

**MECHANISMS OF CATIONIC LIPOSOMES-INDUCED
APOPTOSIS AND ITS PROTECTION
BY ANTIOXIDANTS**

LALANA KONGKANERAMIT

**A THESIS SUBMITTED IN PARTIAL FULFILLMENT
OF THE REQUIREMENTS FOR
THE DEGREE OF DOCTOR OF PHILOSOPHY
(PHARMACEUTICS)
FACULTY OF GRADUATE STUDIES
MAHIDOL UNIVERSITY
2010**

COPYRIGHT OF MAHIDOL UNIVERSITY

Thesis
entitled
**MECHANISMS OF CATIONIC LIPOSOMES-INDUCED
APOPTOSIS AND ITS PROTECTION
BY ANTIOXIDANTS**

.....
Mrs. Lalana Kongkaneromit
Candidate

.....
Prof. Narong Sarisuta, Ph.D.
Major advisor

.....
Prof. Yon Rojanasakul, Ph.D.
Co-advisor

.....
Assoc. Prof. Ramida Watanapokasin,
Ph.D.
Co-advisor

.....
Prof. Banchong Mahaisavariya,
M.D., Dip Thai Board of Orthopedics
Dean
Faculty of Graduate Studies
Mahidol University

.....
Assoc. Prof. Satit Puttipatkhachorn,
Ph.D.
Program Director
Doctor of Philosophy Program in
Pharmaceutics
Faculty of Pharmacy, Mahidol University

Thesis
entitled
**MECHANISMS OF CATIONIC LIPOSOMES-INDUCED
APOPTOSIS AND ITS PROTECTION
BY ANTIOXIDANTS**

was submitted to the Faculty of Graduate Studies, Mahidol University
for the degree of Doctor of Philosophy (Pharmaceutics)

on
May 12, 2010

.....
Mrs. Lalana Kongkaneromit
Candidate

.....
Prof. Sompol Prakongpan, Ph.D.
Chair

.....
Prof. Garnpimol C. Ritthidej, Ph.D.
Member

.....
Prof. Narong Sarisuta, Ph.D.
Member

.....
Assist. Prof. Wichet Leelamanit, Ph.D.
Member

.....
Assoc. Prof. Ramida Watanapokasin, Ph.D.
Member

.....
Prof. Banchong Mahaisavariya,
M.D., Dip Thai Board of Orthopedics
Dean
Faculty of Graduate Studies
Mahidol University

.....
Assoc. Prof. Chuthamanee Suthisisang,
Ph.D.
Dean
Faculty of Pharmacy
Mahidol University

ACKNOWLEDGEMENTS

I would like to express my deepest gratitude to my major advisor, Professor Dr. Narong Sarisuta, for his immense support, significant advice, consideration and encouragement throughout my study. Since I started as graduate student for doctoral degree until now I have learned that he is as the role model teacher for me.

I am greatly grateful to Professor Dr. Yon Rojanasakul, my co-advisor, for his welcome that gave me valuable experience in advanced research and for his generosity, support and encouragement. I am grateful to Assoc. Prof. Dr. Ramida Watanapokasin, my co-advisor, for her kind support and meaningful advice.

I would like to acknowledge The Commission on Higher Education (Staff Development Project) and NANOTEC (Thai Herbal Nano-Cosmeceuticals Coordinated Research Program) for their support for scholarship and research grants.

I appreciate all personnels and faculty members at Faculty of Pharmacy, Mahidol University (MU), Thailand and Department of Pharmaceutical Sciences, West Virginia University (WVU), West Virginia, USA for their assistances.

I am very thankful to Dr. Liying Wang, Dr. Yongju Lu, Dr. Neelam Azad, Dr. Anand Krishnan V. Iyer, Dr. Jirapan Mounjaroen and Dr. Pithi Chanvorachote for their teaching and assistances at Prof. Dr. Yon's lab in WVU and also to Ms. Wasu Witoonsaridsilp (Ph. D. candidate) for her helpful and friendliness at Prof. Dr. Narong's lab in MU. My thanks are extended to all of my friends.

Finally, I wish to express my greatly grateful to my parents, Mr. Sermsak Kongkaneromit and Mrs. Pranee Kongkaneromit, and thankful to my spouse, Mr. Yutthapon Sormpeng, and my family for their love, understanding, support and encouragement throughout my life.

Lalana Kongkaneromit

MECHANISMS OF CATIONIC LIPOSOMES-INDUCED APOPTOSIS AND ITS PROTECTION BY ANTIOXIDANTS

LALANA KONGKANERAMIT 4738645 PYPT/D

Ph.D.(PHARMACEUTICS)

THESIS ADVISORY COMMITTEE : NARONG SARISUTA, Ph.D., YON ROJANASAKUL, Ph.D.,
RAMIDA WATANAPOKASIN, Ph.D.**ABSTRACT**

Cationic liposomes, nonviral gene delivery vectors, have advantages such as opportunities for chemical or physical manipulation and large scale production. Although they are widely used, their disadvantages are cytotoxicity and low transfection efficiency. LipofectamineTM (LF), a commercial cationic liposome, has been reported for its cytotoxicity involving reactive oxygen species (ROS) but the underlying mechanism is still unclear. The aims of this study carried out in human lung epithelial cancer cells (H460 cells) were to determine the mechanism, to identify specific ROS involved, and to reduce its cytotoxicity by various antioxidants such as chemicals, enzymes, or herbal extracts.

The results showed that LF-induced apoptosis of H460 cells occurred through a mechanism involving caspase activation and ROS generation. Inhibition of caspase activity by caspase inhibitors (pan-caspase, caspase-8 or caspase-9 inhibitors) could restrain the apoptotic effect of LF. Overexpression of FLICE-inhibitory protein (FLIP) or B-cell lymphoma-2 (Bcl-2) protein, which are known as inhibitors of the extrinsic and intrinsic death pathway, respectively, could additionally inhibit apoptosis by LF. Induction of apoptosis by LF was shown to require ROS generation since its inhibition by ROS scavengers or by ectopic expression of antioxidant enzyme superoxide dismutase and glutathione peroxidase strongly inhibited the apoptotic effect of LF. The primary ROS that was responsible for LF-induced apoptosis was found to be superoxide. The mechanism by which ROS mediated the apoptotic effect of LF involved down-regulation of FLIP. Apart from ROS scavengers or antioxidant enzymes, herbal root extracts from *Asparagus racemosus* was shown to exhibit protective effect against LF-induced apoptosis in H460 cells. Due to the fact that LF death signaling pathway was elucidated, the use of antioxidant was advised and the promising protective herbal extract from such cytotoxicity was proposed. Consequently, a novel mechanism of apoptosis regulation in LF death signaling may be exploited to decrease cytotoxicity and increase gene transfection efficiency of cationic liposomes.

KEY WORDS: CATIONIC LIPOSOMES / APOPTOSIS / REACTIVE OXYGEN SPECIES / FLIP /
ASPARAGUS RACEMOSUS

121 pages

กลไกการตายของเซลล์ที่ถูกเหนี่ยวนำโดยไลโปโซมประจุบวก และการป้องกันโดยใช้สารต้านอนุมูลอิสระ
MECHANISMS OF CATIONIC LIPOSOMES-INDUCED APOPTOSIS AND ITS PROTECTION BY
ANTIOXIDANTS

ลลนา คงานรมิตร 4738645 PYPT/D

ปร.ศ. (เภสัชการ)

คณะกรรมการที่ปรึกษาวิทยานิพนธ์ : ฌรงค์ สาริสุต, Ph.D., YON ROJANASAKUL, Ph.D., รมีดา วัฒนโกลาสิน,
Ph.D.

บทคัดย่อ

มีการใช้ไลโปโซมประจุบวกเป็นตัวนำส่งยีนชนิดไม่ใช้ไวรัส ซึ่งมีข้อดี เช่น สามารถปรับให้เหมาะสมทางเคมีและกายภาพได้ และสามารถผลิตในปริมาณมากได้ ถึงแม้ว่ามีการใช้ไลโปโซมประจุบวกนี้ยังกว้างขวาง แต่ก็มีข้อด้อย เช่น ความเป็นพิษต่อเซลล์ และมีประสิทธิภาพต่ำในการนำส่งยีน มีรายงานเกี่ยวกับความเป็นพิษต่อเซลล์ของ ไลโปเฟคตามีน (Lipofectamine™, LF) ซึ่งเป็นไลโปโซมประจุบวกที่มีจำหน่าย โดยสัมพันธ์กับ reactive oxygen species (ROS) และยังไม่ทราบถึงกลไกที่ชัดเจน การศึกษานี้ทำการทดสอบกับเซลล์มะเร็งปอด (H460 cells) เพื่อต้องการค้นหากลไกดังกล่าว และระบุถึงชนิดของ ROS ที่เกี่ยวข้อง และต้องการลดความเป็นพิษโดยใช้สารต้านอนุมูลอิสระชนิดต่างๆ เช่น สารเคมี เอนไซม์ หรือสารสกัดจากพืช

ผลการศึกษานี้แสดงให้เห็นว่า LF เหนี่ยวนำให้เซลล์เกิดการตายแบบ apoptosis เนื่องจากมีกลไกที่เกี่ยวข้องกับการกระตุ้นการทำงานของ caspase และพบว่ามีการสร้าง ROS ขึ้นด้วย เมื่อยับยั้งการทำงานของ caspase โดยใช้ตัวยับยั้ง caspase (caspase inhibitors) หลายชนิด พบว่าการตายที่เหนี่ยวนำจาก LF ถูกยับยั้งได้เมื่อทำให้มีปริมาณของโปรตีน FLICE-inhibitory protein (FLIP) และ B-cell lymphoma-2 (Bcl-2) protein เพิ่มขึ้นในเซลล์ (เป็นที่ทราบกันว่าโปรตีนทั้งสองนี้สามารถยับยั้งวิธีการตายแบบ extrinsic และ intrinsic ได้ตามลำดับ) พบว่าการตายที่เหนี่ยวนำจาก LF ถูกยับยั้งได้ นอกจากนี้ การเหนี่ยวนำให้เซลล์ตายโดย LF นี้ต้องการ ROS ร่วมด้วย เพราะเมื่อใช้ ROS scavenger หรือเมื่อมีปริมาณเอนไซม์ที่มีฤทธิ์ต้านอนุมูลอิสระ (superoxide dismutase and glutathione peroxidase) เพิ่มขึ้นในเซลล์ พบว่าสามารถยับยั้งการตายที่เหนี่ยวนำจาก LF ได้ ส่วน ROS หลักที่สัมพันธ์กับการตายนี้คือ superoxide และการสลายของ ROS เมื่อเซลล์ตายจาก LF นี้มีกลไกเกี่ยวข้องกับการทำให้ FLIP ลดลง นอกเหนือจาก ROS scavenger และเอนไซม์ที่มีฤทธิ์ต้านอนุมูลอิสระแล้ว การใช้สารสกัดจากรากพืช คือ รากสามสิบ หรือ สามร้อยราก (*Asparagus racemosus*) มีฤทธิ์ในการป้องกันการตายที่เหนี่ยวนำจาก LF ใน H460 cells ได้ การศึกษาทั้งหมดนี้แสดงถึงวิธีการนำสัญญาณการตายที่เหนี่ยวนำโดย LF แสดงถึงสารต้านอนุมูลอิสระที่ใช้ป้องกัน และนำเสนอสารสกัดจากพืชที่มีฤทธิ์ปกป้องความเป็นพิษ ดังนั้น กลไกการตายที่เกี่ยวข้องกับสัญญาณการตายที่เหนี่ยวนำโดย LF ที่ค้นพบนี้ อาจใช้ประโยชน์ในการช่วยลดความเป็นพิษต่อเซลล์ และเพิ่มประสิทธิภาพในการนำส่งยีนของไลโปโซมประจุบวกได้

CONTENTS

	Page
ACKNOWLEDGEMENTS	iii
ABSTRACT (ENGLISH)	iv
ABSTRACT (THAI)	v
LIST OF TABLES	vii
LIST OF FIGURES	viii
LIST OF ABBREVIATIONS	xiv
PUBLICATIONS AND PRESENTATIONS	xvi
CHAPTER I INTRODUCTION	1
CHAPTER II LITERATURE REVIEW	3
CHAPTER III MATERIALS AND METHODS	39
CHAPTER IV RESULTS AND DISCUSSION	53
4.1 Characterization of Lipofectamine™	53
4.2 Investigation of LF-induced apoptosis	57
4.3 Role of ROS to LF-induced apoptosis	70
4.4 Antioxidant activity of herbal extracts	80
CHAPTER V CONCLUSION	100
REFERENCES	103
APPENDICES	113
Appendix A Overexpression of FLIP, Bcl-2, SOD, GPx in H460 cells	114
Appendix B Electron spin resonance studies	116
Appendix C Ubiquitination pathway studies	118
BIOGRAPHY	120

LIST OF TABLES

Table		Page
2.1	Comparison of different viral vectors for gene therapy	7
2.2	Advantages and limitations of current nonviral gene delivery systems	8
2.3	Subfamily members of caspase family	22
4.1	Particle size of Lipofectamine™ (LF)	55
4.2	Zeta potential of Lipofectamine™ (LF)	56
4.3	R _f values and color zones of TLC fingerprints of OA and AR1-1 in system I and DG and AR1-2 to AR1-5 in system II in white light and under UV (366 nm)	84
4.4	Total saponin content of ARs in terms of diosgenin equivalent (DGE) (µg/mg extract)	88
4.5	The percentage remaining of DPPH for ARs tested at the same concentration (500 µg/ml)	97

LIST OF FIGURES

Figure		Page
2.1	Cationic lipids used in cationic liposome formulations.	15
2.2	Apoptosis signaling by Fas.	23
2.3	Mitochondrial pathway.	24
2.4	Downstream substrates of apoptosis executioner caspases.	26
2.5	Schematic structures of Bcl-2 family proteins.	29
2.6	Two major apoptotic pathways in mammalian cells.	31
2.7	Domain structure of the IAP family. The presence of at least one BIR domain (indicated by blue boxes) is the defining characteristic of the IAP family. Some IAPs contain a RING-zinc finger domain at the carboxy terminus (indicated by green hexagon). cIAP1 and cIAP2 both possess a caspase recruitment domain (CARD) (indicated by yellow boxes) in the linker region between the BIR domains and the RING (Really Interesting New Gene) domain. NAIP possesses a nucleotide binding site domain (indicated by black stripes), as well as a leucine-rich repeat domain (indicated by aquaovals). BRUCE contains a UBC, ubiquitin-conjugation, domain (indicated by red circle).	32
2.8	Composition of the NADPH oxidase in phagocytic cells.	34
2.9	Proposed effects of ROS level to cell homeostasis.	36
4.1	TEM photomicrographs of Lipofectamine [™] (LF) obtained by negative staining technique (magnification 150,000x).	54
4.2	Apoptosis of H460 cells treated with various concentrations of LF (0-50 $\mu\text{g/ml}$) determined by Hoechst 33342 assay after 6 h. Data are mean \pm S.D. (n = 4). *, $p < 0.05$ versus nontreated control.	58

LIST OF FIGURES (cont.)

Figure		Page
4.3	Representative fluorescence micrographs of H460 cells treated with LF (0, 20, 40 µg/ml) for 6 h and stained with the Hoechst dye. Apoptotic cells exhibit condensed nuclei with bright nuclear fluorescence (original magnification, 400X). A, untreated cells as control. B, cells treated with 20 µg/ml of LF. C, cells treated with 40 µg/ml of LF.	59
4.4	Apoptosis of H460 cells treated with LF (20 µg/ml) for 3, 6, 9, 12 h determined by Hoechst 33342 assay. Data are mean ± S.D. (n = 4). *, <i>p</i> < 0.05 versus nontreated control.	60
4.5	DNA fragmentation of H460 cells treated with various concentrations of LF (0-50 µg /ml) analyzed by gel electrophoresis DNA ladder assay after 6 h.	61
4.6	Caspase-8 and caspase-9 activities of H460 cells treated with various concentrations of LF (0-40 µg/ml) for 6 h analyzed by caspase assay. Data are mean ± S.D. (n = 4). *, <i>p</i> < 0.05 versus nontreated control.	63
4.7	Apoptosis of H460 cells treated with LF (20 µg/ml) in the presence or absence of 10 µM of pan-caspase inhibitor (z-VAD-fmk), caspase-8 inhibitor (z-IETD-fmk), or caspase-9 inhibitor (z-LEHD-fmk) determined by Hoechst assay after 6 h. Data are mean ± S.D. (n = 4). *, <i>p</i> < 0.05 versus nontreated control; **, <i>p</i> < 0.05 versus LF-treated control.	64
4.8	Apoptosis of FLIP- or Bcl-2-overexpressing cells treated with LF (20 µg/ml) for 6 h analyzed by Hoechst assay. Data are mean ± S.D. (n = 4). *, <i>p</i> < 0.05 versus nontreated control; **, <i>p</i> < 0.05 versus mock-transfected LF-treated control.	66

LIST OF FIGURES (cont.)

Figure	Page
4.9 Caspase-8 (A) and caspase-9 (B) activation of FLIP- or Bcl-2-overexpressing cells treated with LF (20 µg/ml) for 6 h analyzed by caspase assay. Data are mean ± S.D. (n = 4). *, $p < 0.05$ versus nontreated control; **, $p < 0.05$ versus mock-transfected LF-treated control.	67
4.10 FLIP, FADD, and Fas protein expression in H460 cells treated with LF (0-40 µg/ml) for 6 h analyzed by Western blotting. Plots are mean ± S.D. (n = 3). *, $p < 0.05$ versus nontreated control.	69
4.11 Superoxide and peroxide formation in H460 cells treated with LF (0-40 µg/ml) for 30 min analyzed by fluorometry using DHE and DCF-DA as fluorescent probes. Data are mean ± S.D. (n = 3). *, $p < 0.05$ versus nontreated control.	71
4.12 FLIP level in H460 cells either left untreated or pretreated with MnTBAP (100 µM), CAT (1000 units/mL), or SF (10 mM) for 1 h, after which treated with LF (20 µg/ml) for 6 h analyzed by Western blotting. Plots are mean ± S.D. (n = 3). *, $p < 0.05$ versus nontreated control; **, $p < 0.05$ versus LF-treated control.	73
4.13 Superoxide generation in H460 cells either left untreated or pretreated with DPI (1 µM) or rotenone (1 µM) for 30 min, after which treated with LF (20 µg/ml) and analyzed by DHE fluorescence measurement after 30 min. Plots are mean ± S.D. (n = 3). *, $p < 0.05$ versus nontreated control; **, $p < 0.05$ versus LF-treated control.	75
4.14 SOD- or GPx-overexpressing cells treated with LF (20 µg/ml) for 30 min analyzed by DHE fluorescent measurement. Plots are mean ± S.D. (n = 4). *, $p < 0.05$ versus nontreated control.	76

LIST OF FIGURES (cont.)

Figure	Page
4.15 Apoptosis of H460 cells stably transfected with SOD, GPx, or control plasmid, and treated with LF (20 µg/ml) for 6 h analyzed by Hoechst assay. Plots are mean ± S.D. (n = 4). *, $p < 0.05$ versus nontreated control.	77
4.16 H460 cells were pretreated with MnTBAP or CAT for 1 h, after which they were treated with LF (20 µg/ml) for 6 h and analyzed for apoptosis by Hoechst assay. Plots are mean ± S.D. (n = 3). *, $p < 0.05$ versus nontreated control; **, $p < 0.05$ versus LF-treated control.	79
4.17 TLC fingerprints in white light (A) and under UV (366 nm) (B) of OA and AR1-1 samples in the system I.	82
4.18 TLC fingerprints in white light (A) and under UV (366 nm) (B) of AR1-2 to 1-5 samples in the system II and that of DG sample at the solvent front.	83
4.19 Calibration curve of diosgenin (DG) analyzed by spectrophotometer ($y = 0.0097x + 0.0098$, $r^2 = 0.9991$).	86
4.20 Total saponin in each AR expressed as diosgenin equivalent (DGE, µg/mg extract). Data are mean ± S.D. (n = 3). Significant differences among the groups were determined by one way ANOVA using SPSS with LSD test as post hoc analysis. *, $p < 0.05$ versus other ARs; **, $p < 0.05$ versus AR1-1 and others.	87
4.21 Calibration curve of DPPH analyzed by spectrophotometer ($y = 0.0097x + 0.0024$, $r^2 = 0.9999$).	90
4.22 Reaction kinetics in antioxidant activity testing of ascorbic acid (1 and 2 µg/ml) with DPPH.	91

LIST OF FIGURES (cont.)

Figure		Page
4.23	Reaction kinetics in antioxidant activity testing of AR1-4 (0.5 mg/ml) with DPPH.	92
4.24	Efficient concentration (EC ₅₀) of ascorbic acid (AA).	93
4.25	Efficient concentration (EC ₅₀) of <i>Asparagus racemosus</i> extract; AR1-4.	94
4.26	The percentage remaining amount of DPPH for ARs tested at the same concentration (0.5 mg/ml). Plots are mean ± S.D. (n = 2).	96
4.27	Apoptosis of H460 cells untreated or pretreated with <i>Asparagus racemosus</i> aqueous extract (AR1-4) at various concentrations for 1 h, after which treated with LF (20 µg/ml) for 6 h and analyzed by Hoechst assay. Plots are mean ± S.D. (n = 3). *, <i>p</i> < 0.05 versus LF-treated control.	99
4.28	H460 cells were stably transfected with FLIP, Bcl-2, SOD, GPx or control pcDNA3 plasmid and determined protein expression level by Western blot analysis. A, An increase in FLIP expression level over vector-transfected control. B, An increase in Bcl-2 expression level over vector-transfected control. C, An increase in SOD expression level over vector-transfected control. D, An increase in GPx expression level over vector-transfected control	115
4.29	H460 cells (1x10 ⁶ /ml) were incubated in RPMI medium containing the spin trapper DMPO (10 mM) in the presence or absence of LF (20µg/ml), sodium formate (10 mM), MnTBAP (100 µM), and catalase (1000 units/ml). ESR spectra were then recorded 30 min after the addition of the test agents. The spectrometer settings were as follows: receiver gain at 1.5x10 ⁵ , time constants at 0.3 second, modulation amplitude at 1.0 G, scan time at 4 min, magnetic field at 3470 ± 100 G.	117

LIST OF FIGURES (cont.)

Figure		Page
4.30	H460 cells were transiently transfected with ubiquitin and myc-tagged FLIP plasmids. Thirty six hours later, the cells were treated with LF (20 µg/ml) in the presence or absence of MnTBAP (100 µM) or catalase (1000 units/ml). Cell lysates were immunoprecipitated with anti-myc antibody and the immune complexes were analyzed for ubiquitin by Western blotting. Analysis of ubiquitin was performed at 2 h post-treatment where ubiquitination was found to be maximal. Data are mean ± S.D. (n = 3). *, $p < 0.05$ versus nontreated control; **, $p < 0.05$ versus LF-treated control.	119

LIST OF ABBREVIATIONS

β	beta
$^{\circ}\text{C}$	degree Celsius
%	percent
%CV	percentage of coefficient of variation
μg	microgram
μl	microliter
ml	milliliter
mM	millimolar
μM	micromolar
nm	nanometer
ANOVA	analysis of variance
AA	Ascorbic acid
BCA	bicinchoninic acid
Bcl-2	B-cell lymphoma
CAT	catalase
CO_2	carbon dioxide
DCF-DA	dichlorofluorescein diacetate
DG	diosgenin
DHE	dihydroethidium bromide
DPI	diphenylene iodonium
DPPH	2,2-diphenyl-1-picrylhydrazyl
ESR	electron spin resonance
FBS	fetal bovine serum
FLIP	FLICE inhibitory protein
GPx	glutathione peroxidase
H_2O_2	hydrogen peroxide

LIST OF ABBREVIATIONS (conts.)

LF	Lipofectamine™
MnTBAP	Mn (III) tetrakis (4-benzoic acid) porphyrin chloride
$O_2^{\cdot-}$	superoxide anion
OH^{\cdot}	hydroxyl radical
OA	oleanolic acid
r^2	correlation coefficient
ROS	reactive oxygen species
ROT	rotenone
S.D.	standard deviation
SDS-PAGE	sodium dodecyl sulfate-polyacrylamide gel electrophoresis
SF	sodium formate
SOD	superoxide dismutase
TEM	transmission electron microscope
TM	trade mark
UV	ultraviolet

PUBLICATIONS AND PRESENTATIONS

PUBLICATIONS

Kongkaneramt L, Sarisuta N, Azad N, Lu Y, Iyer AKV, Wang L, Rojanasakul Y. Dependence of reactive oxygen species and FLICE inhibitory protein on Lipofectamine-induced apoptosis in human lung epithelial cells. *Journal of Pharmacology and Experimental Therapeutics*. 2008; 325 (3), 969-977.

Wang L, Azad N, **Kongkaneramt L**, Chen F, Lu Y, Jiang B-H, et al. The Fas death signaling pathway connecting reactive oxygen species generation and FLICE inhibitory protein down-regulation. *The Journal of Immunology*. 2008;180:3072-80.

POSTER PRESENTATIONS

Kongkaneramt L, Witoonsaridsilp W, Peungvicha P, Sarisuta N. Antioxidant activity and cytotoxicity of different fractions from successive extraction of *Asparagus racemosus*. The 7th World Meeting on Pharmaceutics, Biopharmaceutics and Pharmaceutical Technology, Valletta, Malta, March 8-11, 2010.

Kongkaneramt L, Sarisuta N, Azad N, Lu Y, Rojanasakul Y. Cationic liposomes induces apoptosis by reactive oxygen species mediated FLIP downregulation through ubiquitin-proteasomal degradation pathway. The 2007 AAPS Annual Meeting and Exposition, San Diego Convention Center, San Diego, California, USA, November 11-15, 2007.

CHAPTER I

INTRODUCTION

Gene therapy is the new approach for treatment or prevention of diseases. It is defined by the use of nucleic acid transfer, either RNA or DNA (1). The main targets of gene therapy are to repair or replace mutated genes, regulate gene expression and signal transduction, manipulate the immune system, or target malignant and other cells for destruction (2). These require the delivery of appropriate therapeutic gene to the target tissue, however, this step is still the rate-limiting step for the successful gene therapy (1). Therefore, the field of gene delivery systems has been studied and researched very much since they are the significant tool in gene therapy.

The gene delivery systems are available in two groups as viral and nonviral vectors (2-4). Viral vector has been used early and now there is a serious case in clinical trial which by a patient died from viral vector (5). Thus, nonviral vector is the alternative for gene delivery in case of it seems less toxic than the viral vector.

Cationic liposomes are one of the nonviral vectors. Their advantages are such as plasmid independent structure, opportunities for chemical or physical manipulation, large scale production, and cost, although disadvantages are that their transfection efficiency is lower than viral vectors (6) and cytotoxicity (7).

Study of cationic liposomes revealed the significant effect when increase in positive charge density. Lipofectamine (8), polyvalent cationic lipid, has transfection efficiency higher than Lipofectin, and DOTAP (monovalent cationic lipid) in macrophage RAW264.7 cell line (9). Nonetheless, higher positive charge density is generally more toxic (10).

The toxicity study of cationic liposomes has been shown in some reports that liposomes consisting of stearylamine (monovalent positive charge), named stearylamine liposomes, induced apoptosis and production of reactive oxygen species (11) in RAW264.7 cell line (12) and mouse immature B cell line (WEHI 231) (13). LF has been reported that it caused toxicity *in vivo*. Intratracheal instillation of mice with

differently charged liposomes, LF caused much more toxic than DOTAP while neutral and negative liposomes were not toxic at the relevant concentration. LF caused dose-dependent toxicity and ROS generation associating with such toxicity (7).

However, the underlying mechanism of LF-mediated cytotoxicity and the role of ROS are unknown. Thus, insight in the mechanism would lead to applications that may benefit from decrease in the cytotoxicity and improvement of the transfection efficiency. In case of the transfection efficiency, the cytotoxicity limit the dose of LF used and then it could be consequently limit the level of transfection efficiency. If the cytotoxicity can be reduced the transfection efficiency may be improved.

In this study, LF was investigated for induction of cell death, the death pathway, and regulatory factors that would be involved. Moreover, LF-induced ROS generation was investigated for source of generation, types of ROS, and the role of ROS. Thus, the role of specific ROS in LF-induced cell death and the underlying mechanism would be elucidated. Therefore, the objectives of this study were

1. To identify specific ROS involved in cationic liposome-mediated apoptosis and determine the underlying mechanisms.
2. To reduce the oxygen radical-mediated toxicity induced by cationic liposomes by using various types of antioxidants.

CHAPTER II

LITERATURE REVIEW

2.1 Gene therapy

Gene therapy is defined by the use of nucleic acid transfer, either RNA or DNA, to treat or prevent a disease. Apparently, some examples of gene therapy have been shown such as the delivery to tumors of antisense or ribozyme RNA specific to an oncogene, the vaccination against hepatitis by intradermal immunization with DNA-expressing hepatitis S antigen, the treatment of cystic fibrosis (CF) by adenoviral gene transfer of CF transmembrane conductance regulator to lung, and the transplant of genetically modified hematopoietic stem cells *in utero* (1).

The main targets of gene therapy are to repair or replace mutated genes, regulate gene expression and signal transduction, manipulate the immune system or target malignant and other cells for destruction (2). Successful gene therapy requires many important steps such as a clear understanding of the pathogenesis of disease, an appropriate target tissue for gene delivery, an effective therapeutic gene(s) and an animal model that closely simulates disease for preclinical testing. The rate-limiting step is the ability to transfer efficiently the appropriate therapeutic gene to the target tissue (1).

Study of many diseases suggests that the cause of disease would come from the abnormality in gene(s). Thus, gene therapy, which is the only approach, is the effort to cure at the cause of diseases. It has been employed in genetic and acquired diseases. Genetic diseases are typically caused by a single gene mutation or deletion, such as severe combined immunodeficiency (SCID), hemophilia, cystic fibrosis. Acquired diseases are those for which no single gene has been identified as the only cause of the disease state, such as cancer, Parkinson's disease, Alzheimer's disease (14). Among these, cancer is by far the most common targeted disease for gene therapy. Cancer gene therapy accounts for 65.6% of all gene therapy clinical protocols worldwide (with a total of 425 as updated on May 25, 2000) (15). The following

examples of cancer gene therapy will show about some strategies or approaches in gene therapy (16):

1. The introduction of cytokine genes, such as granulocyte-macrophage colony-stimulating factor (GM-CSF), interferon γ (IFN- γ) and interleukins (e.g. Il-2), into cancer cells is employed. These cytokines induce a local inflammatory reaction in the tumor, which destroys a significant fraction of the treated tumor. The inflammation in turn induces an anti-tumor cell immune reaction, which destroys any surviving malignant cells in the primary tumor as well as in distant metastases.

2. "Suicide genes", such as the herpes simplex virus-thymidine kinase (HSV-TK) gene. This enzyme is known to phosphorylate the systemically administered prodrug ganciclovir. Phosphorylated ganciclovir is incorporated into the DNA of dividing cells, which leads to the termination of DNA-chain elongation, resulting in the death of the cell.

3. Tumor suppressor genes, such as p53, which are mutated in a large number of cancers, or antisense genes targeted at oncogenes to reduce or abolish their expression.

4. Protection of hematopoietic stem cells (HSCs) from the toxic effects of chemotherapy by inserting a gene that confers drug resistance, e.g. multiple drug resistance gene MDR-I. The MDR-I gene has been isolated from drug resistant tumor cells, where it pumps anticancer drugs out of the cell.

Conclusively, cytokine gene therapy is intended for treatment of both the primary tumor and distant metastases. Suicide and tumor suppressor genes have been designed to mediate direct cytotoxic or antiproliferative effects on the tumor cells, and are only effective for the treatment of localized tumor. MDR-I gene therapy is expected to allow cancer patients to tolerate higher doses of chemotherapy, thereby increasing the efficacy of the therapy.

2.2 The delivery systems

Gene therapy may be divided into germ-line gene therapy and somatic gene therapy (16). Germ-line gene therapy aims for the introduction of therapeutic genes into germ-cells or omnipotent embryonal cells (at the 4-8 cellular stage). As a result, all the cells of the individual derived from these cells will carry the therapeutic gene,

including his or her germ cells. Further offspring will also carry the therapeutic gene. As the effect of expressing a therapeutic gene in both somatic and germ cells is not known, human germ cell gene therapy is presently not accepted. In somatic gene therapy, gene delivery to somatic cells can take place either *ex vivo* or *in vivo* (16, 17). In the *ex vivo* approach, cells from a number of organs and tissues (e.g. skin, hematopoietic system, liver) or from tumors can be removed from the patient and cultured *ex vivo* in the laboratory. A therapeutic gene may be introduced during further culture of such cells. This introduction is then followed by re-infusion or re-implantation of these transduced cells into the patient. The *in vivo* approach involves administration of the gene of interest either locally or systemically to the patient.

The delivery systems, now, are the important issue for gene therapy, since the weakest point of gene therapy development programs is vector design, followed by gene regulation and avoidance of immune responses (2, 5). Scientists still looking for or develop vectors which are efficient and non-toxic. The delivery systems are available in two types of vectors: viral and nonviral vectors. The choice of appropriate vector for successful gene therapy requires understanding of the drawbacks and advantages of each vector (Table 2.1 for comparison of viral vectors and Table 2.2 for comparison of nonviral vectors) (2).

Viral vectors are able to mediate gene delivery with high efficiency and the possibility of long-term gene expression. The acute immune response, immunogenicity and insertion mutagenesis uncovered in gene therapy clinical trials have raised serious safety concerns about some commonly used viral vectors. The limitation in the size of the transgene that recombinant viruses can carry and issues related to the production of viral vectors present additional practical challenges. Although nonviral vectors have advantages in terms of simplicity of use, ease of large-scale production and lack of specific immune response, they are still much less efficient than viral vectors, especially for *in vivo* gene delivery (3, 4).

There are 70% of gene therapy clinical trials that have used viral vectors. However, the awareness of toxicity from viral vectors is raised, since a patient with an ornithine transcarbamylase deficiency died after hepatic arterial injection of an adenovirus vector carrying a wild-type version of the defective enzyme (5). Thus, the attempts to develop nonviral vectors may be advantageous for alternative.

Two methods of nonviral vectors for gene delivery are physical methods and chemical methods (3, 4):

2.2.1 Naked DNA delivery by physical methods

2.2.1.1 Needle injection

The simplest way for administration of DNA is direct injection of naked plasmid DNA into the tissue or systemic injection from a vessel. The site of the direct injection includes skeletal muscle, liver, thyroid, heart muscle, urological organ, skin and tumor. Systemic injection is also a convenient route for gene administration. However, owing to rapid degradation by nucleases in the serum and clearance by the mononuclear phagocytes system, the expression level and the area after injection of naked DNA are generally limited.

2.2.1.2 Electroporation

The application of controlled electric fields to facilitate cell permeabilization is used for enhancement of gene uptake into cells after injection of naked DNA. In addition, electroporation can achieve long-lasting expression and can be used in various tissues such as skin or muscle that the electrode can access the sites of application. Major drawbacks exist for *in vivo* application of electroporation. First, it has a limited effective range of ~1 cm. Second, a surgical procedure is required to place the electrodes deep into the internal organs. Third, high voltage applied to tissues can result in irreversible tissue damage as a result of thermal heating.

2.2.1.3 Gene gun

DNA is deposited on the surface of gold particles, which are then accelerated by pressurized gas and expelled onto cells or a tissue. The momentum allows the gold particles to penetrate a few millimeters deep into the tissue and release DNA into cells on the path. Gene gun is expected to have application as an effective tool for DNA based immunization. However, a disadvantage of this method is the shallow penetration of DNA into the tissue and tissue damage in some applications.

Table 2.1 Comparison of different viral vectors for gene therapy (2)

Vectors	Advantages	Disadvantages
Retrovirus	Integration into host DNA All viral genes removed Relatively safe	Insertional mutagenesis Requires cell division Relatively low titer
Adenovirus	Higher titer Efficient in nondividing cells	Toxicity Immunological response
Adeno-associated virus	All viral genes removed	Limited size of foreign DNA Labor-intensive production Status of genome not fully elucidated
Lentivirus	Provided long-term and stable gene expression Infect nondividing cells	Similar retrovirus

Table 2.2 Advantages and limitations of current nonviral gene delivery systems (4)

Method	Route of gene delivery	Advantages	Limitations
Needle injection	Intratissue	Simplicity and safety	Low efficiency
Gene gun	Topical	Good efficiency	Tissue damage in some applications
Electroporation	Topical Intratissue	High efficiency	Limited working range; need for surgical procedure for nontopical applications
Hydrodynamic Delivery	Systemic Intravascular	High efficiency, simplicity, effectiveness for liver gene delivery	Extremely effective in small animals; surgical procedure may be needed for localized gene delivery
Ultrasound	Topical Systemic	Good potential for site-specific gene delivery	Low efficiency <i>in vivo</i>
Cationic lipids	Topical Intratissue Systemic Airway	High efficiency <i>in vitro</i> ; low to medium high for local and systemic gene delivery	Acute immune responses; limited activity <i>in vivo</i>
Cationic polymers	Topical Intratissue Systemic Airway	High effective <i>in vitro</i> ; low to medium high for local and systemic gene delivery	Toxicity to cells; acute immune responses
Lipid/polymer hybrids	Intratissue Systemic Airway	Low to medium-high efficiency <i>in vitro</i> and <i>in vivo</i> ; low toxicity	Low activity <i>in vivo</i>

2.2.1.4 Ultrasound

Ultrasound creates membrane pores and facilitates intracellular gene transfer through passive diffusion of DNA across the membrane pores, unlike the electroporation which moves DNA along the electric field. The transfection efficiency of this system is determined by several factors, including the frequency, the output strength of the ultrasound applied, the duration of ultrasound treatment, and the amount of plasmid DNA used. The efficiency can be enhanced by the use of microbubble, contrast agents or conditions that make membranes more fluidic. Ultrasound can apply to a specific area it could become ideal method for noninvasive gene transfer into cells of the internal organs. So far, the major problem for this method is low gene delivery efficiency.

2.2.1.5 Hydrodynamic injection

A rapid injection of a large volume of naked DNA solution via the tail vein of the mouse can induce potent gene transfer in internal organs, especially the liver. It has been proposed that the liver, which has its flexible structure, can accommodate large volume of solution, and the hydrostatic pressure forces DNA into the liver cells before it is mixed with blood. Furthermore, breaking of the endothelial barrier by the pressure has been proposed as the major mechanism responsible for the highly efficient expression in the liver. Enhancing the efficiency have been done in many ways such as massaging of the abdomen after injection via the tail vein, using large-volume injection with high speed via the portal vein of liver, and transiently restricting blood flow through the liver immediately following peripheral intravenous injection of naked DNA. However, the real challenge for gene transfer by the hydrodynamic method is how to translate this procedure to the application in humans. Therefore, it may need the modification of the method when use in humans.

2.2.2 Gene delivery by chemical methods

There are several groups of gene carriers that have been designed:

- (1) those forming condensed complexing with the DNA to protect from nucleases and other blood component;
- (2) those designed to target delivery to specific cell type;

- (3) those designed to increase delivery of DNA to the cytosol or nucleus;
- (4) those designed to dissociate from DNA in the cytosol;
- (5) those designed to release DNA in the tissue to achieve a continuous or controlled expression.

So far, developed systems are described as follows:

2.2.2.1 Cationic polymer-mediated gene delivery

Polyplexes are named of the complexes of cationic polymers and nucleic acids. Cationic polymers used for gene delivery come from synthetic and naturally polymers. One of the first group of cationic polymers used in gene delivery *in vivo* is poly-L-lysine. Later, polyethylenimine (PEI), polyamidoamine and polypropylamine dendrimers, polyallylamine, cationic dextran, chitosan, cationic protein (polylysine, protamine, and histones), and cationic peptides have been explored as carriers for gene delivery. Although most cationic polymers share the function of condensing DNA into small particles and facilitating cellular uptake via endocytosis, their transfection activity and toxicity differ dramatically.

PEI is one of the most densely charged polymers. Linear PEI (LPEI) and branched PEI (BPEI) have excellent transfection activities *in vitro* and exhibit moderate transfection activity *in vivo*. One drawback in the use of PEI relates to its nonbiodegradable nature. It is known that the toxicity and transfection activity of PEI is molecular weight-dependent. Thus, the biodegradable cationic polymers have been designed to reduce the toxicity.

The mechanism of cationic polymer-mediated gene delivery has been explained by a proton sponge hypothesis, especially gene transfer by PEI and its derivatives. The majority of PEI's amine groups are not fully protonated under physiological pH. However, they could be protonated when the pH drops below 6.0 in the endosome compartment. Proton entrance into the endosome also brings chloride counterions into the endosomes, rising the osmotic pressure and causing these vesicles to swell and rupture.

2.2.2.2 Lipid-polymer hybrid system

This system includes DNA precondensed with polycations, then coated with either cationic liposomes, anionic liposomes, or amphiphilic polymers with or without helper lipids. DNA is better protected in these lipid-wrapping polyplexes. The 3-part system appears to be more efficient in transfection than lipid-DNA complexes *in vitro* and is equally active *in vivo*.

2.2.2.3 Cationic liposome-mediated gene delivery

In 1987, cationic liposome-mediated gene delivery was reported by Felgner et al. They shown that this method has more efficient than the calcium phosphate or DEAE dextran transfection technique (18). So far, a large number of cationic lipids have been reported and used. The cationic liposome-mediated gene delivery will be reviewed in detail later.

2.3 Liposomes

In the mid-1950s, Friedman et al. administered phosphatidyl choline dispersed in aqueous phase intravenously with ultrasonic radiation to rabbits and the treatment was very effective for arteriosclerosis. Later in the mid-1960s, Bangham et al. researched about liposomes and then they found that “hand-shaken phospholipids dispersion” in aqueous phase can spontaneously form microscopic closed vesicles. These vesicles consist of water surrounded by bilayered phospholipids membranes. Bangham called these tiny fat bubbles “smectic mesophase”. Later they named “liposomes” by his colleague Gerald Weissman (19, 20). So far, liposomes have been under extensive research and a variety of liposomes is created. In this review, the five major liposomes are mentioned: conventional liposomes, long-circulation liposomes, immunoliposomes, pH-sensitive liposomes, and cationic liposomes (6, 21).

Conventional liposomes are typically composed of only phospholipids (neutral and/or negatively charged) and/or cholesterol. They can be varied widely in their physicochemical properties such as size, lipid composition, surface charge and number and fluidity of the phospholipids bilayers. Conventional liposomes have a relatively short blood circulation time. When administered *in vivo* by a variety of parenteral routes, they show a strong tendency to accumulate rapidly in

reticuloendothelial system (RES). The major organs of accumulation are the liver and the spleen.

Long-circulation liposomes are produced mostly by attaching hydrophilic polymer polyethylene glycol (PEG) covalently to the outer surface. Such PEG-coated liposomes are also called “stealth” or “sterically stabilized” liposomes. They have RES-escaping capability resulting in their long circulation times. This affects to their extravasation at body sites where the permeability of vascular wall is increased such as solid tumors. This concept was used in liposomal anticancer commercial products as Doxil and DaunoXome.

Immunoliposomes have specific antibodies or antibody fragments on their surface to enhance target site binding. Nevertheless, when immunoliposomes were administered intravenously. They tend to accumulate in the liver and the spleen as conventional liposomes. Therefore, to guarantee accessibility of the target receptors, local administration has received some interest. Successful attempts have been made to prolong the half-life of immunoliposomes after intravenous administration by coating with PEG, thus giving them a greater chance to reach the target.

pH-sensitive liposomes are constructed from pH-sensitive component. Endocytosed by cells, pH-sensitive liposomes can fuse with endosomal membrane as the result of lower pH inside the endosome, and release their contents into the cytoplasm. This type of liposomes is intended for cytosolic delivery.

Cationic liposomes are effective for gene delivery since cationic lipid can disrupt endosomal membrane and then genes will be released into cytoplasm. Their detail will be reviewed in the following topic.

2.4 Cationic liposomes

Cationic liposomes are nonviral vector for gene delivery. Although, they have many advantages such as low immunogenicity, plasmid independent structure, opportunities for chemical or physical manipulation (e.g. targeting potential), large scale production, and cost, their disadvantages are transfection efficiency that lower than viral vectors (6), and toxicity (7) which has been reported increasingly.

From their disadvantages, much effort has been tried to improve the transfection efficiency of cationic liposomes such as a study of lipoplex structure, a

study of chemical property of lipids, optimization of lipid and DNA ratio or lipoplex preparation, a study of lipoplex-cell interaction and release mechanism of cationic liposomes. Thus, these studies will be reviewed.

2.4.1 Studies of lipoplex structure

Lipoplex was named from the complex of cationic liposomes and nucleic acids. The cationic lipid is used to neutralize the polyanionic nucleic acid chain to form a highly compact microstructure. There are attempts to determine structure of lipoplexes. In 1994, Sternberg and co-workers found the aggregated spherical structures together with elongated fibrils forming what has been described as “the spaghetti-meatball” appearance. The spherical units are believed to comprise condensed DNA associated with cationic lamellar lipid, where as the fibrils appear to be strands of DNA surrounded by lipid bilayer in tubular form (22). In 2003, Almofti et al. showed atomic force microscopy (AFM) images from charge ratios study of lipoplexes. The images showed that lipoplexes were formed from extensively fusion among liposome particles that encapsulated DNA rather than aggregation of several independent liposome particles with DNA (11). In 2006, Safinya et al. have reviewed the structure of lipoplex determined by synchrotron X-ray diffraction. Using DOTAP alone or DOTAP with DOPC, per DNA at some ratio the lipoplex can occur as lamellar phase, DNA sandwiched between the lipid bilayers. Transfection efficiency of lamellar lipoplex depends on charge density. In other formula, using DOTAP with DOPE, cone-shaped lipid which confer a negative curvature to membranes, their structure tends to be columnar inverted hexagonal structure where the DNA molecules are inserted in tubes composed of inverse lipid micelles and assembled on a hexagonal lattice. This structure is independent of charge density. Its high transfection efficiency probably related to the observed rapid fusion between the membranes of complexes and the membranes of the plasma membrane or endosome (23). Thus, study of the lipoplex structure is one of approaches for enhancing the transfection efficiency.

2.4.2 The study of chemical property of lipids

The study of chemical property of lipids has been investigated particularly in charge density and chemical structure. Lipids used in cationic liposome

formulations will be grouped into neutral lipids and cationic lipids. Neutral lipids are often used as co-lipid in the formulation such as cholesterol, dioleoyl phosphatidyl choline (DOPC), and dioleoyl phosphatidylethanolamine (DOPE)(24). DOPE has an endosomal membrane-destabilizing property by a change in its geometrical shape from inverted cone shape to cylindrical shape after its protonation in an acidic environment within endosome and then transfer of DOPE into endosomal membrane, to promote leakage and escape of cargo molecules (25). Thereby, it helps to delivery DNA to cytosol and promote transfection efficiency of lipoplex.

Cationic lipids used in cationic liposome formation vary widely with respect to their polar head group, hydrophobic tail, and the interlinking region of the molecule. All are dependent on amine-containing head groups for their positive charge, and in the majority the lipophilic region consists of two fatty acyl chains as in conventional phospholipids (22). DOTMA (*N*-[1-(2,3,-dioleoyloxy)propyl]-*N,N,N*-trimethylammonium chloride) is the first cationic lipid that was introduced by Felgner co-workers in 1987. Thereafter, many cationic lipids have been synthesized and become commercial available such as DOTAP (26), Lipofectamine, and DC-Chol.

DOTMA and DOTAP are monovalent cationic lipids. DOTAP (1,2-diacyl-3-trimethylammonium propane) has lipids with ester as linker bonds and DOTMA has lipids attached to the propyl backbone via ether instead of ester bonds (24). Lipofectamine (LF) is the mixing of a 3:1 (w/w) of polyvalent cationic lipid DOSPA (2,3-dioleoyloxy- *N* - [2(sperminocarboxamido)ethyl] - *N,N* - dimethyl-1-propanaminium trifluoroacetate) and neutral lipid DOPE (27). DC-Chol (cholesteryl-3 β -carboxyamidoethylenedimethylamine) has a basic structure of cholesterol and commonly used by mixing with DOPE (28). Structures of these lipids are shown in Figure 2.1. Interestingly, there is a report shown that the number of positively charge groups seems to affect transfection efficiency. Using the more number of positively charge groups as LF (polyvalent cationic lipid) have more transfection efficient than Lipofectin (DOTMA/DOPE, 1:1 w/w) and DOTAP (monovalent cationic lipid) in macrophage RAW 264.7 cell line (9).

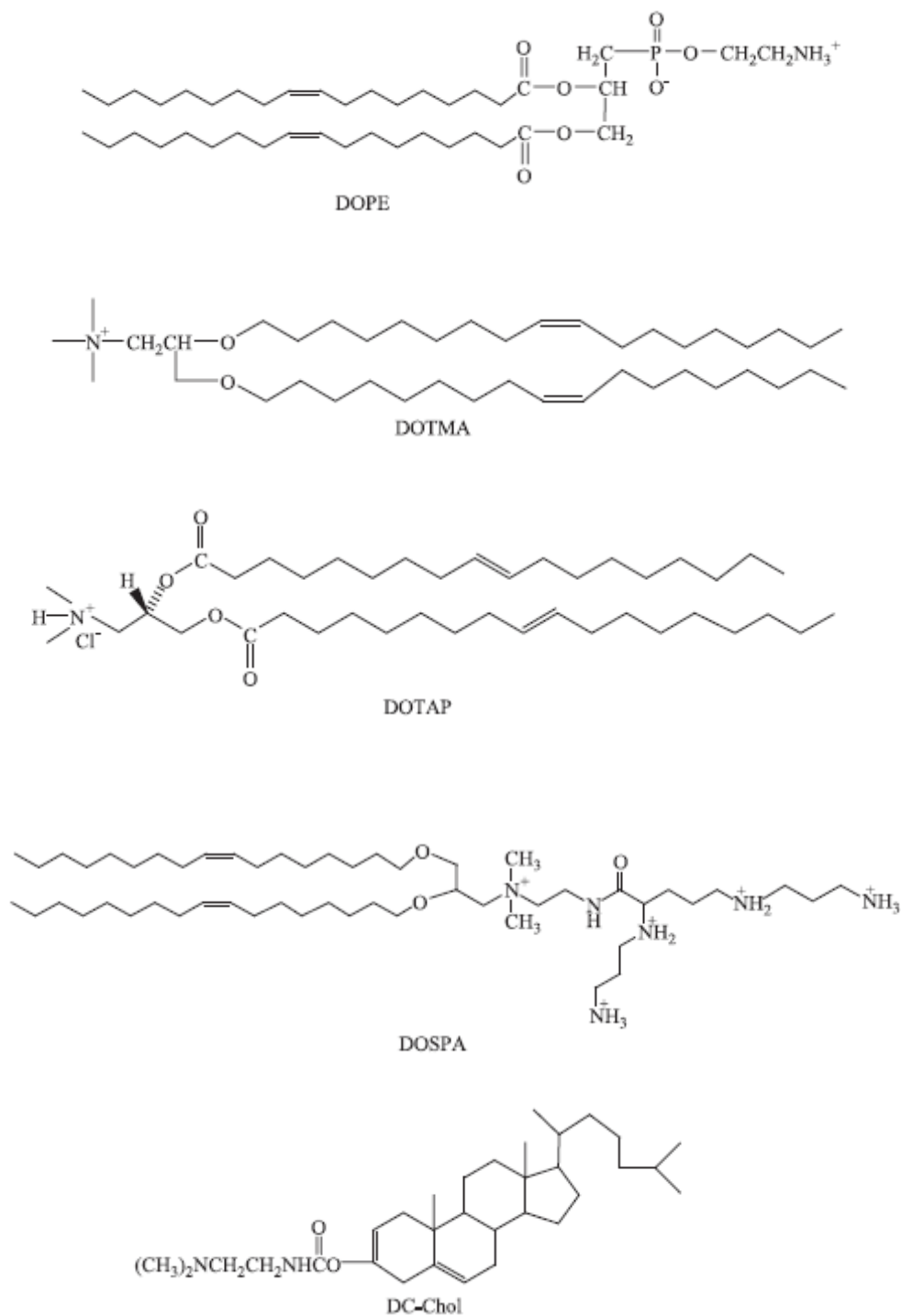


Figure 2.1 Cationic lipids used in cationic liposome formulations (24).

2.4.3 The optimization of lipid and DNA ratio or lipoplex preparation

Sakurai et al. showed that DNA/liposome mixing ratio affects transfection efficiency (29). They prepared DOTMA/DOPE liposomes complexing with plasmid DNA at different DNA/liposome mixing ratios (DNA:lipid, w/w) and tested with cultured cells. They found that efficient gene expression in transfection experiments for MBT-2 cells (mouse bladder tumor), NLH3T3 cells (mouse fibroblasts), HUVEC (human umbilical vein endothelial cells) was obtained at an optimal ratio of 1:5, 1:7.5, 1:5, respectively. The study about lipoplex preparation especially in incubation time or mixing was shown by Zhang et al. They studied interactions between plasmid DNA and cationic liposomes by using fluorescence resonance energy transfer (FRET). FRET data showed that binding of cationic liposomes to DNA occurs immediately upon mixing within 1 min. They found that lipoplexes with a 1-h incubation have much higher transfection efficiencies than samples with 1-min or 5-h incubation (30).

2.4.4 The study of lipoplex-cell interaction and release mechanism of cationic liposomes

The lipoplex-cell interaction has been reported. Cellular uptake of cationic liposomes occur via endocytosis. DOTAP/DNA lipoplexes were shown that lipoplexes are internalized by cells by mean of clathrin-mediated endocytosis (31). After endocytosis, DNA will be released into cytosol thus transfection efficiencies depend on the escape of DNA from lipoplex and endosome to cytosol, and transfer DNA into nucleus for expression. A report which proposed about the release of nucleic acids was shown that the complex (cationic liposome/ oligonucleotide complexes) induces flip-flop of anionic lipids of endosome from the cytoplasmic facing monolayer. Anionic lipids laterally diffuse into the complex and form a charged neutralized ion-pair with the cationic lipids. This leads to displacement of the oligonucleotide from the cationic lipid and its release into the cytoplasm (32).

Although huge attempts in such studies have been shown, transfection efficiency of cationic liposomes still is not high. Therefore, the perspective on toxicity of lipoplex is one of alternative ways to investigate. If toxicity can be reduced when using cationic liposomes as the delivery system, the transfection efficiency may be improved.

2.5 Toxicity of cationic liposomes

The study of toxicity is valuable. Especially, an understanding of the mechanism of toxicity is of both practical and theoretical importance. Such information provides a rational basis for interpreting descriptive toxicity data, estimating the probability that a chemical will cause harmful effects, establishing procedures to prevent or antagonize the toxic effect, designing drugs and industrial chemicals that are less hazardous, and developing pesticides that are more selectively toxic for their target organisms (33).

Similarly, studying the mechanism of cationic liposome-mediated cytotoxicity will give valuable information for using in lipoplex application such as prevention of cytotoxicity or enhancement of transfection efficiency. For instance, Kim et al. showed that there was a positive correlation between doses and cytotoxicity with a cationic lipid and rat primary osteoblasts (34). Therefore, decrease in cytotoxicity may be widen the therapeutic index. Consequently, they could be used in higher dose and may possibly transfect in more cells.

In the past 30 years, the study of toxicity of cationic liposomes gradually has been published, such as, for stearylamine liposomes (35), DDAB (dimethyldioctadecyl-ammonium bromide) liposomes (36), GL-67 liposomes (37), DOTAP liposomes (38), and LF (7). Such liposomes are frequently used together with DOPE because of their enhancing transfection efficiency but its disadvantage is enhancement of the toxicity (38).

There are some instances of mechanism of cytotoxicity from cationic liposomes such as stearylamine and DOTAP. Stearylamine liposomes have been shown that they can inhibit cell dividing more efficient than neutral or negative charge liposomes in L1210 cells (35). Also, they have hemolytic activity to rabbit erythrocyte by interacting with the negative charges of the erythrocyte membrane and this activity depends on the amount of stearylamine in the liposome membrane (39). Furthermore, they can induce apoptosis in mouse splenic macrophages, macrophage-like cell line (RAW264.7 cells) (12), and mouse immature B cell line (WEHI 231 cells) (13). In 2006, Iwaoka et al. have investigated that stearylamine liposomes induce apoptosis of RAW264.7 by the mitogen-activated protein kinase (MAPK) p38

and a caspase-8-dependent Bid-cleavage pathway, and reactive oxygen species (ROS) involved intimately to this pathway (40).

For DOTAP, in 1997, Filion and Phillips have revealed that the DOTAP/DOPE liposomes are toxic to mouse macrophages and human monocyte-like U937 cells by using lactate dehydrogenase (LDH) assay. When DNA (antisense oligonucleotide or plasmid vector) was incorporated into the liposomes, the toxicity was lower. The replacement of DOPE by DPPC (dipalmitoylphosphatidylcholine) significantly reduced liposome toxicity. Thus, toxicity was enhanced by DOPE. Furthermore, they can elucidate the effect of the liposomes on the production of nitric oxide (NO) and tumor necrosis factor- α (TNF- α) by showing that the DOTAP/DOPE liposomes inhibited *in vitro* and *in situ* nitric oxide (NO) and tumor necrosis factor- α (TNF- α) (38).

LF are widely used as nonviral gene delivery vector but the mechanism of its cytotoxicity has not been elucidated. There is an only report showing about LF-induced toxicity *in vivo*. Intratracheal instillation of mice with differently charged liposomes, the multivalent cationic liposome LF caused much more toxic than monovalent cationic liposome DOTAP, and neutral and negative liposomes were not toxic at the relevant concentration. LF cause dose-dependent toxicity and pulmonary inflammation. Lactate dehydrogenase (LDH) assay and polymorphonuclear leukocytes (PMN) cell counts were performed to measure toxicity and pulmonary inflammation, respectively. Furthermore, LF caused reactive oxygen species (ROS) generation that associated with such toxicity (7). So far, there is no report that elucidates the mechanism of cytotoxicity of LF. Thus, insight in LF-induced cytotoxicity would be valuable for searching the way to lower the toxic and to enhance the transfection efficiency.

2.6 Cell death and apoptosis

Toxic compounds can damage cells in target organs in a variety of ways and the cellular injury caused by such compounds leads to a complex sequence of events. The eventual response may be reversible injury or an irreversible change leading to cell death that is the point of no return (41). Regarding cell death, two modes of cell death are broadly discussed: apoptosis and necrosis. Apoptosis, or

programmed cell death, is an active process mediated by programmed signaling pathways, whose activation can be initiated by a variety of extracellular or intracellular stimuli. Apoptosis plays a pivotal role in regulating growth, development and immune response, and clearing excessive or abnormal cells in organisms. It is also deeply involved in the pathogenesis of many human disorders, such as cancer, AIDS, other immune disorders, cardiovascular diseases and many neurodegenerative diseases including Alzheimer disease, Parkinson disease, stroke, and ischemia (42, 43). For necrosis, it has been characterized as passive, accidental cell death resulting from environmental perturbations (44).

The term “Apoptosis” was named by Currie and colleagues in 1972 to describe a common type of programmed cell death that they repeatedly observed in various tissue and cell types (45). Apoptosis is accompanied by a characteristic change of nuclear morphology (chromatin condensation, nuclear fragmentation) and of chromatin biochemistry (DNA fragmentation). It also involves the activation of specific cysteine proteases (caspases). Phosphatidylserine residues, normally on the inner membrane leaflet, exposing on the surface will allow for the recognition and elimination of apoptotic cells by their healthy neighbor, before the membrane breaks up and cytosol or organelles spill into the intercellular space and elicit inflammatory reactions. In contrast to apoptosis, necrosis does not involve any regular DNA and protein degradation pattern and is accompanied by swelling of the entire cytoplasm and of the mitochondrial matrix, which occur shortly before cell ruptures (46).

At present, there is satisfactory information about caspases in apoptosis signaling pathways. It is useful for profound explaining about how caspases work and how cells change. Caspases was discovered in 1993 by investigation of worm as *Caenorhabditis elegans*. A cell death gene from *C. elegans*, *ced-3*, encoded a protein that has a sequence homology to a cysteine protease in mammals: the interleukin-1 β -converting enzyme (ICE), a mammalian protease, is responsible for proteolytic maturation of pro- interleukin-1 β (8, 42).

Caspase structure has been investigated by sequence analysis and x-ray crystallography. Data suggest that all caspases share a common structure. Each caspase is pro-enzyme containing an N-terminal prodomain, a large subunit containing the active site cysteine within a conserved QACXG motif, and a C-terminal small

subunit, and an interdomain linker containing one or two aspartate cleavage sites separates the large and small subunits. Caspase activation occurs when proteolysis of the interdomain linker. Each procaspase is cleaved in order to produce one large subunit (pL) and one small subunit (pS), thereby forming a tetrameric (pL₂pS₂) active form from two molecules of procaspase (8, 42).

Fourteen caspases have been identified and they are all aspartate-specific cysteine proteases. Caspases are divided into three subfamilies based on their homology in amino acid sequences, as shown in Table 2.3. Caspases in subfamily I and II are involved in apoptosis but in subfamily III are involved in inflammation (43). Caspases in subfamily I and II having roles about apoptosis activator and apoptosis executioner are also called initiator caspases and effector caspases, respectively. The roles of initiator and effector caspases are relative as caspase cascade. This cascade will confirm that apoptosis is an ordered or programmed cell death and it will be described in the following topic.

2.7 Caspase-cascade signaling pathway

For apoptosis, there are two pathways through which the caspase family proteases can be activated: death receptor and mitochondrial pathway. Moreover, caspase activation or inactivation requires regulating factors in the cell death or cell survival processes such as FLIP, Bcl-2, IAP (43).

Death receptor pathway, initially, requires death ligands and death receptors binding together and then triggering the signal along the pathway. The death receptors contain in addition a homologous cytoplasmic sequence termed the “death domain” (DD). The best characterized death receptors are CD95 (also called Fas or Apo1) and TNFR1 (tumor necrosis factor receptor 1) (also called p55 or CD120a). Additional death receptors are avian CAR1; DR3 (death receptor 3) (also called Apo3, WSL-1, TRAMP, or LARD); DR4; and DR5 (also called Apo2, TRAIL-R2, TRICK 2 or KILLER). The ligands that activate these receptors are structurally related molecules that belong to the TNF gene superfamily. CD95 ligand (CD95L or FasL) bind to CD95 (Fas); TNF and lymphotoxin α bind TNFR1; Apo3 ligand (Apo3L, also called TWEAK) binds to DR3; and Apo2 ligand (Apo2L, also called TRAIL) binds to DR4 and DR5 (47).

Signaling by Fas receptors, Fas ligation leads to clustering of the receptors' death domains (Figure 2.2). An adapter protein called FADD (Fas-associated death domain) then binds through its own death domain to the clustered receptor death domains (DDs). FADD also contains a "death effector domain"(DED) that the exposed DEDs interact with the DEDs in the prodomain of procaspase-8, which will induce the oligomerization of procaspase-8. Then the molecule complex known as the death-inducing signal complex (DISC) is formed. In DISC, two linear subunits of procaspase-8 compact to each other followed by procaspase-8 autoactivation to caspase-8. Caspase-8 then activates downstream effector caspases.

For TNF, binding to TNFR1 will induce association of the receptors' death domains. Subsequently, an adapter termed TRADD (TNFR-associated death domain) binds through its own death domain to the clustered receptor death domains. TRADD functions as a platform adapter that recruits several signaling molecules to the activated receptor: TNFR-associated factor-2 (TRAF2), receptor-interacting protein (RIP), and FADD. Regarding FADD, it couples the TNFR1-TRADD complex to activation of procaspase-8, thereby initiating apoptosis (43, 47).

For the mitochondrial pathway, when the cellular stress (e.g. DNA damage) occurs, proapoptotic proteins in the cytosol will be activated, which will in turn induce the opening of mitochondrion permeability transition pores (MPTPs). As a result, cytochrome c localized in mitochondria will be released to the cytosol. With the presence of cytosolic dATP (deoxyadenosine triphosphate) or ATP, Apaf-1 (apoptotic protease activation factor-1) oligomerizes. Together with procaspase-9, dATP, cytochrome c, oligomerized Apaf-1 can result in the formation of molecular complex known as apoptosome. The N-terminal of Apaf-1 and the prodomain of procaspase-9 both have the caspase recruitment domain (CARD), with complementary shapes and opposite charges. They interact with each other by CARDS and form a complex in the proportion of 1:1. Activated caspase-9 can in turn activate apoptosis effectors: procaspase-3 and procaspase-7. The activated caspase-3 will then activate procaspase-9 and form a positive feedback activation pathway (Figure 2.3).

Table 2.3 Subfamily members of caspase family (43)

Subfamily	Role	Members
I	Apoptosis activator	Caspase-2 Caspase-8 Caspase-9 Caspase-10
II	Apoptosis executioner	Caspase-3 Caspase-6 Caspase-7
III	Inflammatory mediator	Caspase-1 Caspase-5 Caspase-11 Caspase-12 Caspase-13 Caspase-14

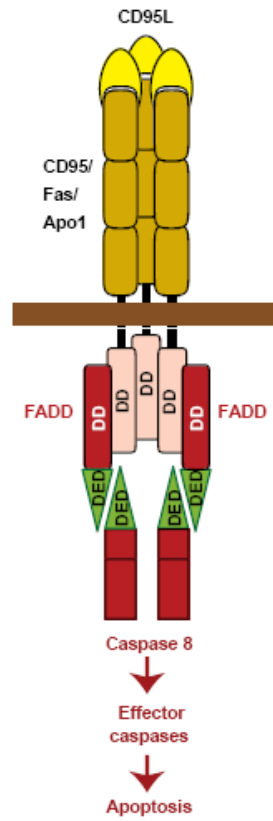


Figure 2.2 Apoptosis signaling by Fas (47).

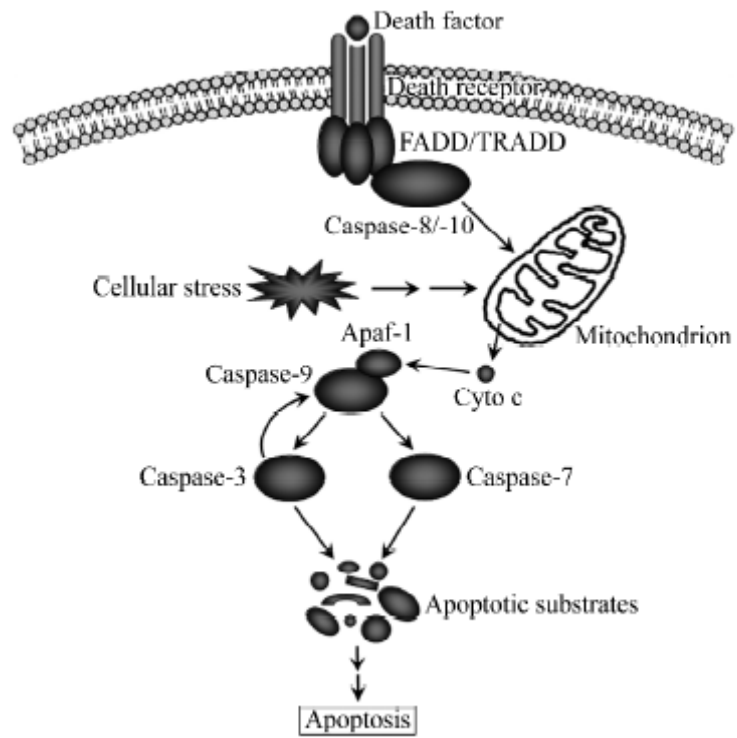


Figure 2.3 Mitochondrial pathway (43).

Two death pathways described above are the direct signal from death receptor or mitochondria to effector caspases that is independently of each other. However, the signal transmission for caspase activation in death receptor and mitochondria pathway can sometimes be interconnected. There are some reports showing about the signal initiated from death receptor affects to mitochondrial pathway, for example, caspase-8 cleaves not only the downstream caspases, but also other substrate proteins, including Bid. The truncated Bid (tBid) that is produced by caspase-8-mediated proteolysis then moves to the mitochondria, and there stimulates a release of cytochrome c into the cytoplasm. This is followed by an enhancement of the apoptosome formation and the activation of caspase-9 (42). In the case of the signal initiated from mitochondria that can affect to caspase-8 activation, for example, after cytochrome c is released from mitochondria to the cytosol, caspase-6 is the only cytosolic caspase with the ability to activate procaspase-8, which depends solely on procaspase-6 activation by prodomain cleaving. It means that, in the cytochrome c-dependent pathway, the activation of procaspase-8 requires neither the interaction with FADD nor the formation of a DISC complex (43).

When the initiator caspases are activated and transmitted until reaching to the effector caspases including caspase-3, -6, -7, then the activated effector caspases will affect to cell, especially in cell morphology. Caspase-3 will activate procaspase-6. Caspase-6 can also activate procaspase-3 by a positive feedback pathway. The downstream substrate of caspase-3 and caspase-7 is such as PARP [poly (ADP-ribose) polymerase], CAD (caspase-activated deoxyribonuclease) and ICAD (inhibitor of CAD). CAD and ICAD form complex by binding together reside in the nucleus. Caspase-3 and caspase-7 can cleave ICAD and the complex then releases CAD, which can result in *DNA fragmentation*. Moreover, caspase-3 can cleave lamin A, the component of the nuclear skeleton, leading to *nuclear shrinkage and fragmentation*. Fodrin, cytoskeleton protein, is cleaved by caspase-3 probably leading to *loss of overall cell shape*. *Plasma membrane blebbing* results from the caspase-mediated activation of gelsolin, an actin depolymerizing enzyme. Caspase-mediated cleavage of PAK2, a member of the p21-activated kinase family, participates in the formation of *apoptotic bodies* (43, 44) (Figure 2.4).

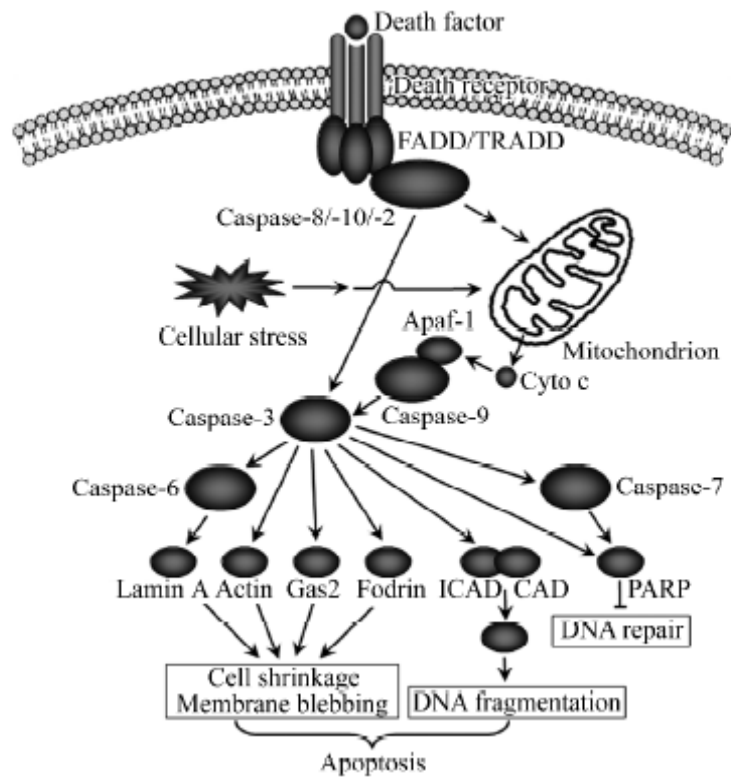


Figure 2.4 Downstream substrates of apoptosis executioner caspases (43).

2.8 Caspase family protease regulating factors

Besides caspases, several cellular proteins have been identified as either anti-apoptotic or pro-apoptotic proteins. For examples, FLIP, Bcl-2, and IAP, have also been identified that they can regulate caspase activation. Smac/DIABLO can also regulate IAP activity. Thus, the sum of anti-apoptotic and pro-apoptotic effect may lead the cell to decide to survive or die. Additionally, the imbalance of apoptosis such as overexpression of anti-apoptotic protein will increase the possibility of tumor growth or cancer. Thus, such proteins are described as follows.

FLIP (FADD-like ICE inhibitory protein or FLICE-inhibitory protein), initially, was first characterized in virus and later it was found that it is involved in death receptor pathway. In 1997, Thome et al. reported that equine herpesvirus-2 (EHV-2) and certain γ -herpesviruses contain ORFs predicted to code for proteins consisting of two DED motives and they called these proteins vFLIP (viral FLICE inhibitory protein). Two DEDs of vFLIP interact with FADD at DISC. This inhibits the recruitment and activation of FLICE (caspase-8) by the CD95 death receptor. Cells expressing vFLIP are protected against apoptosis induced by CD95 or by the related death receptor TRAMP and TRAIL-R (48). Later, FLICE-inhibitory protein in human cell was discovered and designated FLIP. It can be classified to two types as FLIP_S (short) and FLIP_L (long). FLIP_S has the structure similar to vFLIP and its molecular mass is around 28 K. FLIP_L also has the structure similar to vFLIP but two DEDs are followed at the C terminus by a caspase-like domain. The molecular mass of FLIP_L is around 55 K. For their role in inhibition of apoptosis, FLIP_S and FLIP_L inhibit apoptosis induced by Fas, TRAMP and TNFR1 by interact with FADD and FLICE (49), and interfere the activation of FLICE (50).

Bcl-2 family proteins were named after the *bcl-2* (B-cell leukemia/lymphoma 2) gene. Bcl-2 gene mutation are translocations that result in overexpression of Bcl-2 protein in B cells. Such mutation or overexpression has been associated with follicular lymphoma (51, 52). Although Bcl-2 proteins in follicular lymphomas producing from either translocating or no translocating *bcl-2* gene are identical to the normal Bcl-2 protein (51), the excess of Bcl-2 proteins having anti-apoptotic effect may promote the survival of cancer cells.

Bcl-2 family is comprised of over a dozen proteins, which have been classified into three functional groups. Proteins of the first group, such as Bcl-2 and Bcl-X_L, are characterized by four short, conserved Bcl-2 homology (BH) domains (BH1-BH4). The key feature of group I proteins is that they all possess anti-apoptotic activity. In contrast, group II consists of Bcl-2 family proteins with pro-apoptotic activity. The proteins of group II, such as Bax and Bak, have a similar overall structure to group I proteins but lack of BH4. Group III consists of a large and diverse collection of proteins whose only common feature is the presence of the ~12-16 amino-acid BH3 domain. The proteins of group III are such as Bid and Bik, which also have pro-apoptotic activity (45) (Figure 2.5).

Bcl-2 protein, as describe above, has the anti-apoptotic activity that results in promotion of cell survival in follicular lymphoma. The mechanism of Bcl-2 protein has been attempted to clarify. In 1997, Yang et al. reported that human acute myeloid leukemia (HL-60) cells which overexpress Bcl-2 resist apoptosis induced by either staurosporine or etoposide. They found that cytochrome c is released from mitochondria early in apoptosis before mitochondrial depolarization, activation of caspases, and DNA fragmentation. Cytochrome c has the specificity in activation of caspase-3 and may lead to apoptosis. Overexpression of Bcl-2 prevents the release of cytochrome c from the mitochondria to the cytosol (53). At the same year, Kluck et al. had studied the release of cytochrome c in a cell-free apoptosis system and reported that mitochondria spontaneously release cytochrome c, which activates DEVD-specific caspases, leading to fodrin cleavage and apoptotic nuclear morphology. Bcl-2 acts *in situ* on mitochondria to prevent the release of cytochrome c and thus caspase activation. Testing with intact cells was found that cytochrome c translocation is similarly blocked by Bcl-2 but not by a caspase inhibitor, zVAD-fmk. Testing *in vitro*, exogenous cytochrome c bypasses the inhibitory effect of Bcl-2. Cytochrome c release is unaccompanied by changes in mitochondrial membrane potential (54). From these studies, mitochondria release cytochrome c which can cause apoptosis by activation to caspase-3. Bcl-2 prevent cytochrome c translocation from mitochondria to cytosol, thereby resulting in anti-apoptotic effect.

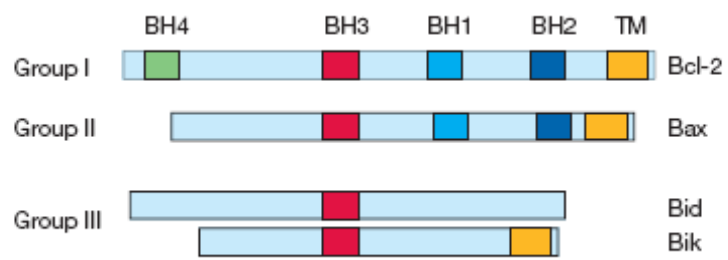


Figure 2.5 Schematic structures of Bcl-2 family proteins (45).

Therefore, Bcl-2 is a significant regulator of apoptosis via mitochondria pathway and FLIP is a significant regulator of apoptosis via death receptor pathway. The overview of the two apoptotic pathways is shown in Figure 2.6.

The inhibitors of apoptosis (IAP) proteins are an important regulator of apoptosis as well as FLIP and Bcl-2. By far, the mammalian IAP family was identified up to eight proteins. The first IAP, which is NAIP (Neuronal Apoptosis Inhibitory Protein), was identified in 1995. Later, others were discovered as cIAP1, cIAP2, XIAP (X-linked inhibitor of apoptosis), Livin, Ts-IAP (Testis-specific IAP), survivin, BRUCE (BIR-containing ubiquitin conjugating enzyme). The IAPs are structurally similar in that all contain one or more 70-80 amino acid Baculovirus IAP Repeat (BIR) domains (55). The schematic structure of mammalian IAP family is shown in Figure 2.7.

The mechanism of IAPs is involved with blocking of apoptotic events. In 1998, Deveraux et al. have shown that XIAP, cIAP1 and cIAP2 can block cytochrome c-induced activation of caspase-9, thus preventing the activation of caspases -3, -6 and -7. By contrast, IAPs can not block caspase-3 activation induced by caspase-8. However, the IAPs bind to and inhibit the enzymatic activity of caspase-3 following its activation, thereby preventing the proteolytic cascade initiated by caspase-8 (56, 57).

The regulators of IAPs are such as XAF1 (XIAP-Associated Factor 1), Smac/DIABLO, and Omi/HtrA2. Smac/DIABLO (Second mitochondrial activator of caspases, or Direct IAP Binding protein with Low PI) is a 25-kDa mitochondrial protein (55) that can be released from the mitochondria when cells are exposed to apoptotic stimuli. Smac/DIABLO is shown to bind and inhibit IAPs, thereby accelerating apoptosis (42).

2.9 Reactive oxygen species (ROS)

ROS, at present, are very attractive because of their activities not only about oxidative stress but also about signaling. Moreover, other than mitochondria, the source of ROS generation which is the NADPH oxidase (Nox) family members in plasma membrane has been studied intensively (58).

Mitochondria, the sites of electron transport chain (or respiratory chain) and oxidative phosphorylation, are function for energy (ATP) production.

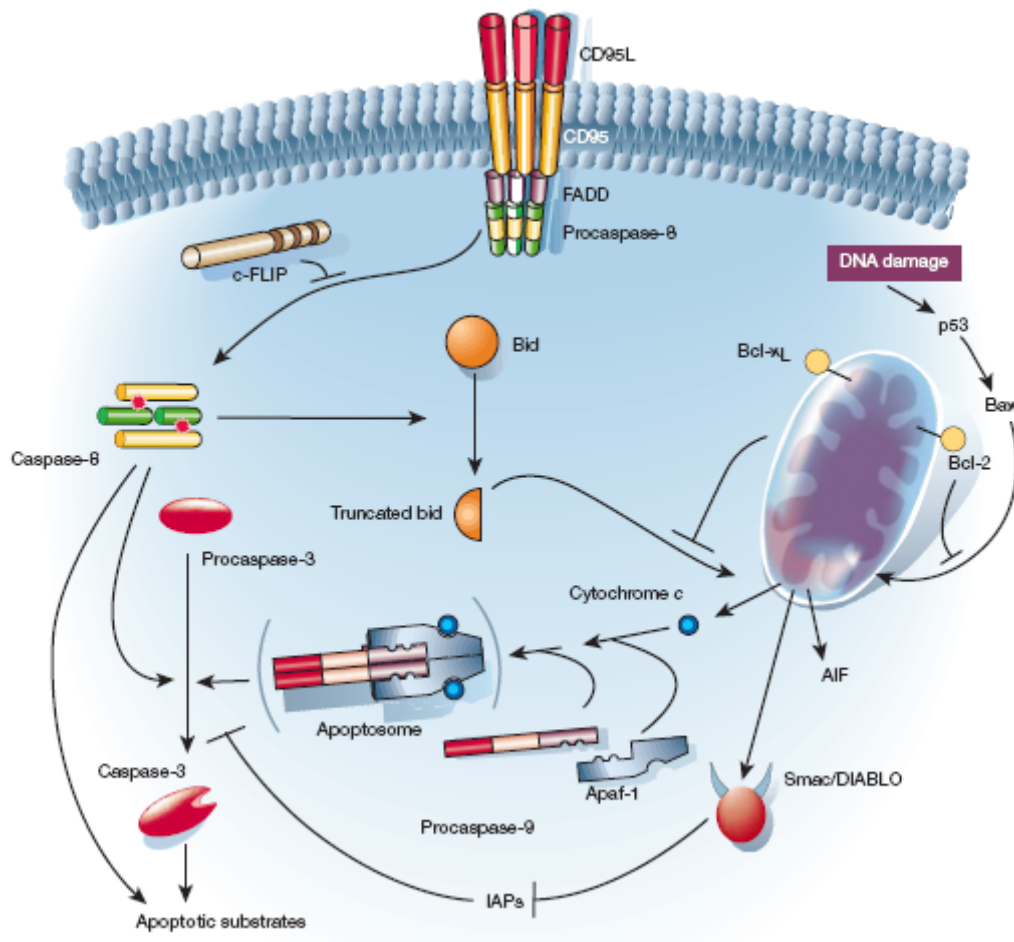


Figure 2.6 Two major apoptotic pathways in mammalian cells (45).

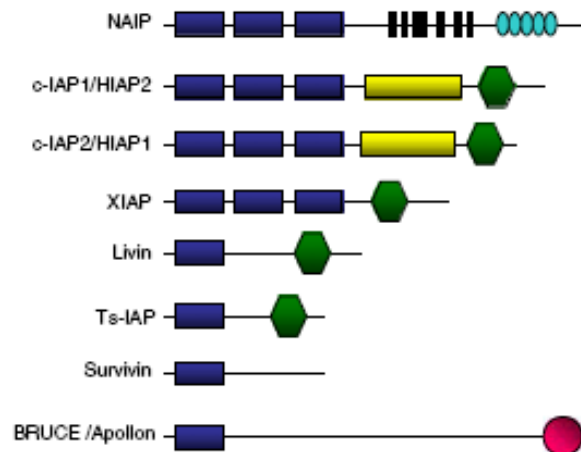


Figure 2.7 Domain structure of the IAP family. The presence of at least one BIR domain (indicated by blue boxes) is the defining characteristic of the IAP family. Some IAPs contain a RING-zinc finger domain at the carboxy terminus (indicated by green hexagon). cIAP1 and cIAP2 both possess a caspase recruitment domain (CARD) (indicated by yellow boxes) in the linker region between the BIR domains and the RING (Really Interesting New Gene) domain. NAIP possesses a nucleotide binding site domain (indicated by black stripes), as well as a leucine-rich repeat domain (indicated by aquaovals). BRUCE contains a UBC, ubiquitin-conjugation, domain (indicated by red circle) (55).

Nonetheless, mitochondria are also the sites for ROS generation because of rarely efficient 100% electron transfer. In the terminal step in electron transport, O_2 serves as the final electron acceptor for cytochrome oxidase that catalyzes the four-electron reduction of O_2 to H_2O . Partially reduced and highly reactive metabolites of O_2 may be formed during these electron transfer reactions. These O_2 metabolites include superoxide anion ($O_2^{\cdot-}$) and hydrogen peroxide (H_2O_2), formed by one- and two-electron reductions of O_2 , respectively. In the presence of transition metal ions, the even more reactive hydroxyl radical (OH^{\cdot}) can be formed. These partially reduced metabolites of O_2 are often referred to as “reactive oxygen species” (ROS) due to their higher reactivities relative to molecular O_2 (59, 60).

As discussed above, the plasma membrane is one of the sites for ROS generation as well. In phagocyte, the NADPH oxidase in plasma membrane serves a specialized function in host defense against invading microorganisms. This multicomponent enzyme catalyzes the one-electron reduction of O_2 to $O_2^{\cdot-}$, with NADPH as the electron donor through the transmembrane protein cytochrome b_{558} (a heterodimeric complex of gp91^{phox} and p22^{phox} protein subunits). The transfer of electron occurs from NADPH on the inner aspect of the plasma membrane to O_2 on the outside (Figure 2.8). During phagocytosis, the plasma membrane is internalized as the wall of the phagocytic vesicle, with what was once the outer membrane surface now facing the interior of the vesicle. This targets the delivery of $O_2^{\cdot-}$ and its reactive metabolites internally for localized microbicidal activity (60).

In non-phagocytic cells, recent studies have suggested that NADPH oxidase components have been detected in cells such as vascular smooth muscle cells (61, 62), fibroblast cells, and mesangial cells (60). However, NADPH oxidase components are similar, but not identical, to the classical phagocytic NADPH oxidase (62).

ROS have been traditionally regarded as toxic by-products of metabolism. When cellular production of ROS overwhelms its antioxidant activity, damage to cellular macromolecules such as lipid, protein, and DNA may succeed. Thus, oxidative stress has been implicated in a large number of human diseases including atherosclerosis, pulmonary fibrosis, cancer, neurodegenerative diseases, and aging. Interestingly, accumulating evidence suggests that ROS are not only toxic by-product

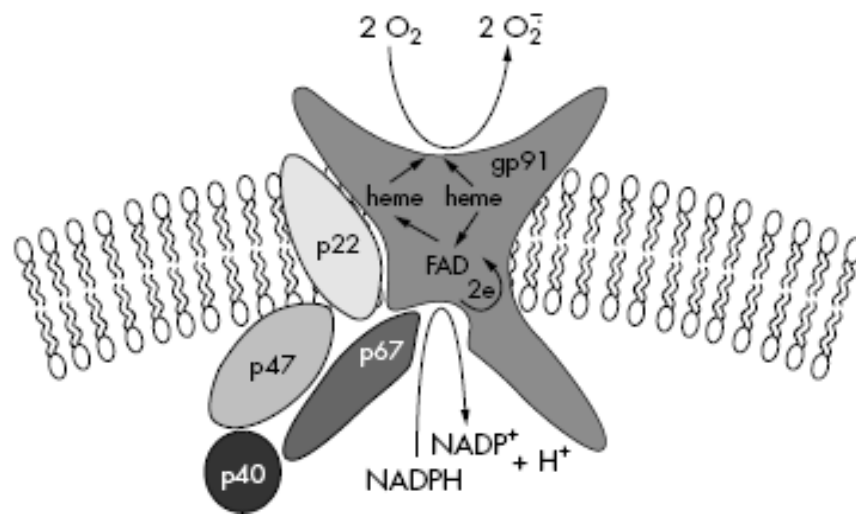


Figure 2.8 Composition of the NADPH oxidase in phagocytic cells (61).

of cellular metabolism but also essential participants in cell signaling and regulation such as cell proliferation, cell hypertrophy, or apoptosis (58, 60). For clear insight of the role of ROS, Finkel and Holbrook have reviewed and shown the picture that illustrated the source of ROS and level of ROS that have affect to cell homeostasis as shown in Figure 2.9 (63).

ROS which are involved in apoptosis have been reported (64). For instances, blastocoele fluid containing hydrogen peroxide is toxic to malignant pretrrophectodermal cells (ECa 247) by induction of apopsis, but catalase can inhibit such toxic (65). ROS participating in paclitaxel cytotoxicity was shown that accumulation of hydrogen peroxide is an early and crucial step for paclitaxel-induced cancer cell death before the commitment of the cells into apoptosis (66).

Mechanism of ROS-induced apoptosis has been investigated. For examples, tumor necrosis factor-related apoptosis-inducing ligand (TRAIL/Apo2L) – induced HeLa cells apoptosis is mediated by ROS-activated p38 MAP kinase followed by caspase activation (67); TRAIL-resistant human colon carcinoma cell lines (RKO, HT29, and HCT8) are sensitized to TRAIL-induced apoptosis by mitochondrial-derived ROS inducing from carbonyl cyanide m-chlorophenylhydrazone (CCCP), the uncoupler of oxidative phosphorylation. In the presence of mitochondrial-derived ROS, TRAIL induces mitochondrial release of Smac/DIABLO and activation of XIAP through caspase-9-independent activation of caspase-3 (68); α -Lipoic acid-induces apoptosis in human lung epithelial cells (H460) by induction of ROS generation from mitochondria. Down-regulation of Bcl-2 protein by mitochondrial ROS, especially hydrogen peroxide, affects to caspase-9 activation because of α -lipoic acid-induced apoptosis in H460 via the mitochondrial death pathway (69).

From these reports, ROS are one of factors that induce apoptosis. Such ROS have the role of regulation. Therefore, investigation of ROS whether they are involved in apoptosis or about their role will be worth to clarify the death pathway and the factors involved. Modulating of such pathway may protect from cell death.

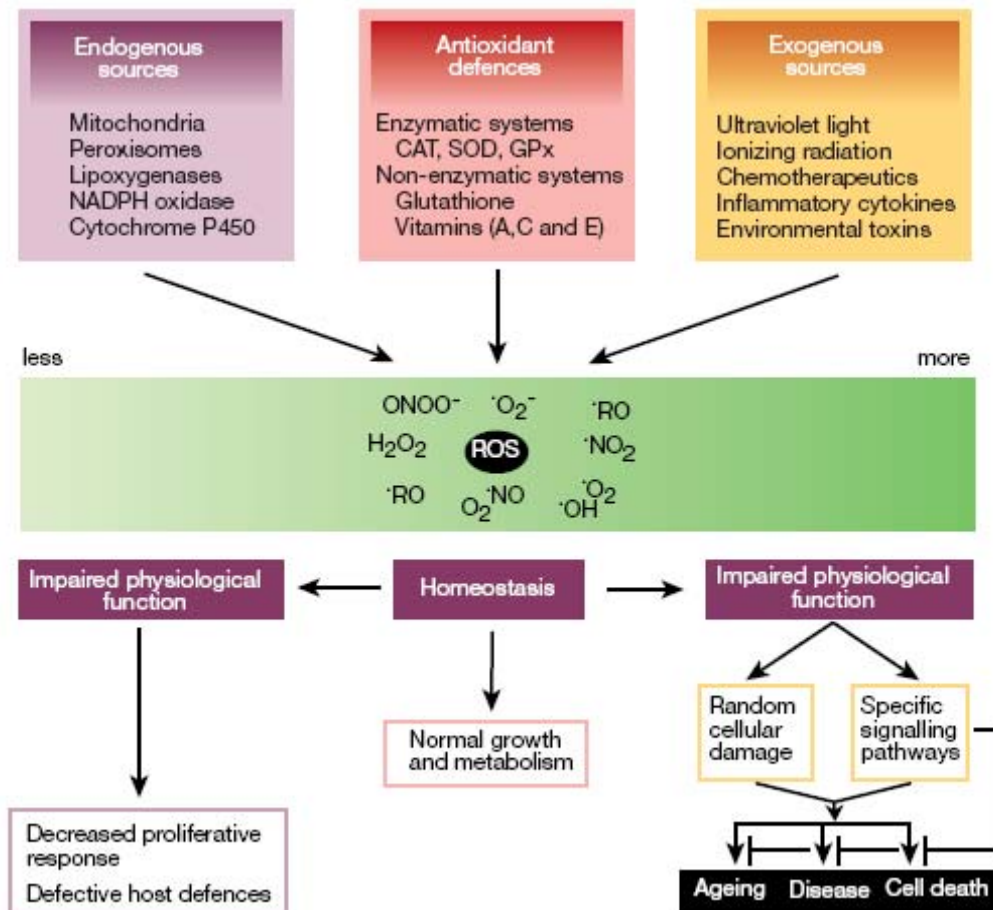


Figure 2.9 Proposed effects of ROS level to cell homeostasis (63).

2.10 Antioxidant from *Asparagus racemosus*

The plant *Asparagus racemosus* Willd (family Asparagaceae; Liliaceae), is commonly called, in India, Satavari, Satawar or Satmuli in Hindi; Satavari in Sanskrit; Shatamuli in Bengali, etc (70). In Thai, it is called, for example, Sam-Sib (สามสิบ), Sam-Roi-Rak (สามร้อยราก) (71). The plant is a spinous under-shrub, with tuberous, short rootstock bearing numerous succulent tuberous roots (30-100 cm long and 1-2 cm thick) that are silvery white or ash coloured externally and white internally (70).

In 2007, Bopana and Saxeba reviewed of the pharmacological applications of *Asparagus racemosus* (AR) that are phytoestrogenic effect, effect on neurodegenerative disorders, anti-diarrhoeal effects, anti-dyspepsia effects, adaptogenic effects, cardio protective effects, anti-bacterial effects, immunoadjuvant effects, and anti-tussive effects. AR is applied in two major forms as methanolic extract and aqueous extract and the products of AR are in the preparations such as root extract in tablet, root powder in tablet, root extract in syrup (70).

AR has many biological activities including the anti-oxidant activity. Several reports of antioxidant effect of AR were shown and can be classified into two groups in term of the type of extracting solvent: organic or aqueous solvent. For the methanolic extract, Sairam et al. reported in 2003 that AR methanolic extract given orally to rat with cold restraint stress alleviated stress-induced gastric ulcer with mark decrease in lipid peroxidase product (malondialdehyde) and increase in catalase activity (72). Bhatnagar et al. reported in 2005 that AR, methanolic extract, was effective in reducing gastric ulcer in indomethacin-treated gastric ulcerative rats. They found that superoxide dismutase, catalase, and ascorbic acid, increased significantly, whereas a significant decrease in lipid peroxidation was observed (73). Recently, in 2008, Hayes et al. have shown that the methanolic extract from the root of AR has ten steroidal saponins when they were isolated by RP-HPLC and characterized by spectroscopic (NMR) and spectrometric (LCMS) methods (74). However, other than these saponin, Wiboonpun also found the antioxidant compound from dichloromethane extract of AR root and named it as racemofuran in 2004 (75).

For the aqueous extract, Kamat et al reported in 2000 that crude extract and a purified aqueous fraction (polysaccharide component, MW 2000 kDa), extracting by

petroleum ether and then hot water, have an anti-oxidant effect in membrane damage induced by γ -radiation in rat liver mitochondria by protecting against radiation-induced loss of protein thiols and inactivation of superoxide dismutase (76). Recently, in 2008, Agrawal et al. have shown that the aqueous extract of AR root, extracting by soaking the powdered roots in water for 24 h, showed the positive results of the presence of saponins and anthraquinones. Furthermore, pretreatment of Wistar rats with such extract leads to an amelioration of oxidative stress and hepatotoxicity brought about by the treatment with diethylnitrosamine (77).

The antioxidant effect of AR root extract is confirmed by many reports that it attracts to use as antioxidant from herb for protecting cells from apoptosis which is related with ROS generation. Using herb provides the alternative way for scavenging of ROS and later it would be useful for application in therapy.

CHAPTER III

MATERIALS AND METHODS

3.1 Chemicals and reagents

1. Lipofectamine[™] reagent (LF) (Lot no. 413303; 671244, Invitrogen, Carlsbad, CA, USA)
2. RPMI 1640 medium (Invitrogen, Carlsbad, CA, USA)
3. Dulbecco's phosphate buffered saline (DPBS) (Sigma Chemical, St. Louis, MO)
4. Fetal bovine serum (FBS) (Invitrogen, Carlsbad, CA)
5. L-glutamine (Sigma Chemical, St. Louis, MO)
6. Penicillin / Streptomycin (Sigma Chemical, St. Louis, MO)
7. 0.05% Trypsin-EDTA (Invitrogen, New York, USA)
8. Hoechst 33342 (Sigma Chemical, St. Louis, MO)
9. CaspGLOW[®] caspase-8 assay kit (Biovision, Mountain View, CA)
10. CaspGLOW[®] caspase-9 assay kit (Biovision, Mountain View, CA)
11. Pan-caspase inhibitor, z-VAD-fmk (Biovision, Mountain View, CA)
12. Caspase-8 inhibitor, z-IETD-fmk (Biovision, Mountain View, CA)
13. Caspase-9 inhibitor, z-LETD-fmk (Biovision, Mountain View, CA)
14. BCA[™] protein assay kit (Pierce, Rockford, IL)
15. Mn (III) tetrakis (4-benzoic acid) porphyrin chloride (MnTBAP) (Calbiochem, La Jolla, CA)
16. Catalase (CAT) (Roche Diagnostics, Indianapolis, IN)
17. Sodium formate (SF) (Sigma Chemical, St. Louis, MO)
18. Diphenylene iodonium (DPI) (Sigma Chemical, St. Louis, MO)
19. Rotenone (ROT) (Sigma Chemical, St. Louis, MO)
20. Dihydroethidium bromide (DHE) (Sigma Chemical, St. Louis, MO)
21. Dichlorofluorescein diacetate (DCF-DA) (Sigma Chemical, St. Louis, MO)

22. Oleanolic acid (OA) (Lot no. 093K0961, Sigma Chemical, St. Louis, MO)
23. Diosgenin (DG) (Lot no. 037K1176, Sigma Chemical, St. Louis, MO)
24. 2,2-Diphenyl-1-picrylhydrazyl (DPPH) (Sigma Chemical, St. Louis, MO)
25. Ascorbic acid (AA) (Fluka, Buchs SG, Switzerland)
26. Hexane (Lab-Scan, Bangkok, Thailand)
27. Ethyl acetate (Fisher, Leicestershire, UK)
28. Dichloromethane (Lab-Scan, Bangkok, Thailand)
29. Chloroform (Lab-Scan, Bangkok, Thailand)
30. Methanol (Fisher, Leicestershire, UK)
31. Ethanol (Lab-Scan, Bangkok, Thailand)
32. PCR markers (G3161) (Promega, Madison, WI)
33. Monoclonal antibody against FLIP (Dave-2) (Alexis Biochemical, San Diego, CA)
34. Peroxidase-conjugated anti-Myc antibody (9E10) (Santa Cruz Biotechnology, Santa Cruz, CA)
35. Anti-Myc agarose beads (Santa Cruz Biotechnology, Santa Cruz, CA)
36. Protein A-agarose (Santa Cruz Biotechnology, Santa Cruz, CA)
37. β -actin antibody (Sigma Chemical, St. Louis, MO)
38. Ubiquitin antibody (Sigma Chemical, St. Louis, MO)
39. Peroxidase-conjugated secondary antibody (Sigma Chemical, St. Louis, MO)
40. Supersignal West Pico Chemiluminescent (Pierce, Rockford, IL)

3.2 Cell lines

1. HTB-177 (NCI-H460) (American Type Culture Collection, Manassas, VA, USA)
2. FLIP-, Bcl-2-, SOD- or GPx-overexpressing H460 cells (Professor Dr. Yon Rojanasakul, West Virginia University, WV, USA)

3.3 Equipment

1. Autospot (Camag[®] Limonat V, Switzerland) , scanner, camera
2. Centrifuger (Hermle[®] Z300K, Hermle Laboratechnik, Germany)
3. Class IIA/B3 biological safety cabinet (Forma Scientific, Marietta OH)
4. CO₂ incubator (Thermo Electron[®] , Marietta, OH)
5. Fluorescence microscopy (Leica[®] DMIL, Wetzlar, Germany)
6. Freezer -80 °C (Reveo[®] , Thermo Electron, Asheville, NC)
7. Imaging densitometer with automated digitizing software UN-SCAN-IT[®] (Silk Scientific Inc., Orem, UT, USA).
8. Multiwell plate reader (FLUOstar[®] OPTIMA, BMG Labtech Inc., Durham, NC)
9. Transmission electron microscope (Model JEM-2100[®] , JEOL, Tokyo, Japan)
10. UV spectrophotometer (Eppendorf[®] Biophotometer, Westbury, NY)
11. UV transilluminator (UV & Fluorchem[™] SP with Software Alpha Innotech, Alexandria, VA)
12. Water bath (Thermo Electron[®] , Marietta, OH)
13. X-ray film processor (ALLPRO Imaging[®] 100 Plus, Melville, NY)
14. Zetasizer[®] (Model Nano ZS series, Malvern instrument, Worcestershire , UK)

3.4 Methods

3.4.1 Characterization of Lipofectamine[™] (LF)

3.4.1.1 Transmission electron microscopy (TEM)

Transmission electron microscopy was used to examine vesicle type and lamella structure of LF. The microscopic appearance of the vesicles was examined using negative staining TEM. A former-coated grid was floated on a droplet of sample on parafilm for 5-10 min to permit adsorption of the sample. Most of the liquid was blotted with a filter paper. The grid was then transferred onto a nearby drop of 2% uranyl acetate (negative stain) for 15 seconds, blotted with a filter paper, and then air-dried for 1 min and kept in the desiccators prior to use.

3.4.1.2 Particle size

A Zetasizer[®] Nanoseries was used to determine the size and size distribution of LF by measuring the rate of fluctuation in laser light intensity scattered by particles as they diffuse through the LF dispersion at 25°C. The measurement was performed with the samples in deionized water (100 µg/ml). The intensity of scattered light was detected by photomultiplier at an angle of 173 degrees. The measurements were done in triplicate.

3.4.1.3 Surface charge

A Zetasizer[®] Nanoseries was used to examine the charge and zeta potential of LF. The measurement was performed with the samples in deionized water (100 µg/ml) at room temperature. The zeta-potential was detected by the movement of a charged surface with respect to an adjacent liquid phase and the mean value of zeta potential from three determinations was reported with standard deviation.

3.4.2 Cell culture

Cells were cultured in RPMI-1640 medium supplemented with 5% fetal bovine serum (FBS) and 2 mM L-glutamine, 100 units/ml of penicillin and 100 µg/ml of streptomycin. Cells were grown in a humidified atmosphere of 5% CO₂ at 37°C until they reached over 60% confluence. Then cells were passaged by the use of a solution containing 0.05% trypsin and 0.5 mM EDTA.

3.4.3 Apoptosis assay

Cells were incubated with 10 µg/ml of the Hoechst[®] 33342 dye at 37 °C for 30 min. Analyzing for apoptosis was done by scoring the percentage of cells having intensely condensed chromatin and/or fragmented nuclei by fluorescence microscopy. Approximately 1,000 nuclei from random fields were analyzed for each sample. The percentage of apoptosis was calculated as (apoptotic nuclei/total nuclei) x 100 (%).

3.4.4 DNA ladder assay

Cells were washed once with cold phosphate buffer saline (PBS) and lysed with a lysis buffer (5 mM Tris-HCl, pH 8.0; 20 mM EDTA; 0.5% Triton X-100) on ice for 45 min and centrifuged at 14,000 g at 4 °C for 30 min. DNA in the supernatant was extracted twice with 25:24:1 (v/v)-phenol/chloroform/isoamyl alcohol and once with chloroform, then precipitated with ethanol and salt. The DNA pellet was washed once with 70% ethanol and resuspended in TE buffer, pH 8.0, containing 100 µg/ml RNase at 37 °C for 2 h. The DNA fragments were separated by gel electrophoresis at 20 V for 18 h through a 2% Tris borate EDTA agarose gel containing 1 µg/ml ethidium bromide. The separated DNA fragments were examined under a UV transilluminator and photographed.

3.4.5 Caspase activity assay

Caspase activity was determined by fluorometry using CaspGLOW[®] caspase-8 and caspase-9 assay kits. Cells were incubated with 3 µl/ml of CaspGLOW[®] caspase-8 or caspase-9 at 37 °C for 30 min. Subsequently, cells were washed with CaspGLOW[®] wash buffer twice and then added with CaspGLOW[®] wash buffer. Finally, caspase-specific fluorescent products were detected on a multiwell plate reader at the excitation and emission wavelengths of 400 nm and 530 nm, respectively.

3.4.6 ROS detection

Fluorometric analysis of superoxide and peroxide formation was performed using DHE and DCF-DA as fluorescent probes. Cells were incubated with the probes (10 µM) at 37 °C for 30 min, after which they were washed, resuspended in PBS, and immediately analyzed for fluorescence intensity using a multiwell plate reader at the excitation/emission wavelengths of 485/610 nm for DHE measurements and at 485/530 nm for DCF measurements.

3.4.7 Western blotting

Cell extracts were performed by incubating the cells in lysis buffer containing 20 mM Tris-HCl, pH 7.5, 1% Triton X-100, 150 mM sodium chloride, 10% glycerol, 1 mM sodium orthovanadate, 50 mM sodium fluoride, 100 mM

phenylmethylsulfonyl fluoride, and a protease inhibitor mixture for 30 min on ice. After insoluble debris was pelleted by centrifugation at 14,000 *g* for 15 min at 4 °C, the supernatants of which were collected and analyzed for protein content using bicinchoninic acid protein assay. Proteins (20 µg) were resolved on a 10% sodium dodecyl sulfate-polyacrylamide gel electrophoresis (SDS-PAGE) and transferred onto 0.45-µm nitrocellulose membranes. The transferred membranes were blocked for 1 h in 5% non-fat dry milk in TBST (25 mM Tris-HCl, pH 7.4, 125 mM NaCl, 0.05% Tween 20) and incubated with appropriate primary antibodies at 4 °C overnight. Membranes were washed three times with TBST for 10 min and incubated with peroxidase-conjugated secondary antibodies for 1 h at room temperature. The immune complexes were detected by chemiluminescence and quantified by an imaging densitometer with automated digitizing software. Mean densitometry data from independent experiment were normalized to the control.

3.4.8 Plasmids and stable transfection

FLIP, Bcl-2, superoxide dismutase (SOD), and glutathione peroxidase (GPx) plasmids were generously provided by Dr. Christian Stehlik (Northwestern University, Chicago, IL). Authenticity of the plasmid constructs was verified by DNA sequencing. Stable transfectants were generated by culturing H460 cells in a 6-well plate until they reached 80% confluence. One microgram of cytomegalovirus-neo vector and 15 µl of LF reagent with 2 µg of FLIP, Bcl-2, SOD, GPx, or control pcDNA3 plasmid were used to transfect the cells in the absence of serum. Ten hours later, the medium was replaced with culture medium containing 5% FBS, and approximately 36 h after the beginning of the transfection, the cells were digested with 0.03% trypsin and the cell suspensions were plated onto 75-ml culture flasks. The cells were cultured for 4 weeks with G418 selection (400 µg/ml). Resistant transfectants were isolated using cloning cylinders and transferred for expansion and analysis by Western blotting. Stable transfectants were grown in G418-free RPMI medium for at least two passages before each experiment.

3.4.9 DPPH assay

Antioxidant sample solution in methanol (200 μ l) was added to 1400 μ l of a 6×10^{-5} mol/L methanol DPPH \cdot solution. The decrease in absorbance was determined at 515 nm at 0 min, 1 min and every 15 min until to 60 min. The exact DPPH \cdot concentration in the reduction medium was calculated from a calibration curve. The percentage of DPPH \cdot remaining at 60 min was determined and the values were plotted as a function of the molar ratio of antioxidant to DPPH \cdot . Antioxidant activity was defined as the amount of antioxidant necessary to decrease the initial DPPH \cdot concentration by 50% (78).

3.4.10 Gene delivery

H460 cells were grown for 24 h until they reached 80% confluence before the transfection. The plasmid DNA of green fluorescent protein (GFP) as a reporter plasmid was diluted in RPMI and LF was also diluted in RPMI. They were combined and incubated at room temperature for 15-20 min. The cultured medium was removed and cells were washed once with PBS. Then, cells were transfected with the lipoplexes for 4 h. After that, transfection medium was replaced with cultured medium. Cells were cultured for an additional 48 h. The level of gene expression was determined at 24 and/or 48 h by using fluorescent microscope and microplate reader for detection of GFP (7).

3.4.11 Investigation of LF-induced apoptosis

3.4.11.1 Investigation of LF-induced apoptosis of H460 cells by varying concentration of LF or varying treatment time

Cells were seeded in 96-well plate with 3×10^4 cells/well in 100 μ l of culture medium and grown for 24 h. The subconfluent (80%) monolayer of cells was washed once with PBS and then once with RPMI. Subsequently, 100 μ l of RPMI was added and cells were treated with various concentrations of LF for 6 h. or with various time intervals with LF (20 μ g/ml). Untreated cells were used as control. Apoptosis was determined by Hoechst 33342 assay as mentioned above.

3.4.11.2 Analysis for DNA fragmentation in H460 cells treated with LF

Cells were seeded in 6-well plate with 0.5×10^6 cells/well in 3 ml of culture medium and grown for 24 h. The subconfluent monolayer of cells was washed once with PBS and then once with RPMI. Subsequently, 1,000 μ l of RPMI was added and cells were treated with various concentrations of LF for 6 h. Untreated cells were used as control. DNA fragmentation was analyzed by DNA ladder assay as mentioned above.

3.4.11.3 Investigation of LF-induced H460 cells apoptosis in the presence or absence of caspase inhibitors

Cells were seeded in 96-well plate with 3×10^4 cells/well in 100 μ l of culture medium and grown for 24 h. The subconfluent monolayer of cells was washed once with PBS and then once with RPMI. Subsequently, 100 μ l of RPMI was added and cells were untreated or pretreated with 10 μ M of pan-caspase inhibitor (z-VAD-fmk), caspase-8 inhibitor (z-IETD-fmk), or caspase-9 inhibitor (z-LEHD-fmk) for 1 h, and then treated with LF (20 μ g/ml) for 6 h. Untreated cells were used as control. Apoptosis was determined by Hoechst 33342 assay as mentioned above.

3.4.11.4 Investigation of LF-induced apoptosis in FLIP- or Bcl-2-overexpressing cells

H460 cells stably transfected with FLIP, Bcl-2, or control pcDNA3 plasmid were seeded in 96-well plate with 3×10^4 cells/well in 100 μ l of culture medium and grown for 24 h. The subconfluent monolayer of cells was washed once with PBS and then once with RPMI. Subsequently, 100 μ l of RPMI was added and cells were treated with LF (20 μ g/ml) for 6 h. Untreated cells were used as control. Apoptosis was determined by Hoechst 33342 assay as mentioned above.

3.4.11.5 Investigation of caspase activity in H460 cells treated with LF

Cells were seeded in 96-well plate with 3×10^4 cells/well in 100 μ l of culture medium and grown for 24 h. The subconfluent monolayer of cells was

washed once with PBS and then once with RPMI. Subsequently, 100 μ l of RPMI was added and cells were treated with various concentrations of LF for 6 h. Untreated cells were used as control. Caspase-8 and caspase-9 activity was determined by caspase activity assay as mentioned above.

3.4.11.6 Investigation of caspase activity in FLIP- or Bcl-2-overexpressing cells treated with LF

H460 cells stably transfected with FLIP, Bcl-2, or control pcDNA3 plasmid were seeded in 96-well plate with 3×10^4 cells/well in 100 μ l of culture medium and grown for 24 h. The subconfluent monolayer of cells was washed once with PBS and then once with RPMI. Subsequently, 100 μ l of RPMI was added and cells were treated with LF (20 μ g/ml) for 6 h. Untreated cells were used as control. Caspase-8 and caspase-9 activity was determined by caspase activity assay as mentioned above.

3.4.11.7 Detection of FLIP in H460 cells treated with LF by Western blotting

Cells were seeded in 6-well plate with 0.5×10^6 cells/well in 3 ml of culture medium and grown for 24 h. The subconfluent monolayer of cells was washed once with PBS and then once with RPMI. Subsequently, 1,000 μ l of RPMI was added and cells were treated with various concentrations of LF for 6 h. Untreated cells were used as control. FLIP was determined by Western blotting as stated above.

3.4.12 Study of the role of ROS in LF-induced apoptosis

3.4.12.1 Investigation of LF-induced ROS production in H460 cells

Cells were cultured and grown until they reached 80% confluence. Then, cells were washed with PBS once, after which they were scraped and suspended in RPMI. The cells (1×10^6 cells/ml) were treated with LF at various concentrations for 30 min. Untreated cells were used as control. Finally, ROS was detected by fluorometric assay in ROS detection method mentioned above.

3.4.12.2 Investigation of LF-induced ROS production in SOD or GPx overexpressing cells

H460 cells stably transfected with SOD, GPx, or control pcDNA3 plasmid were cultured and grown until they reached 80% confluence. Then, cells were washed with PBS once, after which they were scraped and suspended in RPMI. The cells (1×10^6 cells/ml) were treated with LF (20 μ g/ml) for 30 min. Untreated cells were used as control. Finally, ROS was detected by fluorometric assay in ROS detection method mentioned above.

3.4.12.3 Investigation of the cellular source of ROS production after treatment with LF

Cells were cultured and grown until they reached 80% confluence. Then, cells were washed with PBS once, after which they were scraped and suspended in RPMI. The cells (1×10^6 cells/ml) were untreated or pretreated with 1 μ M of diphenylene iodonium (DPI) or 1 μ M of rotenone (ROT) for 30 min, and then treated with LF (20 μ g/ml) for 30 min. Untreated cells were used as control. Finally, ROS was detected by fluorometric assay in ROS detection method mentioned above.

3.4.12.4 Detection of FLIP in H460 cells treated with LF in the presence or absence of antioxidant (MnTBAP, CAT, SF) by Western blotting

Cells were seeded in 6-well plate with 0.5×10^6 cells/well in 3 ml of culture medium and grown for 24 h. The subconfluent monolayer of cells was washed once with PBS and then once with RPMI. Subsequently, 1,000 μ l of RPMI was added and cells were untreated or pretreated with 100 μ M of MnTBAP, 1,000 units/ml of CAT, or 10 mM of SF for 1 h, and then treated with LF (20 μ g/ml) for 6 h. Untreated cells were used as control. FLIP was determined by Western blotting as stated above.

3.4.12.5 Investigation of LF-induced apoptosis in SOD- or GPx-overexpressing cells

H460 cells stably transfected with SOD, GPx, or control pcDNA3 plasmid were seeded in 96-well plate with 3×10^4 cells/well in 100 μ l of

culture medium and grown for 24 h. The subconfluent monolayer of cells was washed once with PBS and then once with RPMI. Subsequently, 100 µl of RPMI was added and cells were treated with LF (20 µg/ml) for 6 h. Untreated cells were used as control. Apoptosis was determined by Hoechst 33342 assay as mentioned above.

3.4.12.6 Investigation of LF-induced H460 cells apoptosis in the presence or absence of antioxidant (MnTBAP, CAT)

Cells were seeded in 96-well plate with 3×10^4 cells/well in 100 µl of culture medium and grown for 24 h. The subconfluent monolayer of cells was washed once with PBS and then once with RPMI. Subsequently, 100 µl of RPMI was added and cells were untreated or pretreated with 100 µM of MnTBAP, 1,000 units/ml of CAT for 1 h, and then treated with LF (20 µg/ml) for 6 h. Untreated cells were used as control. Apoptosis was determined by Hoechst 33342 assay as stated above.

3.4.13 Antioxidant activity of herbal extracts

3.4.13.1 Successive extraction processes of 5 fractions (AR1-1, 1-2, 1-3, 1-4, 1-5) of *Asparagus racemosus* extracts (ARs)

ARs were obtained from Assoc. Prof. Kornkanok Ingkaninan, Faculty of Pharmaceutical Sciences, Naresuan University. Briefly, extraction processes of AR could be described as follows. AR roots were collected from Tak Province, Thailand. They were dried and minced into powder and then successive extracted with solvents starting from non polar to more polar solvents.

Hexane was the first solvent for extraction of AR roots. The hexane extract was filtered and evaporated by rotary evaporator, after which soft yellow paste was obtained and named as **AR1-1**. The marc of AR roots was extracted further with 95% ethanol. After filtration and evaporation, the 95% ethanol extract with dark brown viscous liquid was named as **AR1-2**. The residual marc was extracted further with water (80°C). After filtration, the aqueous extract was divided into two portions, one of which was evaporated and freeze-dried till brown powder was obtained and named as **AR1-3**. The other portion was added with acetone so that precipitation was occurred and separated out from such solution. Both solution and

precipitate were evaporated and freeze-dried, which were named as **AR1-4** and **AR1-5**, respectively.

3.4.13.2 Standardization of *Asparagus racemosus* extracts (ARs)

(1) Qualitative test by thin layer chromatography (TLC)

TLC was performed on silica gel plates, 60F₂₅₄. In this experiment, two developing systems (I and II) were used. System I was hexane : ethyl acetate (2:1) and system II was chloroform : methanol : water (6.4:5:1). Solutions of oleanolic acid (OA) (0.5 mg/ml) and diosgenin (DG) (0.5 mg/ml) in methanol were prepared and they were known references in system I and II, respectively.

AR samples were prepared as following methods. AR1-1, AR1-2, AR1-3 to 1-5 (10 mg/ml) were dissolved in ethyl acetate, methanol, and water, respectively. All samples were filtered through 0.2- μ m nylon membrane filter before use.

Samples of 8 μ l were spotted by Autospot on the TLC plates. The plates were then air-dried for 5 min. OA and AR1-1 samples were run with developing system I while DG and AR1-2 to AR1-5 samples were run with developing system II. When running was complete, the plates were dried in the oven at 100-110 °C for 5 min., sprayed with anisaldehyde-sulfuric acid reagent around 10 ml, and then heated at 105 °C for 5-10 min. Then, the plates were visualized under white and UV light (366 nm) and TLC fingerprints were photographed. This experiment was performed in duplicate.

(2) Quantitative test for total saponin by spectrophotometry

DG standard curve were prepared as follows. Stock solution of DG (0.5 mg/ml) in methanol was prepared, after which 0, 50, 100, 150, 250 μ l of this stock solution were transferred to tubes and then adjusted to 250 μ l with methanol. A 250- μ l methanol was used as a blank. A 250- μ l portion of 8% w/v vanillin solution in absolute ethanol was added to 250- μ l of sample, which was subsequently mixed with 2.5 ml 72% v/v sulfuric acid, then incubated in water bath at 60 °C for 10 min, and finally cooled in ice bath for 5 min. The absorbance of this mixture was measured at

544 nm. The final concentrations of DG were 8.3, 16.6, 25.0, 41.6 $\mu\text{g/ml}$, respectively. This experiment was performed in triplicate.

AR samples were prepared as followings. AR1-1, AR1-2, AR1-3 to 1-5 (4 mg/ml) were dissolved in dichloromethane, methanol, and water, respectively. All samples were filtered through 0.2- μm nylon membrane filter before use.

A 100- μl portion of AR1-1 stock solution and 50- μl portion of AR1-2, 1-3, 1-4, 1-5 stock solution were adjusted to 250 μl with methanol. Sample was added with 8% w/v vanillin solution, then with 72% v/v sulfuric acid, then incubated in water bath at 60 $^{\circ}\text{C}$ for 10 min, and finally cooled in ice bath for 5 min. The absorbance of this mixture was measured at 544 nm. The final concentrations of AR1-1 and AR1-2 to 1-5 were 133.3 and 66.6 $\mu\text{g/ml}$, respectively. Diosgenin equivalents (DGE) ($\mu\text{g/mg}$ extract) were used to approximately determine the total saponin content of ARs. This experiment was performed in triplicate.

3.4.13.3 Antioxidant activity testing by DPPH assay

(1) Standard curve of DPPH

DPPH assay for antioxidant activity of ARs was carried out as described by Brand-Williams et al. with minor modification (78). Standard curve was prepared from DPPH solution in methanol at concentrations of 10 to 100 μM . The absorbance was measured at 515 nm with methanol as a blank. The standard curve was performed in quadruplicate.

(2) Investigation of reaction kinetic of ascorbic acid and AR1-4

Ascorbic acid (AA) (10 $\mu\text{g/ml}$) and AR1-4 (4 mg/ml) were dissolved in water, 200 μl of which was mixed with 1,400 μl of 60 μM DPPH solution, kept at dark room temperature for a given time. The final concentrations of AA and AR1-4 were 1.25 $\mu\text{g/ml}$ and 0.5 mg/ml, respectively. The absorbance of this mixture was measured at 515 nm. AA was measured every 5 min and AR1-4 was measured every 30 min until they reached the steady state.

(3) Investigation of efficient concentration (EC₅₀) of ascorbic acid and AR1-4

AA (8, 12, 16, 18 µg/ml) and AR1-4 (0.8, 4, 8, 16 mg/ml) were prepared in water, 200 µl of sample was mixed with 1400 µl of 60 µM DPPH solution, kept at dark room temperature. After 5 and 60 min incubation of AA and AR1-4, respectively, the absorbance of this mixture was measured at 515 nm. The final concentrations of AA were 1.0, 1.5, 2.0, 2.25 µg/ml and of AR1-4 were 0.1, 0.5, 1.0, 2.0 mg/ml. AA and AR1-4 experiments were performed in duplicate and triplicate, respectively.

(4) Comparison of antioxidant activity among ARs

AR1-1, AR1-2, AR1-3 to 1-5 (4 mg/ml) were dissolved in dichloromethane, methanol, and water, respectively. Each 200 µl of sample was mixed with 1,400 µl of 60 µM DPPH solution, kept at dark room temperature for 60 min. The final concentrations of AR samples were 0.5 mg/ml. The absorbance of this mixture was measured at 515 nm. This experiment was performed in duplicate.

(5) Investigation of LF-induced apoptosis of H460 cells in the presence or absence of AR1-4

AR1-4 (10 mg/ml) was dissolved in water, and filtered through 0.2-µm nylon membrane filter before use. Cells were seeded in 96-well plate with 3×10^4 cells/well in 100 µl of culture medium and grown for 24 h. The subconfluent monolayer of cells was washed once with PBS and then once with RPMI. Subsequently, 100 µl of RPMI was added and cells were untreated or pretreated with various concentrations of AR1-4 for 1 h and then treated with LF (20 µg/ml) for 6 h. Untreated cells were used as control. Apoptosis was determined by Hoechst 33342 assay as stated above.

3.4.14 Statistical analysis

Data were expressed as mean \pm S.D. of three or more independent experiments. Statistical analysis was performed using an unpaired two-tail student's *t* test at a significance level of $p < 0.05$.

CHAPTER IV

RESULTS AND DISCUSSION

4.1 Characterization of Lipofectamine™ (LF)

4.1.1 Transmission electron microscopy (TEM)

The transmission electron photomicrograph (TEM) of LF is illustrated in Figure 4.1. The existence of the phospholipid bilayers could be evidenced by the lamella structure shown in the TEM, the number of which appeared to be around 4 bilayers. The TEM photomicrograph in this Figure suggests the oligolamellar structure of LF which is the typical characteristics.

4.1.2 Particle size

The particle sizes of LF measured by means of light scattering method are shown in Table 4.1, the mean size of which was 140.5 ± 8.3 nm. This agreed well in the order of magnitude with that reported by Dokka et al. to be 160 nm that was measured by dynamic laser scattering (7).

4.1.3 Surface charge

The zeta potentials of LF are shown in Table 4.2, the mean value of which was confirmed to be cationic with 35.1 ± 4.2 mV. The positive surface charges of LF would ensure repulsive force preventing from aggregation of vesicles.

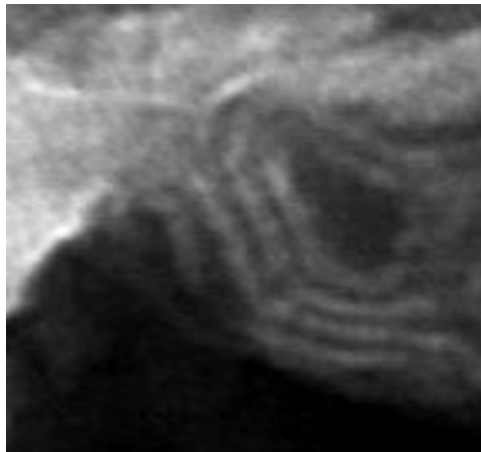


Figure 4.1 TEM photomicrographs of Lipofectamine[™] (LF) obtained by negative staining technique (magnification 150,000x).

Table 4.1 Particle size of Lipofectamine™ (LF)

Samples	Particle size (nm)					
	1	2	3	Mean	SD	%CV
I	144.8	142.4	141.0	142.7	1.9	1.4
II	134.7	133.4	125.7	131.3	4.9	3.7
III	145.1	151.8	145.5	147.5	3.8	2.5
			Total	140.5	8.3	5.9

Table 4.2 Zeta potential of Lipofectamine™ (LF)

Samples	Zeta potential (mV)					
	1	2	3	Mean	SD	%CV
I	41.4	40.6	37.0	39.7	2.3	5.9
II	32.3	34.6	35.7	34.2	1.7	5.1
III	29.4	31.9	33.3	31.5	2.0	6.3
			Total	35.1	4.2	11.8

4.2 Investigation of LF-induced apoptosis

4.2.1 Characterization of LF-induced apoptosis

Aramaki et al. have shown that cationic liposomes induced apoptosis as the primary mode of cell death in various cell types. Their reports showed that stearylamine liposomes induced apoptosis in mouse splenic macrophages, macrophage-like cell line (RAW264.7 cells), and mouse immature B cell line (WEHI 231 cells), while neutral and anionic liposomes did not have such effect (12, 13). For cationic liposome LF, although Dokka et al. have shown that LF caused toxicity in mice administered by intratracheal instillation (7), it has never been reported about underlying mechanism for apoptosis. Therefore, the apoptotic response to LF treatment in H460 cells was investigated. Hoechst 33342 and gel electrophoresis DNA ladder assays were used together to confirm the hallmark of apoptosis that are chromatin condensation and DNA fragmentation, respectively (46).

The results of Hoechst assay showed that treatment of the cells with LF (0-50 µg/ml) caused a dose-dependent increase in apoptosis over control level (Figure 4.2) and condensed nuclei in apoptotic cells exhibited with intense nuclear fluorescence (Figure 4.3). LF also caused apoptosis in time-dependent manner over control level as shown in Figure 4.4. The results suggest that the apoptotic response in dose- or time-dependent could be attributed to LF treatment. Moreover, DNA ladder assay also showed that LF induced a dose-dependent increase in fragmented DNA levels (Figure 4.5), which is consistent with Hoechst assay. These evidences suggest that LF would induce apoptosis in H460 cells.

4.2.2 Investigation of mechanism of LF-induced apoptosis

To study apoptosis, there are two pathways that are well characterized: death receptor (extrinsic) pathway and mitochondrial (intrinsic) pathway. Enzymes that usually involve and that are important in such pathways are caspases. This investigation focused on caspase-8 and caspase-9 which have a role for apoptosis activator or initiator in death receptor pathway and in mitochondrial pathway, respectively. Moreover, FLIP and Bcl-2, regulating factors or proteins, that their function closely relate to caspase-8 and caspase-9 were studied (43, 47).

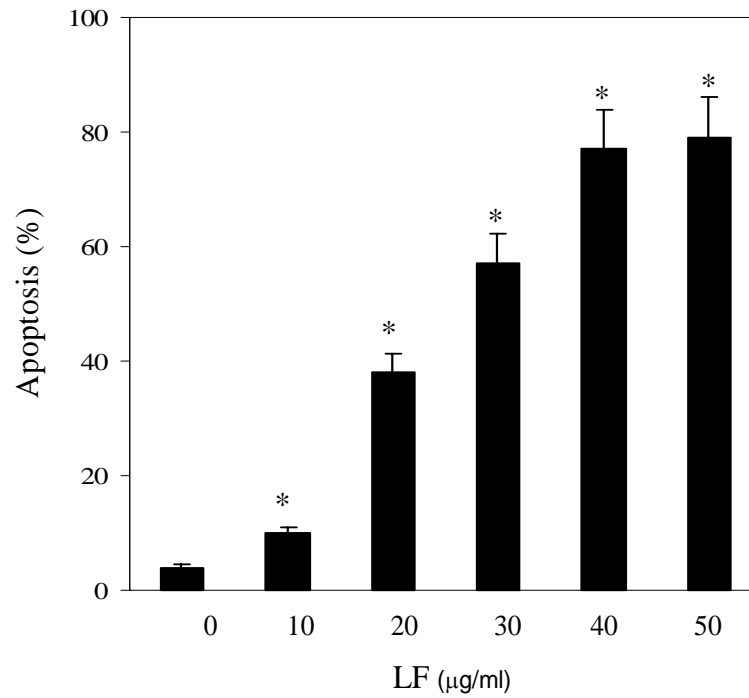


Figure 4.2 Apoptosis of H460 cells treated with various concentrations of LF (0-50 µg/ml) determined by Hoechst 33342 assay after 6 h. Data are mean \pm S.D. (n = 4). *, $p < 0.05$ versus nontreated control.

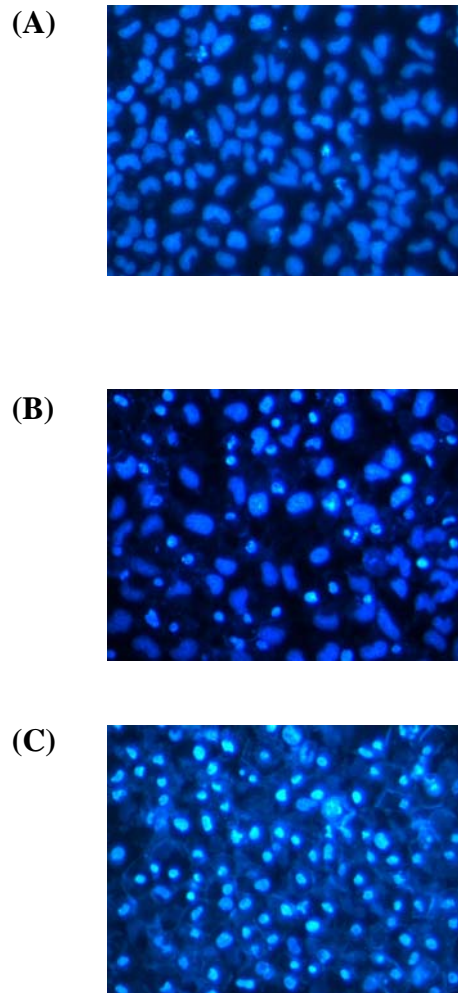


Figure 4.3 Representative fluorescence micrographs of H460 cells treated with LF (0, 20, 40 µg/ml) for 6 h and stained with the Hoechst dye. Apoptotic cells exhibit condensed nuclei with bright nuclear fluorescence (original magnification, 400X).

A, untreated cells as control.

B, cells treated with 20 µg/ml of LF.

C, cells treated with 40 µg/ml of LF.

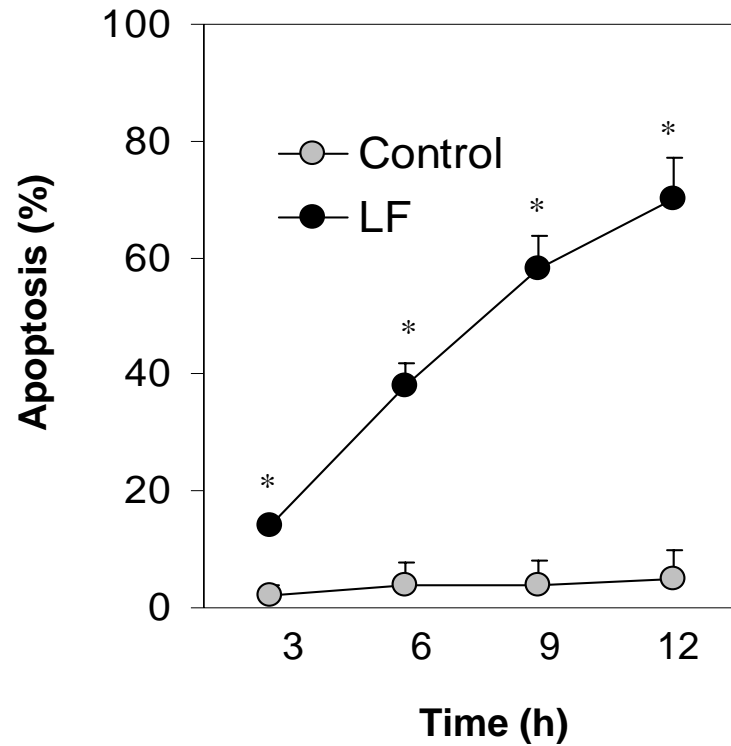


Figure 4.4 Apoptosis of H460 cells treated with LF (20 $\mu\text{g/ml}$) for 3, 6, 9, 12 h determined by Hoechst 33342 assay. Data are mean \pm S.D. (n = 4).

*, $p < 0.05$ versus nontreated control.

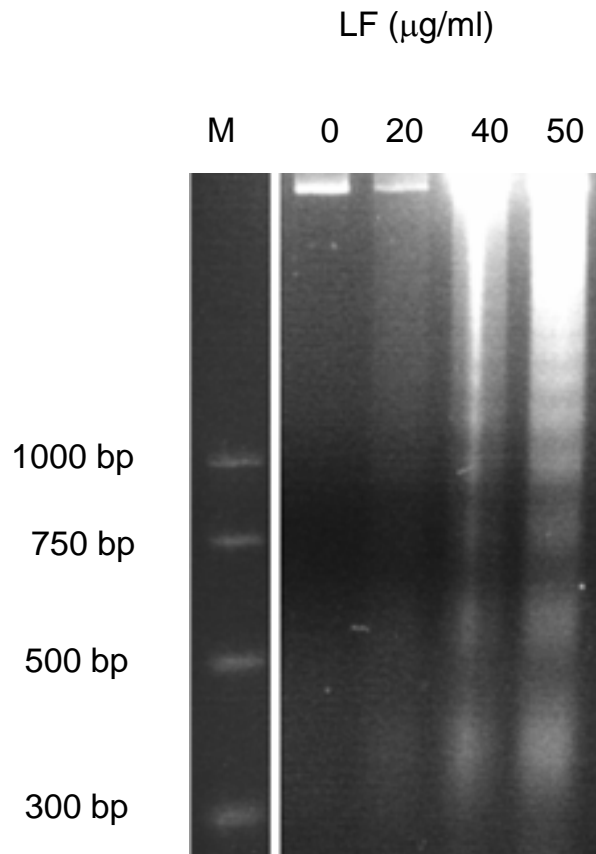


Figure 4.5 DNA fragmentation of H460 cells treated with various concentrations of LF (0-50 $\mu\text{g/ml}$) analyzed by gel electrophoresis DNA ladder assay after 6 h.

The underlying mechanism of LF-induced apoptosis was determined by various techniques such as inhibitors (caspase-8 inhibitor, caspase-9 inhibitor, and pan-caspase inhibitor); FLIP- or Bcl-2-overexpressing cells; caspase activity assay; Hoechst assay; and Western blot analysis.

4.2.2.1 Caspase activity in H460 cells treated with LF

Caspase-8 and caspase-9 activities in LF-treated H460 cells were analyzed to determine the requirement of caspases in the induction of apoptosis by LF. Caspase activity was determined by using caspase inhibitors, CaspGLOW[®] caspase-8 and caspase-9 assay kits, which were conjugated to FITC and irreversibly bind to the activated caspases in apoptotic cells. The caspase-specific fluorescent products can be detected later by fluorometric assay.

Treating H460 cells with the same condition as in LF-induced apoptosis, both caspase-8 and caspase-9 were activated by the LF treatment in a dose-dependent manner (Figure 4.6). As mention above, caspase-8 serves as the initiator caspase of the death receptor pathway whereas caspase-9 serves as the initiator caspase of the mitochondrial pathway (79, 80), these results suggest that the two pathways are involved in the induction of apoptosis by LF.

4.2.2.2 Apoptosis in H460 cells pretreated with caspase inhibitor and treated with LF

To inhibit caspase activity in cells, caspase inhibitors are an alternative choice. H460 cells were pretreated with specific caspase inhibitor or pan-caspase inhibitor and later treated with the same condition as in LF-induced apoptosis. The apoptosis was observed to confirm the involvement of caspases in cell death pathway.

The results in Figure 4.7 showed that specific caspase-8 inhibitor (z-IETD-fmk) and caspase-9 inhibitor (z-LEHD-fmk) exhibited a significant reduction in apoptosis induced by LF, whereas the pan-caspase inhibitor (z-VAD-fmk) almost completely inhibited the apoptotic effect of LF. These results indicate that apoptosis induced by LF is mediated through the caspase-dependent pathways.

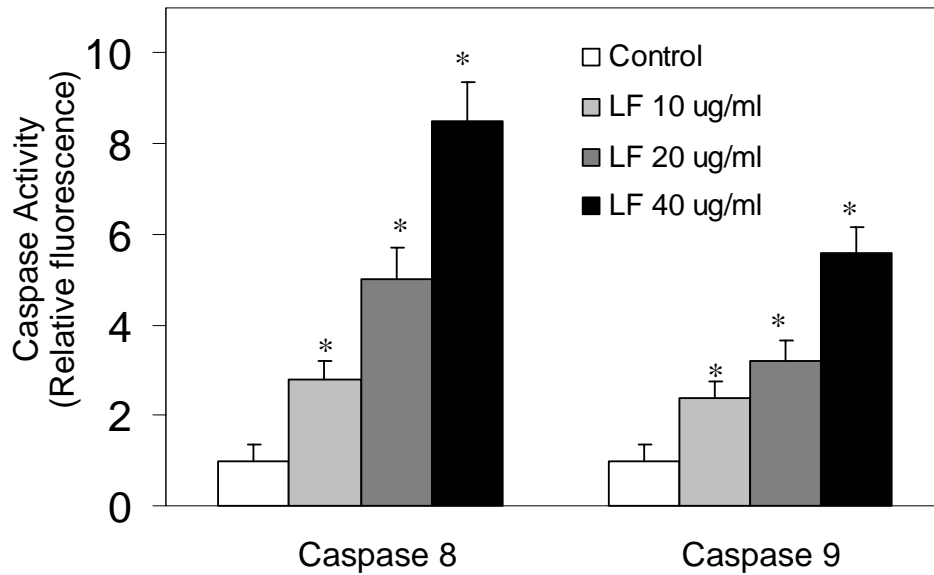


Figure 4.6 Caspase-8 and caspase-9 activities of H460 cells treated with various concentrations of LF (0-40 $\mu\text{g/ml}$) for 6 h analyzed by caspase assay. Data are mean \pm S.D. (n = 4). *, $p < 0.05$ versus nontreated control.

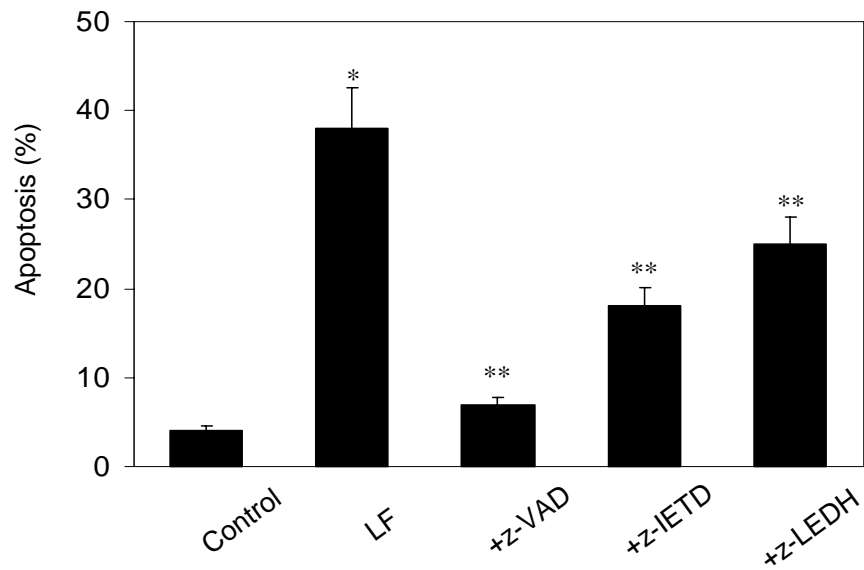


Figure 4.7 Apoptosis of H460 cells treated with LF (20 $\mu\text{g/ml}$) in the presence or absence of 10 μM of pan-caspase inhibitor (z-VAD-fmk), caspase-8 inhibitor (z-IETD-fmk), or caspase-9 inhibitor (z-LEHD-fmk) determined by Hoechst assay after 6 h. Data are mean \pm S.D. (n = 4). *, $p < 0.05$ versus nontreated control; **, $p < 0.05$ versus LF-treated control.

4.2.2.3 Apoptosis in FLIP- or Bcl-2-overexpressing cells treated with LF

H460 cells were stably transfected with FLIP, a known inhibitor of the death receptor pathway (49, 81), Bcl-2, an inhibitor of the mitochondrial death pathway (53, 82, 83), or control pcDNA3 plasmid. FLIP and Bcl-2 gene transfection resulted in a corresponding increase in the protein expression levels over vector-transfected control, as determined by Western blot analysis. The results of FLIP or Bcl-2 overexpression in H460 cells are shown in Appendix A. These cells were used to confirm the involvement of FLIP or Bcl-2 in apoptosis pathway and their effect on LF-induced apoptosis was examined.

These overexpressing cells were treated with the same conditions as in LF-induced apoptosis. The results showed that treatment of the vector-transfected cells with LF caused apoptosis similar to that observed in nontransfected cells, whereas the same treatment produced a significantly lower level of apoptosis in FLIP-overexpressing cells. Apoptosis was also reduced in Bcl-2-overexpressing cells in response to LF treatment; however, such reduction was less pronounced than that observed in FLIP-overexpressing cells (Figure 4.8). These results indicate that apoptosis induced by LF could be effectively inhibited by FLIP. Thus, the death receptor pathway may be the main pathway of cell death signaling.

4.2.2.4 Caspase activity in FLIP- or Bcl-2-overexpressing cells treated with LF

H460 cells stably transfected with FLIP, Bcl-2, or control pcDNA3 plasmid were used. After treated with the same condition as in LF-induced apoptosis caspase-8 and caspase-9 activities were analyzed by caspase assay. This was to examine the relation between regulatory protein (FLIP or Bcl-2) and initiator caspase (caspase-8 or caspase-9). The results showed that FLIP overexpression inhibited LF-induced caspase-8 and caspase-9 activation (Figure 4.9), suggesting the linkage of the two death pathways, i.e., via Bid cleavage, which has previously been shown by other groups using cationic stearylamine liposome (84). Additionally, a review shows about caspase-8 that can activate Bid to tBid and then it moves to the mitochondria and stimulates a release of cytochrome c (42).

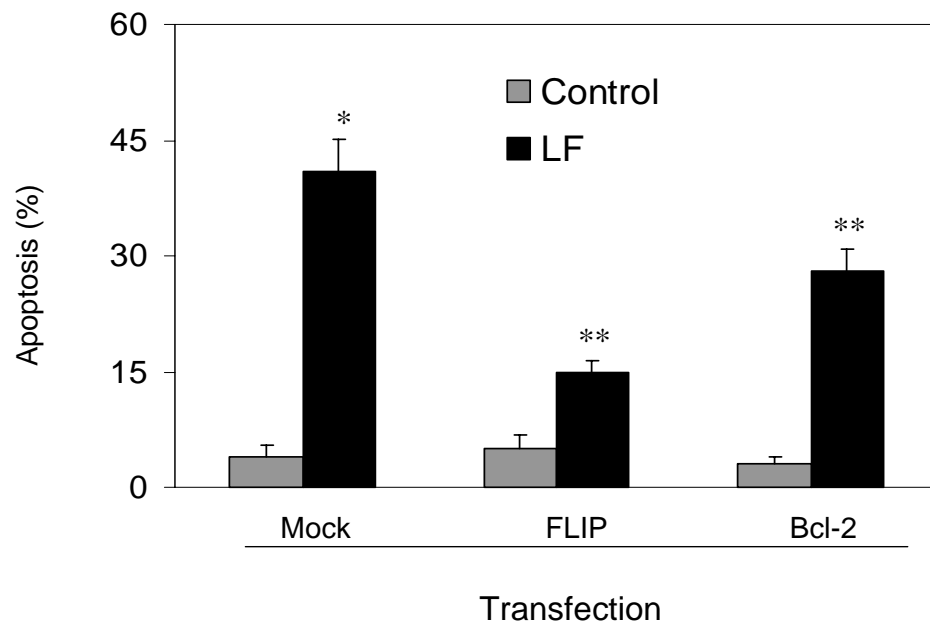


Figure 4.8 Apoptosis of FLIP- or Bcl-2-overexpressing cells treated with LF (20 $\mu\text{g/ml}$) for 6 h analyzed by Hoechst assay. Data are mean \pm S.D. ($n = 4$). *, $p < 0.05$ versus nontreated control; **, $p < 0.05$ versus mock-transfected LF-treated control.

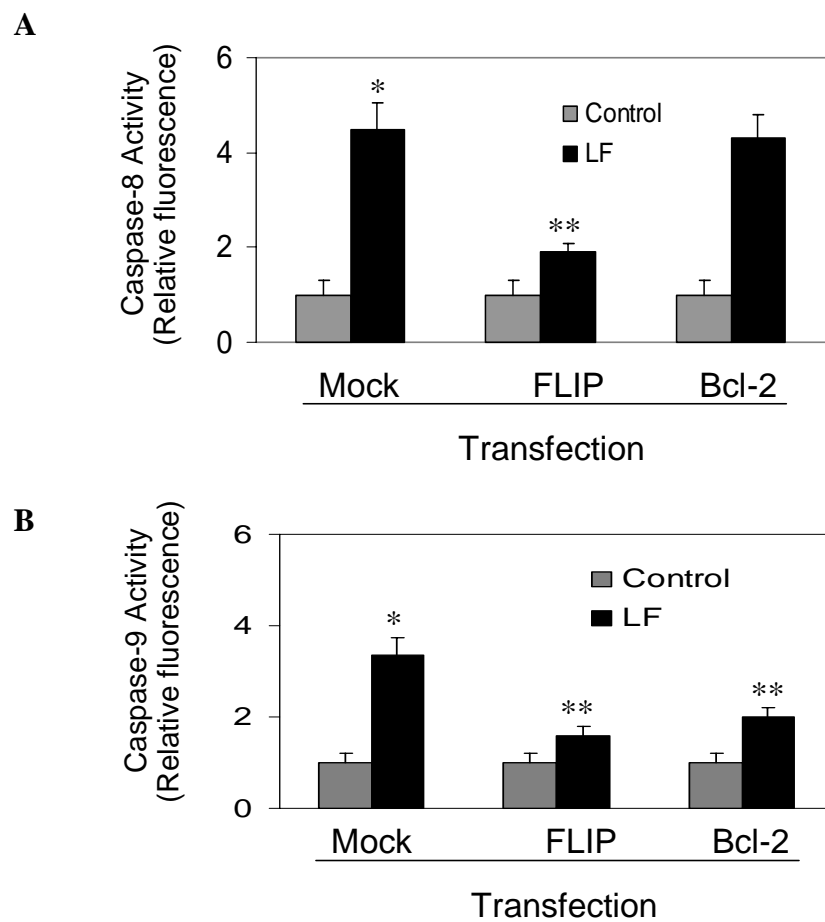


Figure 4.9 Caspase-8 (A) and caspase-9 (B) activation of FLIP- or Bcl-2-overexpressing cells treated with LF (20 μ g/ml) for 6 h analyzed by caspase assay. Data are mean \pm S.D. (n = 4). *, $p < 0.05$ versus nontreated control; **, $p < 0.05$ versus mock-transfected LF-treated control.

Analysis of caspase-8 and caspase-9 activities in Bcl-2-overexpressing cells showed that the increase in Bcl-2 expression had no significant effect on LF-induced caspase-8 activation (Figure 4.9A) but had a partial inhibitory effect on caspase-9 activation (Figure 4.9B). These results suggest that the antiapoptotic effect of Bcl-2 would be mediated downstream of the caspase-8 activation pathway.

4.2.2.5 FLIP detection in H460 cells by Western blotting after treatment by LF

FLIP is the regulator protein involving in death receptor pathway that it can inhibit the recruitment and activation of caspase-8 (FLICE) (48). Down-regulation of FLIP has been shown to sensitize cells to apoptosis in Fas-induced apoptosis (85, 86) or in celecoxib-induced apoptosis (87) through the death receptor pathway. Quantity of FLIP was determined after treatment by LF to observe the relation of the quantity of FLIP and treatment by LF.

Figure 4.10 shows that treatment of the cells with LF caused a dose-dependent decrease in the expression level of FLIP as determined by Western blotting while a similar LF treatment had no significant effect on the expression levels of FADD and Fas, which are known to be involved in the extrinsic death pathway. These results suggest that LF could induce down-regulation of FLIP.

Taking into account together the results of investigation of LF-induced apoptosis, it could be concluded that LF induced apoptosis by activating both the intrinsic (mitochondrial) and extrinsic (death receptor) pathway with the latter pathway playing a more dominant role. The induction of apoptosis through the death receptor pathway involved activation of caspase-8, which was inhibited by the addition of caspase-8-specific inhibitor (z-IETD-fmk) or pan-caspase inhibitor (z-VAD-fmk). Furthermore, overexpression of FLIP, a known inhibitor of the death receptor pathway, strongly inhibited the apoptotic effect of LF, whereas overexpression of Bcl-2, an inhibitor of the mitochondrial death pathway, or addition of caspase-9 inhibitor (z-LEDH-fmk) showed lesser effect to inhibit apoptosis. It is possible that the two death pathways activated by LF are linked. Previous studies by

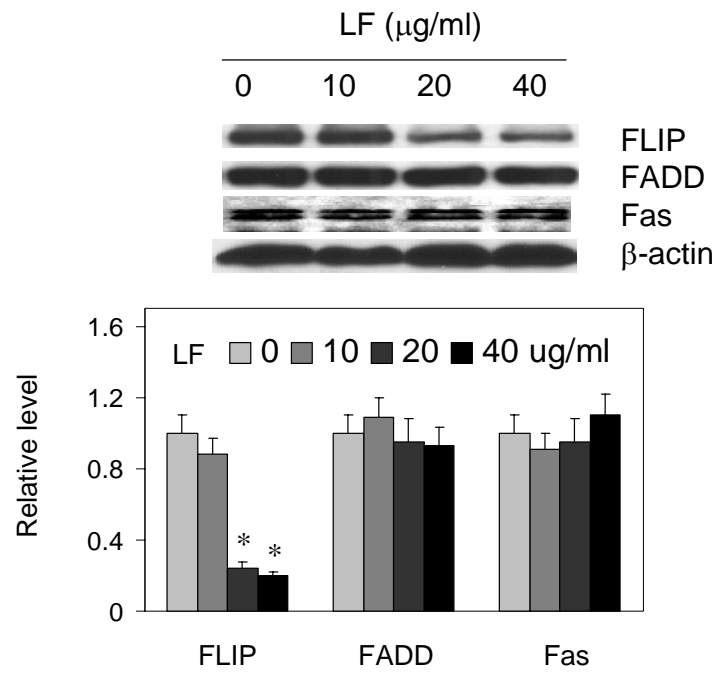


Figure 4.10 FLIP, FADD, and Fas protein expression in H460 cells treated with LF (0-40 $\mu\text{g/ml}$) for 6 h analyzed by Western blotting. Plots are mean \pm S.D. (n = 3). *, $p < 0.05$ versus nontreated control.

Aramaki et al. (12, 13) showed that stearylamine cationic liposome activated caspase-8 and induced Bid cleavage, which led to its translocation into the mitochondria. Such translocation was shown to promote cytochrome c release and subsequent activation of the mitochondrial death pathway (84).

The mechanism by which cationic liposomes activate the death receptor pathway is unknown. Immunoblot analysis of key apoptosis-regulatory proteins involved in the death receptor pathway showed that only FLIP was down-regulated by the LF treatment, whereas FADD and Fas expression levels were relatively unchanged. Ectopic expression of FLIP decreased apoptosis induced by LF, supporting the antiapoptotic role of this protein and suggesting that down-regulation of FLIP by LF is a key event in the death signaling. Overexpression of FLIP also inhibited caspase-8 activation by LF, supporting the role of FLIP. The anti-apoptotic function of FLIP is tightly associated with its expression levels and down-regulation of FLIP is an important mechanism to sensitize cells to death receptor-mediated apoptosis (88).

4.3 Role of ROS to LF-induced apoptosis

There are several reports showing the relation of ROS and apoptosis such as stearylamine liposomes induced apoptosis in RAW264.7 cells in association with ROS production (12), and excessive ROS generation induced by a variety of agents has also been shown to cause apoptotic cell death in various cell types (64, 68, 69). LF also induced cytotoxicity in association with ROS generation (7). To clarify role of ROS and especially the underlying mechanism relating with apoptosis, ROS production in H460 cells treated by LF was studied.

4.3.1 Detection of LF-induced ROS production in H460 cells

ROS production in H460 cells was examined to confirm the report of Dokka et al. (7). The formation of $O_2^{\bullet-}$ and H_2O_2 in the treated cells was detected by spectrofluorometry using fluorescent probes DHE and DCF-DA, respectively. LF-treated H460 cells at various concentrations showed increasing in $O_2^{\bullet-}$ and H_2O_2 as dose-dependent (Figure 4.11). In addition, ESR studies were used to analyzing ROS production with spin trap DMPO and the results are shown in Appendix B.

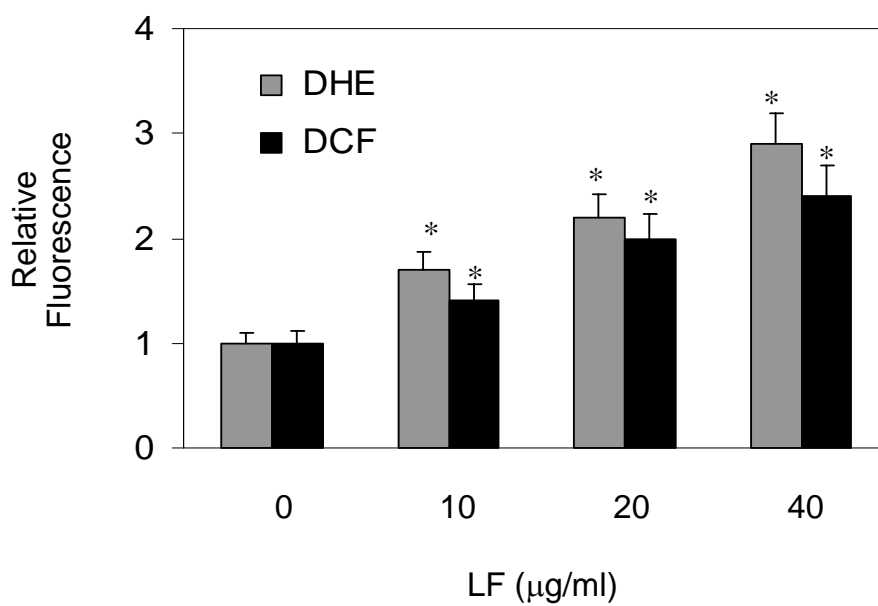


Figure 4.11 Superoxide and peroxide formation in H460 cells treated with LF (0-40 µg/ml) for 30 min analyzed by fluorometry using DHE and DCF-DA as fluorescent probes. Data are mean \pm S.D. (n = 3). *, $p < 0.05$ versus nontreated control.

Consideration of ROS reaction, $O_2^{\bullet-}$ can be converted to H_2O_2 by superoxide dismutase (SOD), and later H_2O_2 can be converted to H_2O by catalase (CAT) or glutathione peroxidase (GPx) or to OH^{\bullet} by the Fenton reaction (in the presence of Fe^{2+} or Cu^+) (59, 89). The ESR results have been shown that OH^{\bullet} was generated in LF-treated cells and $O_2^{\bullet-}$ and H_2O_2 were precursors for OH^{\bullet} generation because addition of SOD mimetic MnTBAP or CAT could inhibit the ESR signal intensity. Therefore, inhibition of $O_2^{\bullet-}$ and H_2O_2 production have affected OH^{\bullet} production in this case.

Alexandre et al. have reported that there was the accumulation of H_2O_2 in an early step for paclitaxel-induced cancer cell apoptosis (66), but for stearylamine liposomes or LF they have never been investigated yet for specific ROS production in cationic liposome-induced apoptosis. The results from this study suggest that $O_2^{\bullet-}$ and H_2O_2 would be initially generated after treatment by LF in H460 cells.

4.3.2 Detection of FLIP in H460 cells treated with LF in the presence or absence of antioxidant (MnTBAP, CAT, SF) by Western blotting

LF treatment in H460 caused FLIP down-regulation as shown in Figure 4.10 and ROS production in Figure 4.11. As shown above, some reports have been shown that ROS could cause apoptosis. As a result, expression of FLIP protein in response to LF treatment in the presence and absence of various antioxidants was analyzed to test whether ROS might mediate the apoptotic effect of LF through FLIP.

Pretreatment of the cells with MnTBAP ($O_2^{\bullet-}$ scavenger) completely inhibited the FLIP down-regulation, whereas pretreatment of the cells with CAT (H_2O_2 scavenger) and SF (OH^{\bullet} scavenger) had partial and no inhibitory effect, respectively, on FLIP down-regulation (Figure 4.12). These results indicate that $O_2^{\bullet-}$, and to a lesser extent H_2O_2 , plays an important role in the regulation of FLIP induced by LF.

4.3.3 The cellular source of ROS production after treatment by LF

To determine the cellular source of ROS generation induced by LF, cells were treated with LF in the presence or absence of DPI, a specific inhibitor of NADPH oxidase (69, 90), or rotenone, a mitochondria respiratory chain inhibitor (90-92), and their effect on $O_2^{\bullet-}$ generation was examined by DHE fluorometry.

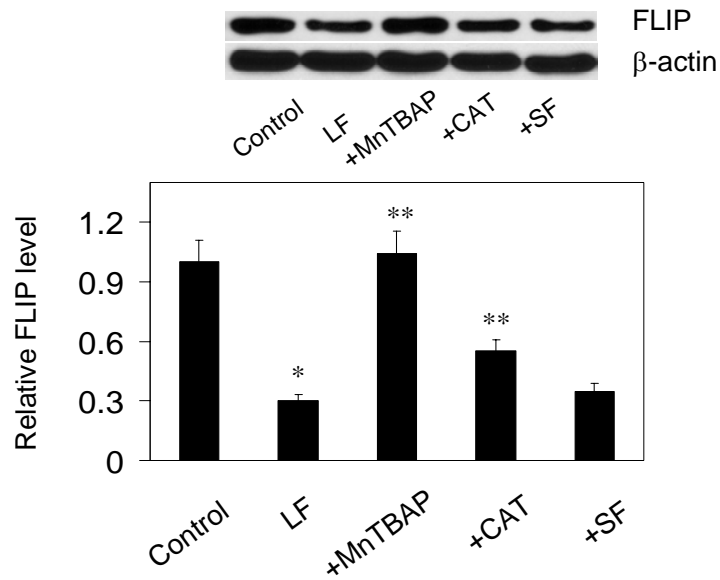


Figure 4.12 FLIP level in H460 cells either left untreated or pretreated with MnTBAP (100 μ M), CAT (1000 units/mL), or SF (10 mM) for 1 h, after which treated with LF (20 μ g/ml) for 6 h analyzed by Western blotting. Plots are mean \pm S.D. (n = 3). *, $p < 0.05$ versus nontreated control; **, $p < 0.05$ versus LF-treated control.

The results showed that DPI strongly inhibited LF-induced DHE fluorescence, whereas rotenone showed minimal effect (Figure 4.13). These results suggest that the plasma membrane NADPH oxidase should be a key source of $O_2^{\cdot-}$ generation induced by LF in H460 cells.

4.3.4 Detection of LF-induced ROS production in SOD or GPx overexpressing cells

H460 cells were stably transfected with SOD, GPx, or control pcDNA3 plasmid. The results of SOD or GPx overexpression in H460 cells as determined by Western blot analysis are shown in Appendix A. To examine the $O_2^{\cdot-}$ level in cells which have overexpression of antioxidant enzymes when treated with LF, $O_2^{\cdot-}$ generation was examined by DHE fluorometry.

Overexpression of SOD potently inhibited LF-induced $O_2^{\cdot-}$ generation compared with vector-transfected control as shown in Figure 4.14. Overexpression of GPx showed less inhibitory effects on LF-induced $O_2^{\cdot-}$ generation. These results suggest that SOD overexpression could work efficiently for lowering the $O_2^{\cdot-}$ level in cells, while GPx overexpression showed less effect.

4.3.5 Investigation of LF-induced apoptosis in SOD- or GPx-overexpressing cells

Cells with overexpressing antioxidant enzymes were used to examine the apoptotic effect after treatment by LF. The results showed that SOD overexpression potently inhibited apoptosis induced by LF, whereas GPx overexpression showed less inhibitory effects on LF-induced apoptosis (Figure 4.15). In relation to the above results, SOD-overexpressing cells generated less $O_2^{\cdot-}$ (Figure 4.14) in association with less apoptosis after treatment by LF. Additionally, GPx-overexpressing cells had more $O_2^{\cdot-}$ generation in association with more apoptosis than SOD-overexpressing had. This indicates that $O_2^{\cdot-}$ would mediate apoptosis in LF-treated cells.

4.3.6 Investigation of LF-induced H460 cells apoptosis in the presence or absence of antioxidant (MnTBAP, CAT)

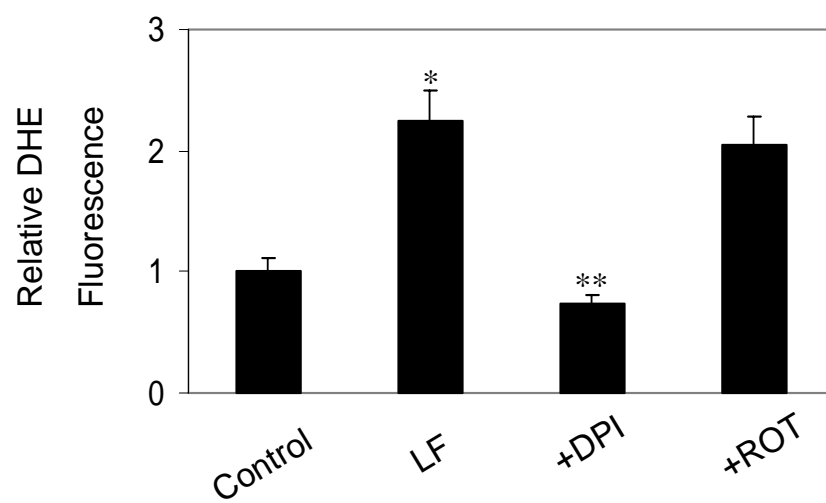


Figure 4.13 Superoxide generation in H460 cells either left untreated or pretreated with DPI (1 μ M) or rotenone (1 μ M) for 30 min, after which treated with LF (20 μ g/ml) and analyzed by DHE fluorescence measurement after 30 min. Plots are mean \pm S.D. (n = 3). *, $p < 0.05$ versus nontreated control; **, $p < 0.05$ versus LF-treated control.

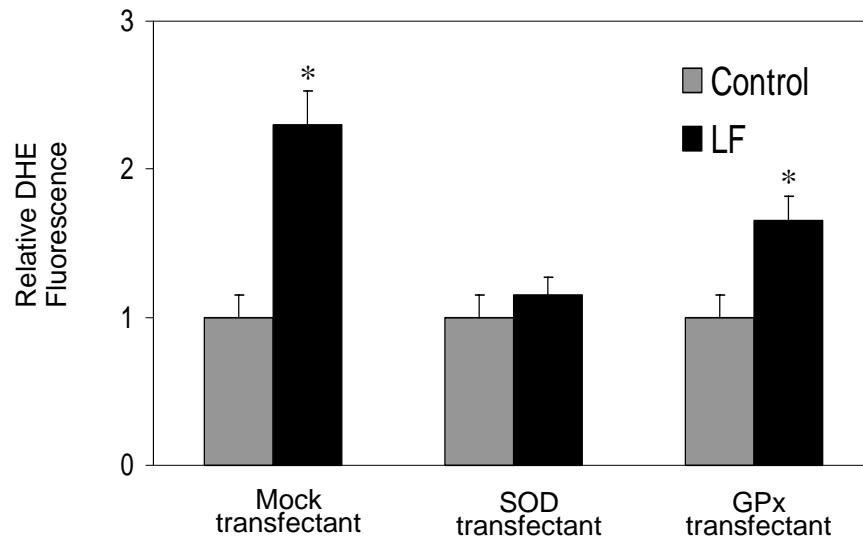


Figure 4.14 SOD- or GPx-overexpressing cells treated with LF (20 μ g/ml) for 30 min analyzed by DHE fluorescent measurement. Plots are mean \pm S.D. (n = 4). *, $p < 0.05$ versus nontreated control.

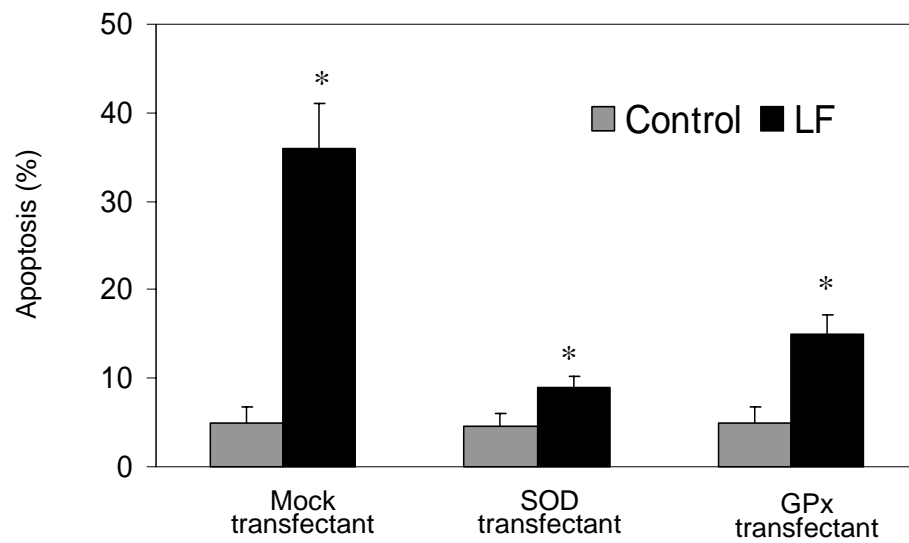


Figure 4.15 Apoptosis of H460 cells stably transfected with SOD, GPx, or control plasmid, and treated with LF (20 $\mu\text{g}/\text{ml}$) for 6 h analyzed by Hoechst assay. Plots are mean \pm S.D. (n = 4). *, $p < 0.05$ versus nontreated control.

Apoptosis studies in H460 cells pretreated with antioxidants followed by LF treatment were investigated to confirm apoptotic response to each antioxidants. The results showed that MnTBAP strongly inhibited the apoptotic effect of LF at the same treatment doses, whereas CAT showed less inhibitory effect (Figure 4.16). The results were consistently with testing in SOD- or GPx-overexpressing cells. This suggests that major ROS mediating apoptosis in LF-treated cells would be $O_2^{\bullet-}$.

Taking into account together the results from the investigation of the role of ROS in LF-induced apoptosis, it could be concluded that LF induced ROS production in dose-dependent manner. Overexpression of SOD showed strongly inhibitory effects on LF-induced $O_2^{\bullet-}$ generation and apoptosis, whereas overexpression of GPx showed less effects. Similar results were obtained in cells treated with MnTBAP ($O_2^{\bullet-}$ scavenger) and CAT (H_2O_2 scavenger). These results indicate that $O_2^{\bullet-}$ is a major oxidative species involved in the apoptotic cell death induced by LF, whereas H_2O_2 plays a lesser role. Furthermore, $O_2^{\bullet-}$ completely inhibited the FLIP down-regulation induced by LF. These results thus support the role of ROS, particular $O_2^{\bullet-}$, in apoptosis and FLIP down-regulation by LF. In addition, source of $O_2^{\bullet-}$ generation was the NADPH oxidase in LF-treated cells.

Although it was shown that after LF-induced ROS production, down-regulation of FLIP, activation of caspase-8 and apoptosis occurred in order, the mechanism by which has not known yet. Several apoptotic stimuli and conditions such as chemotherapeutic agents (93-95), viral infection (96), and p53 and death receptor activation (85, 97), have been shown to induce FLIP down-regulation through the ubiquitination pathway.

The studies of ubiquitination pathway when treated with LF in the presence and absence of MnTBAP or CAT were examined by immunoprecipitation. The results in Appendix C show that LF induced ubiquitination of FLIP and that its inhibition by antioxidants blocked the down-regulation of FLIP by LF. Such results also indicate that $O_2^{\bullet-}$ is the major ROS involving in FLIP ubiquitination since its inhibition by MnTBAP potently inhibited the ubiquitination as compared to catalase. This finding is consistent with the apoptosis and FLIP expression data, indicating the dominant role of $O_2^{\bullet-}$ in LF death signaling. Since many apoptotic stimuli of the death receptor pathway are known to induce ROS generation, the results of this study also suggest

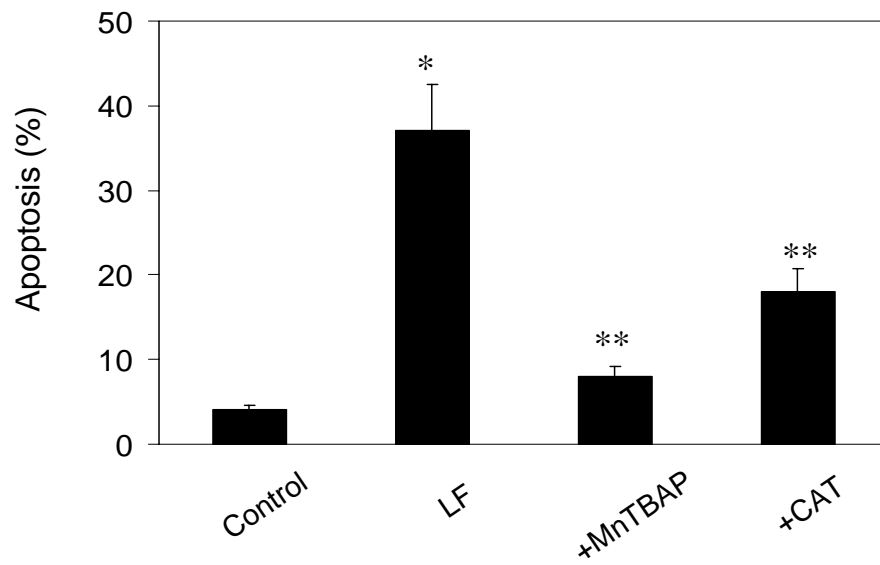


Figure 4.16 H460 cells were pretreated with MnTBAP or CAT for 1 h, after which they were treated with LF (20 $\mu\text{g}/\text{ml}$) for 6 h and analyzed for apoptosis by Hoechst assay. Plots are mean \pm S.D. ($n = 3$). *, $p < 0.05$ versus nontreated control; **, $p < 0.05$ versus LF-treated control.

that ROS may be a common mediator of FLIP ubiquitination and apoptosis induction under various apoptosis conditions.

The mechanism by which ROS mediating the ubiquitination of FLIP remains to be further elucidated. ROS may exert its effect directly on the protein by interacting with specific amino acid residues, leading to conformational changes and increased susceptibility of the protein to ubiquitination by ubiquitin ligases. Down-regulation of FLIP has also been shown to be negatively regulated by nitric oxide (NO), which induces *S*-nitrosylation and inhibits ubiquitination of the protein (85). Since ROS such as $O_2^{\bullet-}$ is known to interact with NO in cellular systems (98, 99) and shown to be critical in FLIP ubiquitination by LF, it is possible that $O_2^{\bullet-}$ may promote FLIP ubiquitination through NO scavenging. Furthermore, ROS may affect FLIP by up-regulating or activating the ubiquitin ligase responsible for FLIP ubiquitination.

4.4 Antioxidant activity of herbal extracts

4.4.1 Standardization of *Asparagus racemosus* (AR) extracts

It has been reported that AR extracts (ARs) contain saponins for the main constituent (100). Until now, it has been found that the major constituents of AR in methanolic extract were steroidal saponins, which were separated, purified, and named as “Shatavarin”. Ten derivatives of Shatavarin were numbered as Shatavarin I to X (70, 74).

For saponins in AR aqueous extract, Gautam et al. analyzed AR aqueous decoction by HPTLC and reported that it presented steroidal saponin, alkaloids, proteins, starch, tannin and mucilage (101). Agrawal et al. carried out screening tests and reported that there were positive for steroids, phytosterols, carbohydrates, tannins, anthraquinones, saponins, glycosides and flavonoids and negative for terpenoids, amino acids and alkaloids (77). Moreover, Visavadiya et al. found that most of phytoconstituents in AR root were saponins (8.833%) and the rest were polyphenols (1.692%), phytosterols (0.79%), ascorbic acid (0.762%), flavonoids (0.476%) (100).

Due to the fact that saponins were in both aqueous and methanolic extracts and some saponins could be purified successfully to pure compounds, there by, saponins were considered as marker in this study. Standardization of AR in this study

was to confirm the presence of saponins and to control the quality of ARs by examining the TLC fingerprints and total saponin content.

4.4.1.1 Qualitative test by Thin layer chromatography (TLC)

TLC is one of several techniques which is useful for identification (102, 103). In this study oleanolic acid (OA) and diosgenin (DG) were used as references for triterpene and steroid saponin, respectively (104, 105).

The TLC fingerprints of OA, DG, and AR1-1 to 1-5 were prepared using two mobile phase systems, that is, system I (2:1-hexane:ethylacetate) and II (6.4:5:1-chloroform:methanol:water). OA and AR1-1 samples were run and generated TLC fingerprints in the system I as shown in Figure 4.17, whereas AR1-2 to 1-5 generated TLC fingerprints in the system II and DG was at the solvent front with the system II as shown in Figure 4.18. The detailed information of R_f values and color zones are shown in Table 4.3.

The anisaldehyde-sulphuric acid reagent was used to detect phenol, sugar, steroid, and terpene that will turn violet, blue, red, grey or green. The results showed that OA and AR1-1 samples exhibited blue color (Figure 4.17) and DG and AR1-2 to 1-5 exhibited yellow-green and green color (Figure 4.18), respectively. These indicate that compounds detected in AR1-1 to 1-5 with this reagent may have the structure of phenol, sugar, steroid, and/or terpene in their molecules. This information was useful for grouping of compounds and TLC fingerprints of ARs would be useful for identification of the extracts and detection of adulteration in the extracts as well.

Among ARs, AR1-1 would have compounds different from those of AR1-2 to 1-5, whereas most of the compounds in AR1-2 to 1-5 would be similar because of the same pattern of TLC fingerprints with 3 main bands and a zone near starting spot (Figure 4.18). Due to the fact that the band of R_f value 0.45 was dominant in AR1-2 whilst a zone near starting spot was more pronounced in AR1-3 to 1-5, solubility of the former would be more in 95% ethanol as extracting solvent and that of the latter would be preferential in aqueous as extracting solvent. Moreover, ARs in this experiment, were obtained from successive extraction, in which the

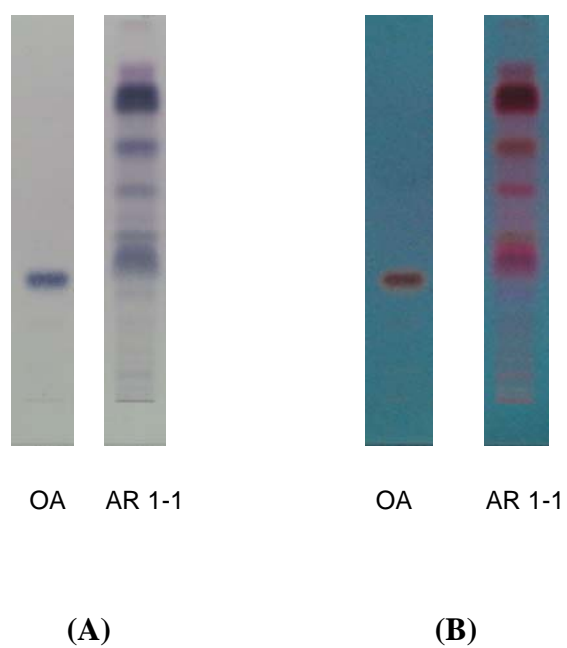


Figure 4.17 TLC fingerprints in white light (A) and under UV (366 nm) (B) of OA and AR1-1 samples in the system I.

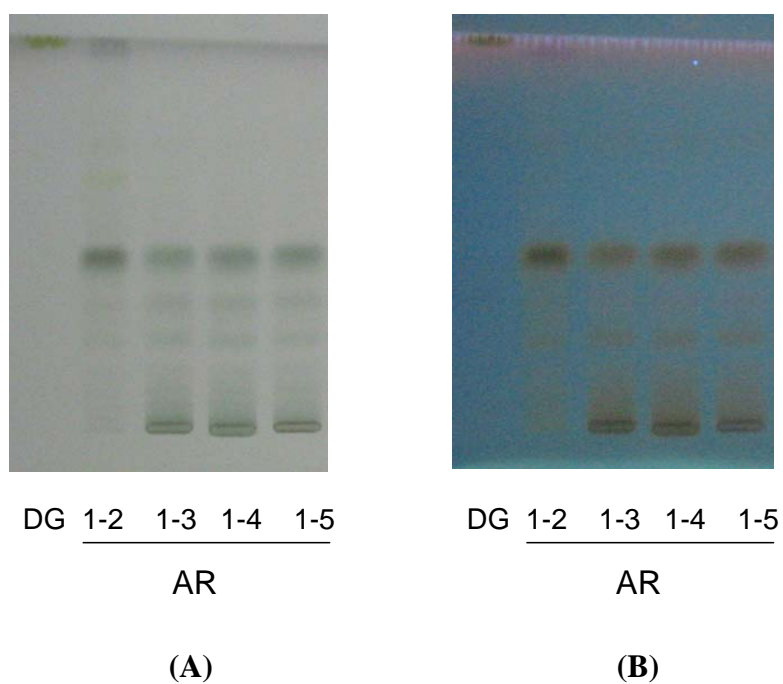


Figure 4.18 TLC fingerprints in white light (A) and under UV (366 nm) (B) of AR1-2 to 1-5 samples in the system II and that of DG sample at the solvent front.

Table 4.3 R_f values and color zones of TLC fingerprints of OA and AR1-1 in system I and DG and AR1-2 to AR1-5 in system II in white light and under UV (366 nm)

Compounds	R_f	Color in white light	Color under UV (366 nm)
OA	0.31	blue	brown
AR1-1	0.38	blue	violet
	0.44	light blue	light brown
	0.56	light blue	pink
	0.69	blue	red
	0.81	dark blue	red
DG	1.00	yellow-green	brown
AR1-2	0.24	light green	light brown
	0.34	light green	light brown
	0.45	dark green	dark brown
AR1-3	0.24	light green	light brown
	0.34	light green	light brown
	0.45	green	brown
AR1-4	0.24	light green	light brown
	0.34	light green	light brown
	0.45	green	brown
AR1-5	0.24	light green	light brown
	0.34	light green	light brown
	0.45	green	brown

extracting solvents were started from non-polar to more polar solvent. Therefore, compounds presenting in each AR extract might have different solubility properties.

4.4.1.2 Quantitative test for total saponins by spectrophotometry

The total saponin content was estimated as previously described by Makkar et al (105), to compare the amount of saponins in each fraction of ARs. DG was used as reference in the determination of total saponins and expressed as diosgenin equivalent, DGE ($\mu\text{g}/\text{mg}$ extract) (106). Vanillin-sulphuric acid reagent was used for derivatization of saponins having an OH group at their C-3 position to give chromogens and the chromogen formed is not dependent on the nature of sugar moieties (105).

The calibration curve of DG was plotted in Figure 4.19 and a high degree of linearity with correlation coefficient (r^2) of 0.9991 was achieved across the specified range of 8.3 – 41.6 $\mu\text{g}/\text{ml}$. The straight line is fitted to an equation:

$$y = 0.0097x + 0.0098 \quad (1)$$

where x and y denote the concentration ($\mu\text{g}/\text{ml}$) and absorbance at 544 nm, respectively. The Absorbances of samples were used to calculate DGE as shown in Table 4.4, and the significant different amounts of DGE are depicted in Figure 4.20.

Among all ARs, the amount of DGE could be ranked in the order as AR1-1 < AR1-5 < AR1-2 = AR1-3 = AR1-4. Therefore, it was apparent that AR contained more amount of saponins in 95% ethanol extract and in aqueous extract as well, but there were differences in type of saponins as discussed in 4.4.1.1.

4.4.2 Antioxidant activity testing by DPPH assay

Dichloromethane, methanolic, and aqueous root extracts of AR have been shown for their antioxidant property. Racemofuran was found and purified from dichloromethane extract which showed the antioxidant activity (75). For methanolic and aqueous root extracts, some reports revealed the antioxidant activity when tested in vivo (72, 73). Moreover, in vitro testing for antioxidant activity of ARs has been

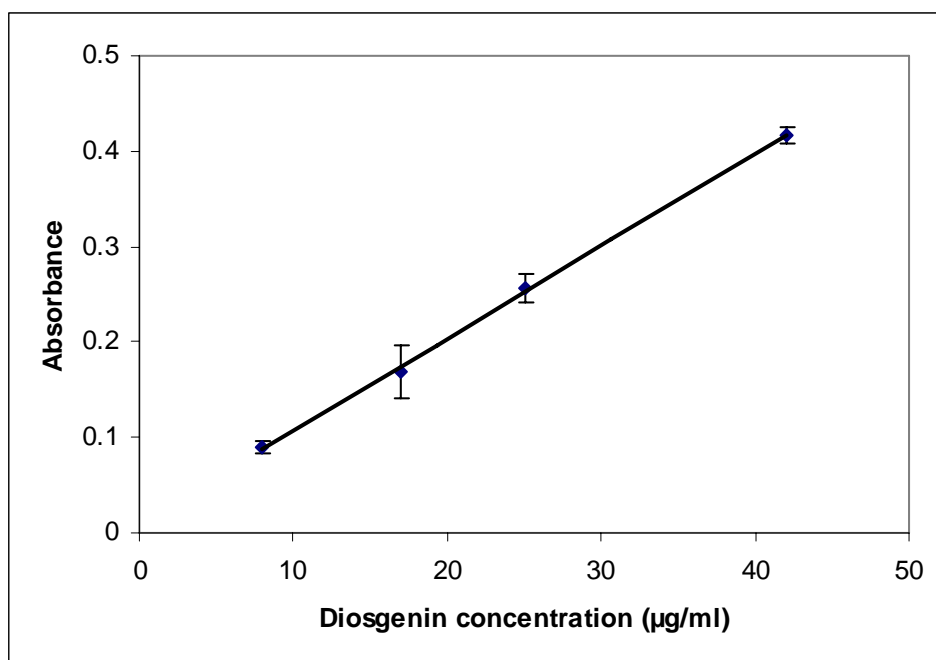


Figure 4.19 Calibration curve of diosgenin (DG) analyzed by spectrophotometer ($y = 0.0097x + 0.0098$, $r^2 = 0.9991$).

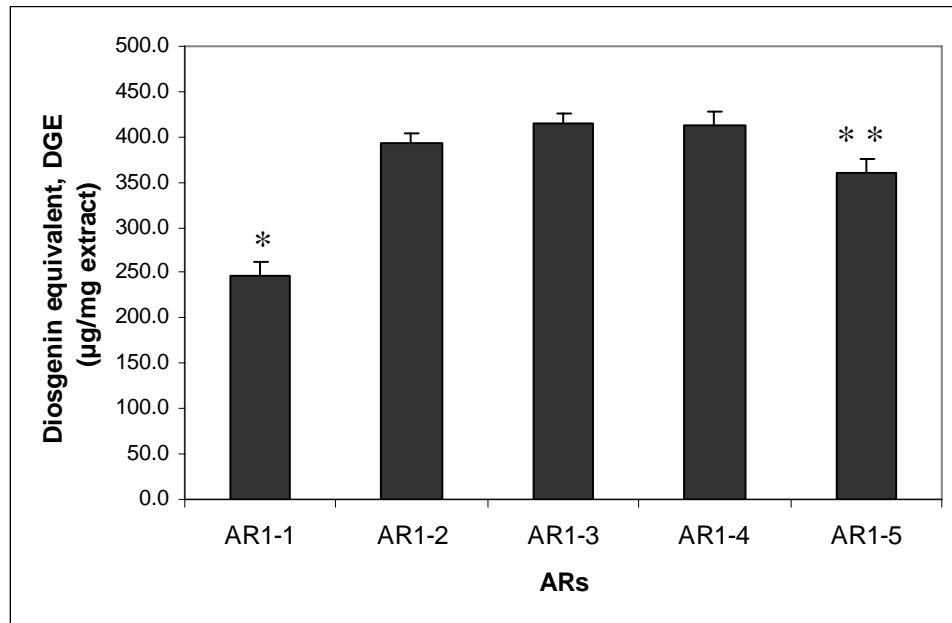


Figure 4.20 Total saponin in each AR expressed as diosgenin equivalent (DGE, µg/mg extract). Data are mean ± S.D. (n = 3). Significant differences among the groups were determined by one way ANOVA using SPSS with LSD test as post hoc analysis. *, $p < 0.05$ versus other ARs; **, $p < 0.05$ versus AR1-1 and others.

Table 4.4 Total saponin content of ARs in terms of diosgenin equivalent (DGE)
($\mu\text{g}/\text{mg}$ extract)

ARs	DGE ($\mu\text{g}/\text{mg}$ extract) Mean \pm SD
AR1-1	247.6 \pm 14.0
AR1-2	392.6 \pm 10.7
AR1-3	414.0 \pm 11.3
AR1-4	413.0 \pm 15.7
AR1-5	361.0 \pm 14.4

conducted by DPPH assay together with TLC for screening purpose (107), or by DPPH assay together with spectrophotometry for determination of efficient concentration (EC_{50}) (100, 108).

In this study, the antioxidant activity was examined by DPPH method (78), which is widely used for evaluation of scavenging capacity of pure compounds or extracts against stable and non-biological radicals such as $DPPH^{\bullet}$ (109, 110). Calibration curve of DPPH was plotted in Figure 4.21 and a very high degree of linearity with correlation coefficient (r^2) of 0.9999 was achieved across the specified range of 10.2 – 102.5 μ M. The straight line is fitted to an equation:

$$y = 0.0097 x + 0.0024 \quad (2)$$

where x and y denote the DPPH concentration (μ M) and absorbance at 515 nm, respectively.

In the investigation of antioxidant activity of ascorbic acid (AA) and AR samples, reaction kinetics of AA and AR1-4 with $DPPH^{\bullet}$ were done to find suitable incubation time before measurement. The results showed that the percentage remaining of DPPH for AA and AR1-4 reached steady state by 1 and 60 min as shown in Figures 4.22 and 4.23, respectively. The time to reach steady state for reaction kinetics, as classified by Brand-William et al. (78), of AA was found to be much more rapid (less than 1 min) than that of AR1-4 (from 1 to 6 h). Active compounds having antioxidant property in AR1-4 would be a large molecule that could result in slow reaction kinetics. On the other hand, AA is smaller molecule which is easily subject to interaction with $DPPH^{\bullet}$.

The efficient concentrations (EC_{50}) of AA and AR1-4 were examined by varying the concentration of samples and the percentage remaining amount of $DPPH^{\bullet}$ were as a function of the sample concentrations. The EC_{50} could be designated as the sample concentration at which % $DPPH^{\bullet}$ remaining decreased from its initial concentration by 50%. The EC_{50} of AA and AR1-4 were shown to be 1.5 and 600 μ g/ml as illustrated in Figures 4.24 and 4.25, respectively. Recently Potduang et al. have shown that the EC_{50} of crude ethanol extract of AR dry powdered root was

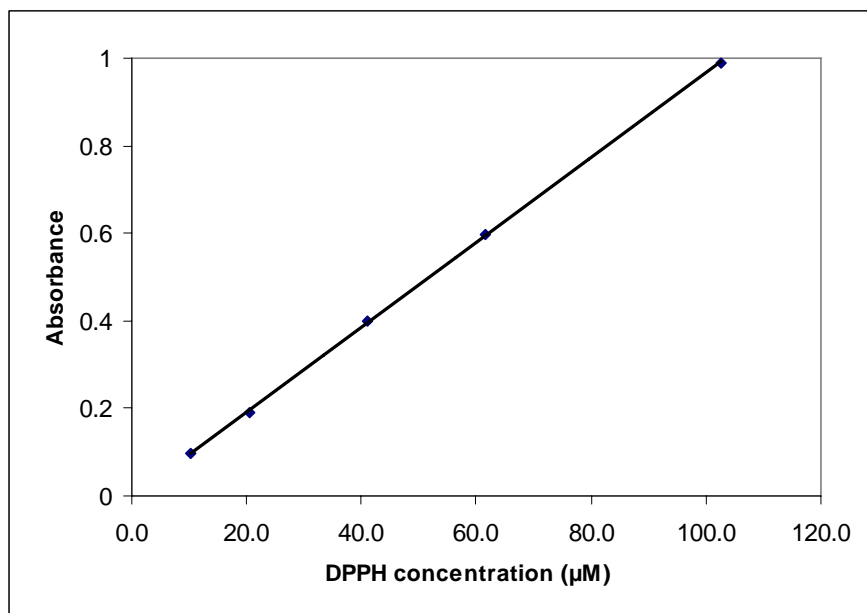


Figure 4.21 Calibration curve of DPPH analyzed by spectrophotometer

$$(y = 0.0097x + 0.0024, r^2 = 0.9999).$$

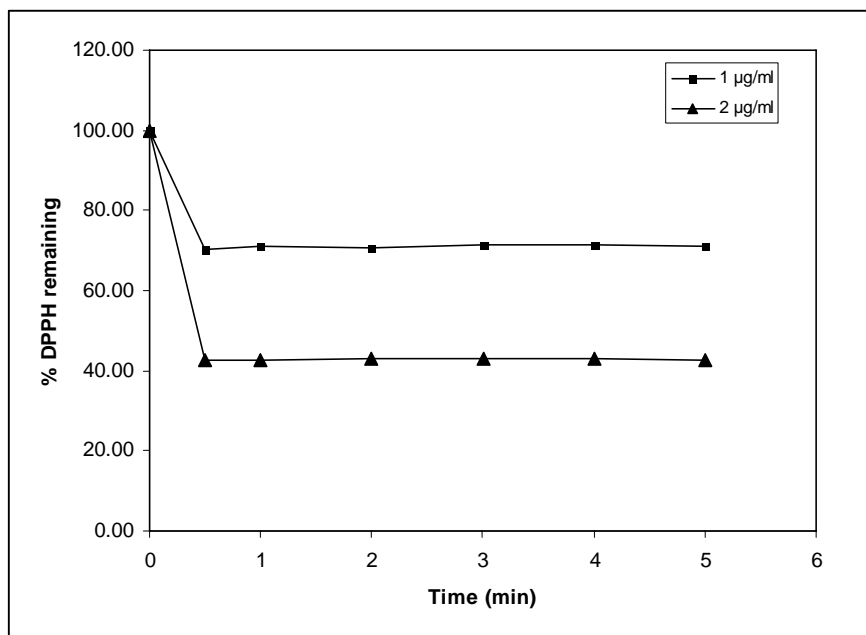


Figure 4.22 Reaction kinetics in antioxidant activity testing of ascorbic acid (1 and 2 µg/ml) with DPPH.

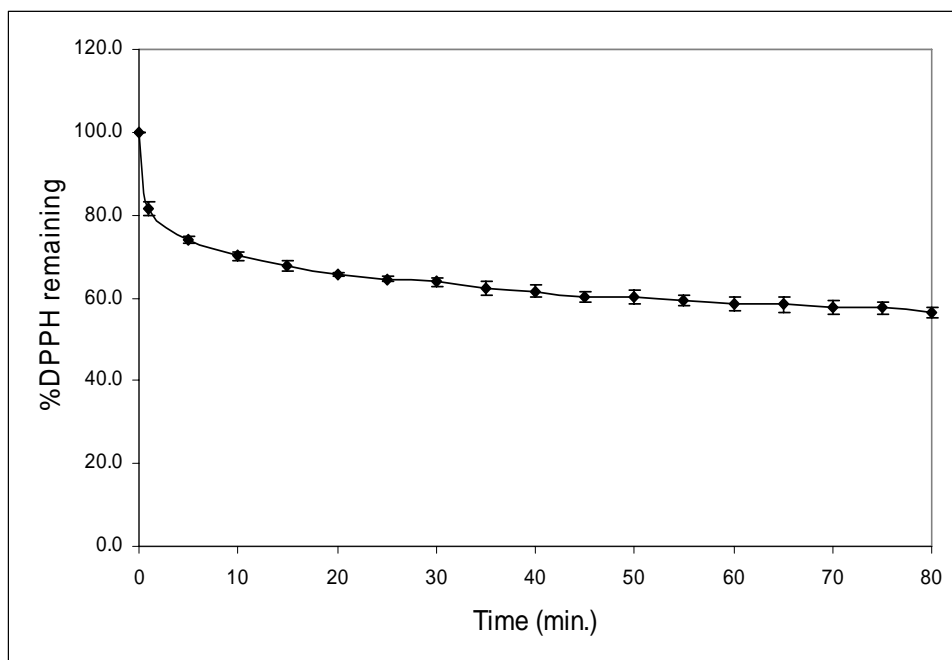


Figure 4.23 Reaction kinetics in antioxidant activity testing of AR1-4 (0.5 mg/ml) with DPPH.

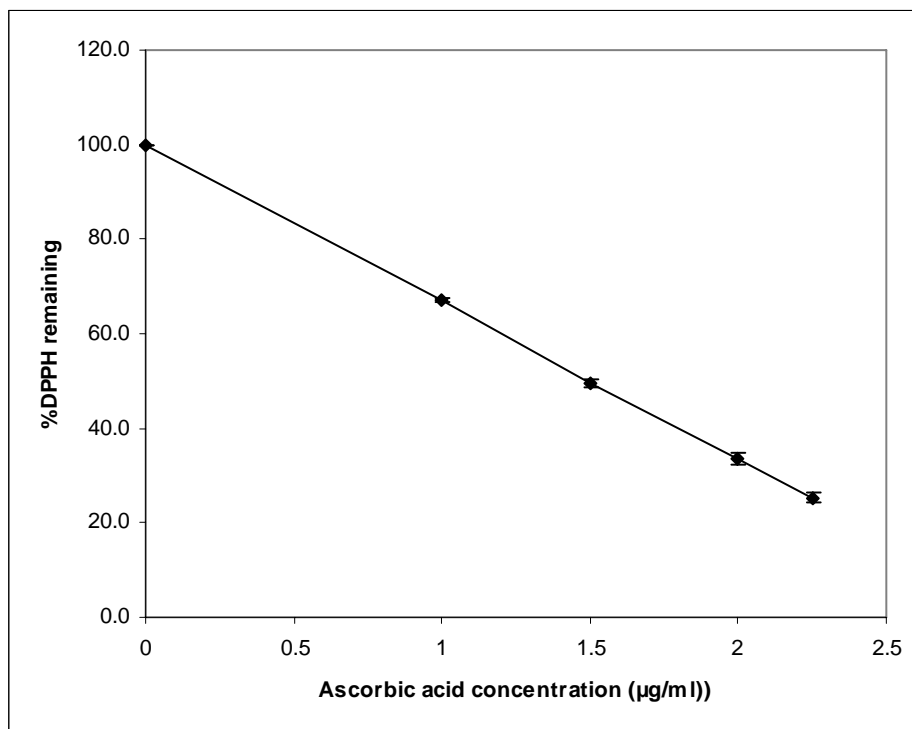


Figure 4.24 Efficient concentration (EC₅₀) of ascorbic acid (AA).

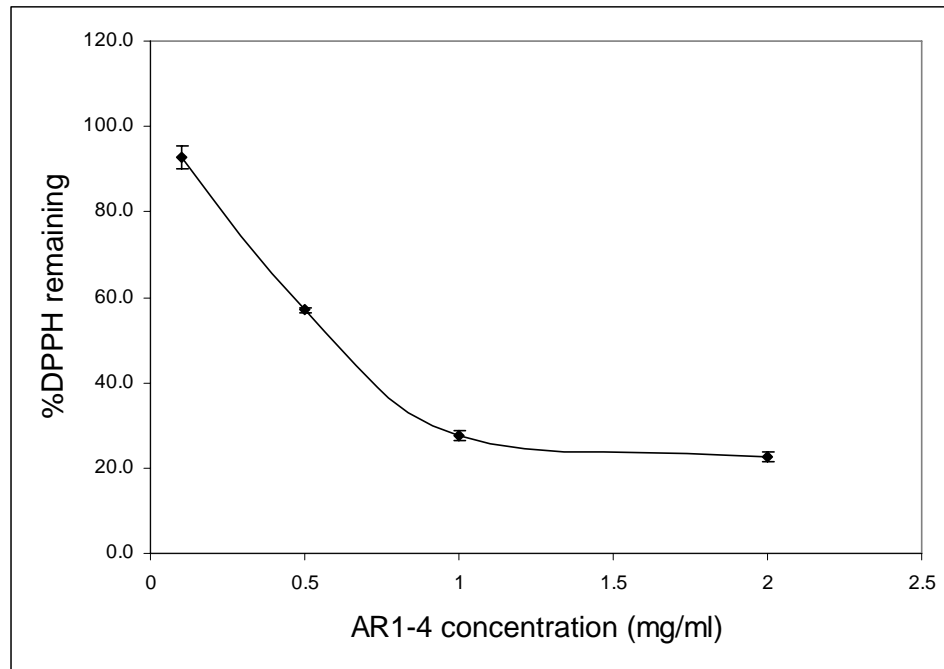


Figure 4.25 Efficient concentration (EC₅₀) of *Asparagus racemosus* extract; AR1-4.

381.91 $\mu\text{g/ml}$ (108). The crude ethanol extract of AR showed more antioxidant activity than aqueous extract AR1-4 from successive extraction.

In order to compare the antioxidant activity among ARs (AR1-1 to AR1-5), they were tested at fixed concentration of 500 $\mu\text{g/ml}$. The results of the % DPPH[•] remaining as shown in Table 4.5 and Figure 4.26 revealed that the AR1-2 (95% ethanol extract) exhibited more antioxidant activity than other ARs. These results were consistent with that reported above. Nonetheless, the antioxidant activity of AR1-2, 95% ethanol extract, was almost in the same order of magnitude as others.

Although ARs possess antioxidant activity much far below than AA when testing with DPPH method, they have been shown to exhibit antioxidant defense in testing *in vivo*. Sairam et al. reported that, having given orally AR methanolic extract to rats with gastric ulcer, it could increase in catalase (CAT) and the ulcer was relieved (72). Bhatnagar et al. also showed that, having given orally AR methanolic extract to rats with NSAID-induced gastric ulcer, it could not only significantly reduce the ulcer index, but also increase the antioxidant defense with significant increase in superoxide dismutase (SOD), catalase (CAT), and ascorbic acid (73). Visavadiya et al. revealed that, having given orally AR root powder in diet to albino rats, it could improve the hepatic antioxidant status (CAT, SOD, ascorbic acid) in hypercholesteremic albino rats (100).

In the *in vitro* testing in rat liver mitochondria by Kamat et al., AR crude and a purified aqueous extracts have been shown to partly protect against radiation-induced loss of protein thiols and inactivation of SOD, which were comparable to glutathione and ascorbic acid (76). According to those previous reports, the antioxidant enzymes, SOD or CAT, were increased from the effect of AR aqueous and methanolic extracts but the underlying mechanism has not known yet. Up to now, there is still no report proving that *saponins of ARs* are the active compound responsible for antioxidant effect.

4.4.3 Investigation of LF-induced H460 cells apoptosis in the presence or absence of AR1-4

AR1-4 aqueous extract was selected for preliminary test of antioxidant effect in cells because its main constituents shown in TLC fingerprint were similar to

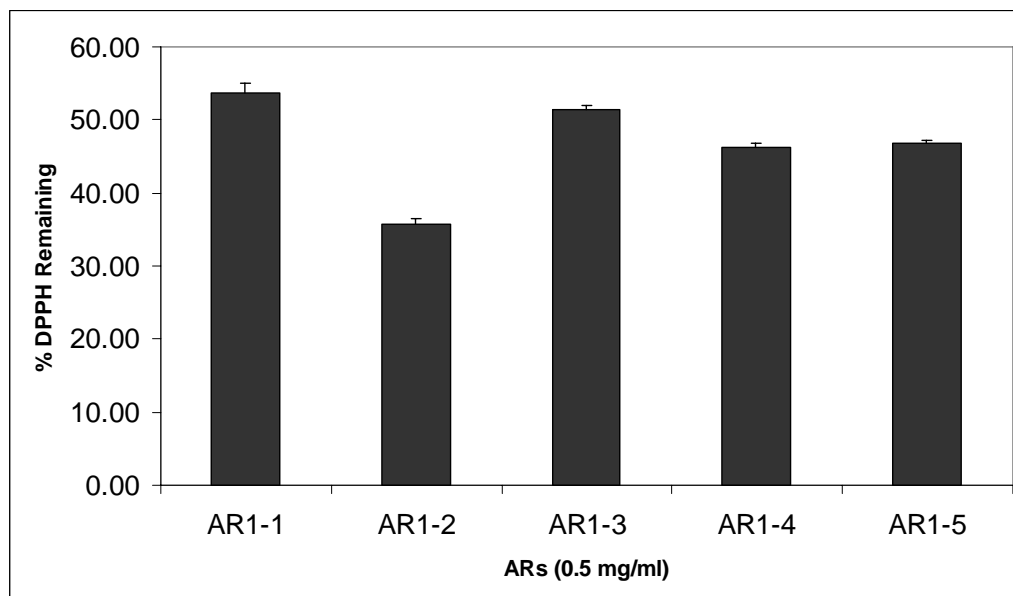


Figure 4.26 The percentage remaining amount of DPPH for ARs tested at the same concentration (0.5 mg/ml). Plots are mean \pm S.D. (n = 2).

Table 4.5 The percentage remaining of DPPH for ARs tested at the same concentration (500 µg/ml)

ARs	% DPPH Remaining (Mean ± SD)
AR1-1	53.60 ± 1.47
AR1-2	35.72 ± 0.85
AR1-3	51.40 ± 0.60
AR1-4	46.16 ± 0.75
AR1-5	46.81 ± 0.41

those of AR1-3 and AR1-5 for both main bands and intensity. Additionally, AR1-4 could more readily be dissolved in water compared to other ARs, which was advantageous in treatment with the cells due to nontoxicity of water solvent.

The purpose of this experiment was to determine the anti-apoptotic effect of AR1-4 against LF-induced apoptosis of H460 cells. The results showed that LF-induced apoptosis was decreased when the concentration of AR1-4 was increased as shown in Figure 4.27.

Numerous studies have reported on the protective effects of AR aqueous extract. Kamat et al. (2000) showed that AR aqueous extract exhibited antioxidant defense by which it could protect the damage of rat liver mitochondria to radiation-induced loss of protein thiols and inactivation of SOD (76). Moreover, Agrawal et al. (2008) reported that pretreatment of AR aqueous extract could lower oxidative stress and hepatotoxicity brought about by treatment with diethylnitrosamine which can induce hepatocarcinogenesis (77).

In this study it was shown that apoptosis was induced by LF treatment through ROS production. ROS scavenger or antioxidant enzymes especially SOD effectively could inhibit apoptosis. Moreover, AR aqueous extract (AR1-4) has protective effect against LF treatment. It would probably be resulted from lower oxidative stress-induced toxicity imposed by its antioxidant activity. However, it is interesting to note that the antioxidant activity of AR1-4 with DPPH in this study was 400 times less than that of AA, whilst it could effectively protect the cells from LF-induced apoptosis almost comparable to untreated ones as shown in Figure 4.27. Such results suggested that this anti-apoptotic effect may probably be caused by the indirect enhancement of antioxidant enzymes such as SOD or CAT rather than the direct antioxidant effect against ROS in the cells.

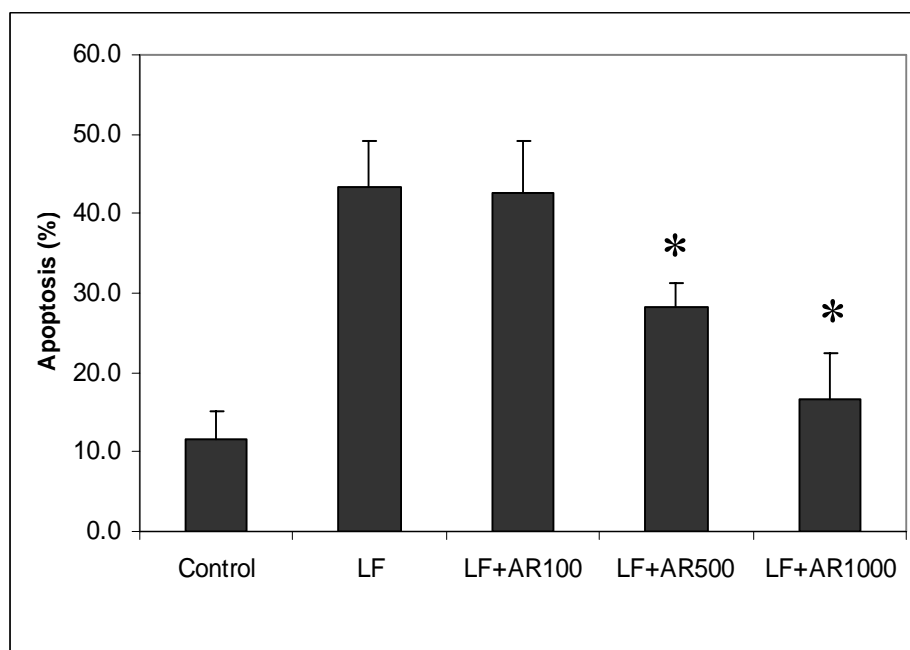


Figure 4.27 Apoptosis of H460 cells untreated or pretreated with *Asparagus racemosus* aqueous extract (AR1-4) at various concentrations for 1 h, after which treated with LF (20 $\mu\text{g}/\text{ml}$) for 6 h and analyzed by Hoechst assay. Plots are mean \pm S.D. (n = 3). *, $p < 0.05$ versus LF-treated control.

CHAPTER V

CONCLUSION

Cationic liposomes are considered as promising tools for gene delivery by forming lipoplex with nucleic acids such as RNA or DNA. Although many studies on toxicity and cationic liposomes-induced apoptosis as well as their mechanisms especially for stearylamine liposomes have been reported to be associated with ROS generation, very few were done with Lipofectamine[™] (LF). This insight information will lead to the development of protocol or formulation or strategy for prevention of cytotoxicity from cationic liposomes while the transfection efficiency may increase if cationic liposome-mediated cytotoxicity could be decreased.

In this study, LF will be investigated for induction of cell death, the kind of cell death (necrosis or apoptosis), the death pathway, and regulatory factors that will be involved. Moreover, LF-induced ROS generation will be investigated for source of generation, types of ROS, and the role of ROS. Thus, the role of specific ROS in LF-induced cell death and the underlying mechanism will be elucidated.

Characteristics of LF

LF used in this study exhibited oligolamellar structure with average size and zeta potential of 140.5 ± 8.3 nm and 35.1 ± 4.2 mV, respectively.

LF-induced apoptosis

It was found that LF caused chromatin condensation and DNA fragmentation in H460 cells and its response was dose- and time-dependent manner. These evidences indicated apoptosis (programmed cell death) which could be attributed to LF treatment. Moreover, the pathway of LF-induced apoptosis was caspase-dependent, which involved both intrinsic (mitochondrial) and extrinsic pathway (death receptor) with the latter as a dominant one. The results also suggested the possible linkage between these 2 pathways. The study on regulatory protein

closely related to initiator caspase especially FLIP (FLICE-inhibitory protein) revealed that overexpression of FLIP could inhibit caspase-8 and -9 activation and reduce the apoptosis as well, while down-regulation of FLIP could sensitize cell to apoptosis. Thus, FLIP would be the important regulatory protein in LF-induced apoptosis and down-regulation of FLIP by LF was a key event in the death signaling.

Role of ROS in LF-induced apoptosis

ROS especially superoxide anion $O_2^{\bullet-}$ were found to be produced in a dose-dependent manner when treatment with LF, and played an important role in FLIP down-regulation. Using antioxidant especially MnTBAP ($O_2^{\bullet-}$ scavenger) could inhibit FLIP down-regulation. Consequently, both antioxidant and antioxidant enzyme, MnTBAP and SOD, could inhibit LF-induced apoptosis.

Antioxidant activity of herbal extracts

The antioxidant activity of extracts from roots of *Asparagus racemosus* (AR) was studied. Five fractions of AR extracts (AR1-1 to 1-5) from successive extraction process ranging from non-polar to more polar solvents were obtained. Total saponins in the extracts were used as marker, which was estimated in terms of diosgenin equivalent value (DGE, $\mu\text{g}/\text{mg}$ extract). The DGE values of ARs were found to be approximately in the range of 240 - 420 $\mu\text{g}/\text{mg}$ extract with higher values for AR1-2 (95% ethanol extract), AR1-3, and 1-4 (aqueous extract).

The antioxidant activity by DPPH method in terms of efficient concentration (EC_{50}) of AR1-4 was found to be 600 $\mu\text{g}/\text{ml}$ compared to 1.5 $\mu\text{g}/\text{ml}$ of ascorbic acid (AA). The antioxidant activity at a given concentration of 500 $\mu\text{g}/\text{ml}$ showed that all ARs exhibited almost the same order of magnitude with the highest one for AR1-4. Further pretreatment of AR1-4 in LF-treated cells was shown to exhibit protective effect against LF-induced apoptosis in H460 cells although the underlying mechanism has not known yet. It could thus be proposed that AR1-4 may inhibit LF-induced apoptosis by the indirect enhancement of antioxidant enzymes such as SOD rather than the direct antioxidant effect against ROS in the cells.

Cell death pathway in LF-induced apoptosis was shown to involve the important factors such as ROS and FLIP. Antioxidants could be used in inhibition of

apoptosis or reduction of toxicity. This is advantageous in gene transfection so that more amount of LF could be delivered. Antioxidants, antioxidant enzymes, or herbal extracts, which can effectively scavenge $O_2^{\bullet-}$, would be alternative choices for such application.

REFERENCES

1. Robbins PD, Ghivizzani SC. Viral vectors for gene therapy. *Pharmacol Therapeut.* 1998;80(1):33-47.
2. Ciftci K, Gupte A. Gene therapy: an overview of the current viral and nonviral vectors. In: Groves MJ, editor. *Pharmaceutical Biotechnology*. 2nd ed. New York: Taylor&Francis; 2006.
3. Niidome T, Huang L. Gene therapy progress and prospects: nonviral vectors. *Gene Ther.* 2002;9:1647-52.
4. Gao X, Kim K-S, Liu D. Nonviral gene delivery: what we know and what is next. *The AAPS Journal.* 2007;9(1):E92-E104.
5. Young LS, Searle PF, Onion D, Mautner V. Viral gene therapy strategies: from basic science to clinical application. *J Pathol.* 2006;208:299-318.
6. Strom G, Crommelin DJA. Liposomes: quo vadis? *PSTT.* 1998;1(1):19-31.
7. Dokka S, Toledo D, Shi X, Castronova V, Rojanasakul Y. Oxygen radical-mediated pulmonary toxicity induced by some cationic liposomes. *Pharm Res.* 2000;17(5):521-5.
8. Wolf BB, Green DR. Suicidal tendencies: apoptotic cell death by caspase family proteinases. *J Biol Chem.* 1999;274:20049-52.
9. Dokka S, Toledo D, Shi X, Ye J, Rojanasakul Y. High-efficiency gene transfection of macrophages by lipoplexes. *Int J Pharm.* 2000;206:97-104.
10. Lv H, Zhang S, Wang B, Cui S, Yan J. Toxicity of cationic lipids and cationic polymers in gene delivery. *J Control Release.* 2006;114:100-9.
11. Almofti MR, Harashima H, Shinohara Y, Almofti A, Baba Y, Kiwada H. Cationic liposome-mediated gene delivery: biophysical study and mechanism of internalization. *Arch Biochem Biophys.* 2003;410:246-53.
12. Aramaki Y, Takano S, Tsuchiya S. Induction of apoptosis in macrophages by cationic liposomes. *FEBS Lett.* 1999;460:472-6.
13. Aramaki Y, Takano S, Arima H, Tsuchiya S. Induction of apoptosis in WEHI 231 cells by cationic liposomes. *Pharm Res.* 2000;17:515-20.

14. Sullivan SM. Introduction to gene therapy and guidelines to pharmaceutical development. In: Rolland A, Sullivan SM, editors. Pharmaceutical gene delivery systems. New York: Marcel Dekker, Inc.; 2003.
15. Lui VW-Y, Huang L. Nonviral approaches for cancer gene therapy. In: Rolland A, Sullivan SM, editors. Pharmaceutical gene delivery systems. New York: Marcel Dekker, Inc.; 2003.
16. Bout A. Gene therapy. In: Crommelin DJA, Sindelar RD, editors. Pharmaceutical biotechnology: an introduction for pharmacists and pharmaceutical scientists. 2nd ed. New York: Taylor&Francis; 2002.
17. Purohit SS, Kakrani HN, Saluja AK. Pharmaceutical biotechnology. Jodhpur, India: Student Edition; 2003.
18. Felgner PL, Gadek TR, Holm M, Roman R, Chan HW, Wenz M, et al. Lipofection: a highly efficient, lipid-mediated DNA-transfection procedure. *Proc Natl Acad Sci.* 1987;84:7413-7.
19. Swarbrick J, Boylan J. Liposomes as pharmaceutical dosage forms. *Encyclopedia of pharmaceutical technology.* USA: Marcel Dekker; 1994. p. 1-9.
20. Hiemenz JW, Walsh TJ. Lipid formulations of amphotericin B: recent progress and future directions. *Clin Infect Dis.* 1996;22(Suppl 2):S133-44.
21. Torchilin VP. Recent advances with liposomes as pharmaceutical carriers. *Nat Rev Drug Discov.* 2005;4:145-60.
22. Kirby CJ, Gregoriadis G. Liposomes. In: Mathiowitz E, editor. *Encyclopedia of controlled drug delivery.* USA: John Wiley & Sons, Inc.; 1999. p. 461-92.
23. Safinya CR, Ewert K, Ahmad A, Evans HM, Raviv U, Needleman DJ, et al. Cationic liposome-DNA complexes: from liquid crystal science to gene delivery applications. *Philos T Roy Soc A.* 2006;364:2573-96.
24. Zhang S, Xu Y, Wang B, Qiao W, Liu D, Li Z. Cationic compounds used in lipoplexes and polyplexes for gene delivery. *J Control Release.* 2004;100:165-80.
25. Fattal E, Couvreur P, Dubernet C. "Smart" delivery of antisense oligonucleotides by anionic pH-sensitive liposomes. *Adv Drug Deliver Rev.* 2004;56:931-46.

26. Simberg D, Weisman S, Talmon Y, Barenholz Y. DOTAP (and other cationic lipids): chemistry, biophysics, and transfection. *Crit Rev Ther Drug.* 2004;21(4):257-317.
27. Borbiev T, Nurmukhambetova S, Liu F, Verin AD, Garcia JGN. Introduction of C3 exoenzyme into cultured endothelium by lipofectamine. *Anal Biochem.* 1999;285:260-4.
28. Congiu A, Pozzi D, Esposito C, Castellano C, Mossa G. Correlation between structure and transfection efficiency: a study of DC-Chol-DOPE/DNA complexes. *Colloid Surface B.* 2004;36:43-8.
29. Sakurai F, Inoue R, Nishino Y, Okuda A, Matsumoto O, Taga T, et al. Effect of DNA/liposome mixing ratio on the physicochemical characteristics, cellular uptake and intercellular trafficking of plasmid DNA/cationic liposome complexes and subsequent gene expression. *J Control Release.* 2000;66:255-69.
30. Zhang Y, Garzon-Rodriguez W, Manning MC, Anchordoquy TJ. The use of fluorescence resonance energy transfer to monitor dynamic changes of lipid-DNA interactions during lipoplex formation. *Biochim Biophys Acta.* 2003;1614:182-92.
31. Rejman J, Bragonzi A, Conese M. Role of clathrin- and caveolae-mediated endocytosis in gene transfer mediated by lipo- and polyplexes. *Mol Ther.* 2005;12(3):468-74.
32. Zelphati O, Szoka FC. Mechanism of oligonucleotide release from cationic liposomes. *Proc Natl Acad Sci.* 1996;93:11493-8.
33. Gregus Z. Mechanisms of toxicity. In: Klaassen CD, editor. *Casarett and Doull's Toxicology: the basic science of poisons.* 7 ed. New York: McGraw-Hill Co., Inc.; 2008. p. 45-106.
34. Kim S-W, Ogawa T, Tabata Y, Nishimura I. Efficacy and cytotoxicity of cationic-agent-mediated nonviral gene transfer into osteoblasts. *J Biomed Mater Res.* 2004;71(A):308-15.
35. Campbell PI. Toxicity of some charged lipids used in liposome preparations. *Cytobios.* 1983;37:21-6.

36. Lappalainen K, Jaaskelainen I, Syrjanen K, Urtti A, Syrjanen S. Comparison of cell proliferation and toxicity assays using two cationic liposomes. *Pharm Res.* 1994;11(8):1127-31.
37. Scheule RK, StGeorge JA, Bagley RG, Marshall J, Kaplan JM, Akita GY, et al. Basis of pulmonary toxicity associated with cationic lipid-mediated gene transfer to the mammalian lung. *Hum Gene Ther.* 1997;8(6):689-707.
38. Fillion MC, Philips NC. Toxicity and immunomodulatory activity of liposomal vectors formulated with cationic lipids toward immune effector cells. *Biochim Biophys Acta.* 1997(1329):345-56.
39. Yoshihara E, Nakae T. Cytolytic activity of liposomes containing stearylamine. *BBA-Biomembranes.* 1986;854(1):93-101.
40. Iwaoka S, Nakamura T, Takano S, Tsuchiya S, Aramaki Y. Cationic liposomes induce apoptosis through p38 MAP kinase-caspase-8-Bid pathway in macrophage-like RAW264.7 cells. *J Leukocyte Biol.* 2006;79:184-91.
41. Timbrell J. Toxic responses of foreign compounds. *Principles of biochemical toxicology.* 3 ed. Philadelphia: Taylor & Francis, Inc.; 2000. p. 175-258.
42. Cho S-G, Choi E-J. Apoptotic signaling pathways: caspases and stress-activated protein kinases. *J Biochem Mol Biol.* 2002;35(1):24-7.
43. Fan T-J, Han L-H, Cong R-S, Liang J. Caspase family proteases and apoptosis. *Acta Bioch Biophys Sin.* 2005;37(11):719-27.
44. Fink SL, Cookson BT. Apoptosis, pyroptosis, and necrosis: mechanistic description of dead and dying eukaryotic cells. *Infect Immun.* 2005(Apr.):1907-16.
45. Hengartner MO. The biochemistry of apoptosis. *Nature.* 2000;407:770-6.
46. Kroemer G, Dallaporta B, Resche-Rigon M. The mitochondrial death/life regulator in apoptosis and necrosis. *Annu Rev Physiol.* 1998;60:619-42.
47. Ashkenazi A, Dixit VM. Death receptors: signaling and modulation. *Science.* 1998;281:1305-8.
48. Thome M, Schneider P, Hofmann K, Fickenscher H, Meini E, Neipel F, et al. Viral FLICE-inhibitory proteins (FLIPs) prevent apoptosis induced by death receptors. *Nature.* 1997;386(3):517-21.

49. Irmeler M, Thome M, Hahne M, Schneider P, Hofmann K, Steiner V, et al. Inhibition of death receptor signals by cellular FLIP. *Nature*. 1997;388:190-5.
50. Scaffidi C, Schmitz I, Krammer PH, Peter ME. The role of c-FLIP in modulation of CD95-induced apoptosis. *J Biol Chem*. 1999;274(3):1541-8.
51. Tsujimoto Y, Croce CM. Analysis of the structure, transcripts, and protein products of bcl-2, the gene involved in human follicular lymphoma. *Proc Natl Acad Sci USA*. 1986;83:5214-8.
52. Hengartner MO, Horvitz HR. Activation of *C. elegans* cell death protein CED-9 by an amino-acid substitution in a domain conserved in Bcl-2. *Nature*. 1994;369:318-20.
53. Yang J, Liu X, Bhalla K, Kim CN, Ibrado AM, Cai J, et al. Prevention of apoptosis by Bcl-2: release of cytochrome c from mitochondria blocked. *Science*. 1997;275:1129-32.
54. Kluck RM, Bossy-Wetzel E, Green DR, Newmeyer DD. The release of cytochrome c from mitochondria: a primary site for Bcl-2 regulation of apoptosis. *Science*. 1997;275:1132-6.
55. Hunter AM, LaCasse EC, Korneluk RG. The inhibitors of apoptosis (IAPs) as cancer targets. *Apoptosis*. 2007;12:1543-68.
56. Deveraux QL, Takahashi R, Salvesen GS, Reed JC. X-linked IAP is a direct inhibitor of cell-death proteases. *Nature*. 1997;388:300-4.
57. Deveraux QL, Roy N, Stennicke HR, Arsdale TV, Zhou Q, Srinivasula SM, et al. IAPs block apoptotic events induced by caspase-8 and cytochrome c by direct inhibition of distinct caspases. *EMBO J*. 1998;17(8):2215-23.
58. Terada LS. Specificity in oxidant signaling: think globally, act locally. *J Cell Biol*. 2006;174(5):615-23.
59. Mathews CK, Holde KE, Ahern KG. *Biochemistry*. 3 ed. San Francisco: Addison Wesley; 2000.
60. Thannickal VJ, Fanburg BL. Reactive oxygen species in cell signaling. *Am J Physiol Lung Cell Mol Physiol*. 2000;279:L1005-L28.

61. Heerebeek LV, Meischl C, Stooker W, Meijer CJLM, Neissen HWM, Roos D. NADPH oxidase(s): new source(s) of reactive oxygen species in the vascular system? *J Clin Pathol*. 2002;55:561-8.
62. Sorescu D, Somers MJ, Lassegue B, Grant S, Harryson DG, Griendling KK. Electron spin resonance characterization of the NAD(P)H oxidase in vascular smooth muscle cells. *Free Radical Bio Med*. 2001;30(6):603-12.
63. Finkel T, Holbrook NJ. Oxidants, oxidative stress and the biology of ageing. *Nature*. 2000;408:239-47.
64. Simon H-U, Haj-Yehia A, Levi-Schaffer F. Role of reactive oxygen species in apoptosis induction. *Apoptosis*. 2000;5:415-8.
65. Pierce GB, Parchment RE, Lewellyn AL. Hydrogen peroxide as a mediator of programmed cell death in the blastocyst. *Differentiation*. 1991;46(3):181-6.
66. Alexandre J, Batteux F, Nicco C, Chereau C, Laurent A, Guillevin L. Accumulation of hydrogen peroxide is an early and crucial step for paclitaxel-induced cancer cell death both *in vitro* and *in vivo*. *Int J Cancer*. 2006;119:41-8.
67. Lee M-W, Park SC, Yang YG, Yim SO, Chae HS, Bach J-H, et al. The involvement of reactive oxygen species (ROS) and p38mitogen-activated protein (MAP) kinase in TRAIL/Apo2L-induced apoptosis. *FEBS Lett*. 2002;512:313-8.
68. Izeradjene K, Douglas L, Tillman DM, Delaney AB, Houghton JA. Reactive oxygen species regulate caspase activation in tumor necrosis factor-related apoptosis-inducing ligand-resistant human colon carcinoma cell lines. *Cancer Res*. 2005;65(16):7436-45.
69. Mounjaroen J, Nimmannit U, Callery PS, Wang L, Azad N, Lipipun V, et al. Reactive oxygen species mediate caspase activation and apoptosis induced by lipoic acid in human lung epithelial cancer cells through Bcl-2 downregulation. *J Pharm Exp Ther*. 2006;319(3):1062-9.
70. Bopana N, Saxena S. *Asparagus racemosus*-Ethnopharmacological evaluation and conservation needs. *J Ethnopharmacol*. 2007;110:1-15.
71. *Asparagus racemosus*. 2008 12/09/08 [cited; Available from: www.pharmacy.mahidol.ac.th/medplantdatabase/dtl_herbal.asp

72. Sairam K, Priyambada S, Aryya NC, Goel RK. Gastroduodenal ulcer protective activity of *Asparagus racemosus*: an experimental, biochemical and histological study. *J Ethnopharmacol.* 2003;86:1-10.
73. Bhatnagar M, Sisodia SS, Bhatnagar R. Antiulcer and antioxidant activity of *Asparagus racemosus* Willd and *Withania somnifera* Dunal in rats. *Ann NY Acad Sci.* 2005;1056:261-78.
74. Hayes PY, Jahidin AH, Lehmann R, Penman K, Kitching W, Voss JJD. Steroidal saponins from the roots of *Asparagus racemosus*. *Phytochemistry.* 2008;69:796-804.
75. Wiboonpun N, Phuwapraisirisan P, Tip-pyang S. Identification of antioxidant compound from *Asparagus racemosus*. *Phytother Res.* 2004;18:771-3.
76. Kamat JP, Bloor KK, Devasagayam TPA, Venkatachalam SR. Antioxidant properties of *Asparagus racemosus* against damage induced by γ -radiation in rat liver mitochondria. *J Ethnopharmacol.* 2000;71:425-35.
77. Agrawal A, Sharma M, Rai SK, Singh B, Tiwari M, Chandra R. The effect of the aqueous extract of the roots of *Asparagus racemosus* on hepatocarcinogenesis initiated by diethylnitrosamine. *Phytother Res.* 2008;22:1175-82.
78. Brand-Williams W, Cuvelier ME, Berset C. Use of a free radical method to evaluate antioxidant activity. *Lebensm-Wiss u-Technol.* 1995;28:25-30.
79. Green DR, Reed JC. Mitochondria and apoptosis. *Science.* 1998;281:1309-12.
80. Wallach D, Varfolomeev EE, Malinin NL, Goltsev YV, Kovalenko AV, Boldin MP. Tumor necrosis factor receptor and Fas signaling mechanisms. *Annu Rev Immunol.* 1999;17:331-67.
81. Chang DW, Xing X, Pan Y, Algeciras-Schimmich A, Barnhart BC, Yaish-Ohad S, et al. c-FLIP_L is a dual function regulator for caspase-8 activation and CD95-mediated apoptosis. *EMBO J.* 2002;21:3704-14.
82. Sun XM, Bratton SB, Butterworth M, MacFarlane M, Cohen GM. Bcl-2 and Bcl-xL inhibit CD95-mediated apoptosis by preventing mitochondrial release of Smac/DIABLO and subsequent inactivation of X-linked inhibitor-of-apoptosis protein. *J Biol Chem.* 2002;277:11345-51.

83. Chanvorachote P, Nimmannit U, Stehlik C, Wang L, Jiang BH, Ongpipatanakul B, et al. Nitric oxide regulates cell sensitivity to cisplatin-induced apoptosis through S-nitrosylation and inhibition of Bcl-2 ubiquitination. *Cancer Res.* 2006;66:6353-60.
84. Iwaoka S, Nakamura T, Takano S, Tsuchiya S, Aramaki Y. Cationic liposomes induce apoptosis through p38-MAP kinase-caspase-8-Bid pathway in macrophage-like RAW264.7 cells. *J Leukocyte Biol.* 2006;79:184-91.
85. Chanvorachote P, Mimmannit U, Wang L, Stehlik C, Lu B, Azad N, et al. Nitric oxide negatively regulates Fas CD95-induced apoptosis through inhibition of ubiquitin-proteasome-mediated degradation of FLICE inhibitory protein. *J Biol Chem.* 2005;280(51):42044-50.
86. Wang L, Azad N, Kongkaneramt L, Chen F, Lu Y, Jiang B-H, et al. The Fas death signaling pathway connecting reactive oxygen species generation and FLICE inhibitory protein down-regulation. *J Immunol.* 2008;180:3072-80.
87. Liu X, Yue P, Schönthal AH, Khuri FR, Sun S-Y. Cellular FLICE-inhibitory protein down-regulation contributes to celecoxib-induced apoptosis in human lung cancer cells. *Cancer Res.* 2006;66(23):11115-9.
88. Krueger A, Buamann S, Krammer PH, Kirchhoff S. FLICE-inhibitory proteins: regulators of death receptor-mediated apoptosis. *Mol Cell Biol.* 2001;21:8247-54.
89. Thabrew I, Ayling RM. *Biochemistry for clinical medicine.* London: Greenwich Medical Media; 2001.
90. Irani K, Xia Y, Zweier JL, Sollott SJ, Der CJ, Fearon ER, et al. Mitogenic signaling mediated by oxidants in Ras-transformed fibroblasts. *Science.* 1997;275:1649-52.
91. Chen Q, Vazquez EJ, Moghaddas S, Hoppel CL, Lesnefsky EJ. Production of reactive oxygen species by mitochondria: central role of complex III. *J Biol Chem.* 2003;278:36027-31.
92. Mayes PA, Botham KM. The respiratory chain & oxidative phosphorylation. In: Murray RK, Granner DK, Mayes PA, Rodwell VW, editors. *Harper's illustrated biochemistry.* 21 ed. New York: The McGraw-Hill Companies, Inc.; 2003. p. 92-101.

93. Kim Y, Suh N, Sporn M, Reed JC. An inducible pathway for degradation of FLIP protein sensitizes tumor cells to TRAIL-induced apoptosis. *J Biol Chem.* 2002;277:22320-9.
94. Nitobe J, Yamaguchi S, Okuyama M, Nozaki N, Sata M, Miyamoto T, et al. Reactive oxygen species regulate FLICE inhibitory protein (FLIP) and susceptibility to Fas-mediated apoptosis in cardiac myocytes. *Cardiovasc Res.* 2003;57:119-28.
95. Day TW, Najafi F, Wu C-H, Safa AR. Cellular FLICE-like inhibitory protein (c-FLIP): a novel target for Taxol-induced apoptosis *Biochem Pharmacol.* 2006;71:1551-61.
96. Perez D, White E. E1A sensitizes cells to tumor necrosis factor α by downregulating c-FLIP_s. *J Virol.* 2003;77:2651-62.
97. Fukazawa T, Fujiwara T, Uno F, Teraishi F, Kadowaki Y, Itoshima T, et al. Accelerated degradation of cellular FLIP protein through the ubiquitin-proteasome pathway in p53-mediated apoptosis of human cancer cells. *Oncogene.* 2001;20:5225-31.
98. Wenzel U, Kuntz S, De UJS, Daniel H. Nitric oxide suppresses apoptosis in human colon cancer cells by scavenging mitochondrial superoxide anions. *Int J Cancer.* 2003;106:666-75.
99. Borutaite V, Brown GC. Nitric oxide induces apoptosis via hydrogen peroxide, but necrosis via energy and thiol depletion. *Free Radical Bio Med.* 2003;35:1457-68.
100. Visavadiya NP, Narasimhacharya AVRL. Asparagus root regulates cholesterol metabolism and improves antioxidant status in hypercholesteremic rats. *eCAM.* 2009;6(2):219-26.
101. Gautam M, Diwanay S, Gairola S, Shinde Y, Patki P, Patwardhan B. Immunoadjuvant potential of *Asparagus racemosus* aqueous extract in experimental system. *J Ethnopharmacol.* 2004;91:251-5.
102. Uematsu Y, Hirata K, Suzuki K, Iida K, Kamata K. Investigation of spectrophotometrically determined substances in *Yucca* extracts by GC/MS, TLC and on-column injection GC. *J Food Hyg Soc Japan.* 2004;45(3):141-5.

103. Zhao L, Huang C, Shan Z, Xiang B, Mei L. Fingerprint analysis of *Psoralea corylifolia* L. by HPLC and LC-MS. *J Chromatogr B*. 2005;821:67-74.
104. Wojciak-Kosior M. Application of high performance thin-layer chromatography to separation of oleanolic acid, ursolic and belulinic acids. *Journal of Pre-Clinical and Clinical Research*. 2007;1(2):176-8.
105. Makkar HPS, Siddhuraju P, Becker K. Plant secondary metabolites. *Methods in molecular biology*. New Jersey: Humana Press Inc; 2007. p. 93-100.
106. Xi M, Hai C, Tang H, Chen M, Fang K, Liang X. Antioxidant and antiglycation properties of total saponins extracted from traditional chinese medicine used to treat diabetes mellitus. *Phytother Res*. 2008;22:228-37.
107. Patnibul S, Puangmalai S, Mounng-on A, Sriprang S. Screening for antioxidant activity in eighteen local northeastern vegetables using silica gel thin-layer chromatography followed by spraying with DPPH. *NU Science Journal*. 2008;5(1):1-6.
108. Potduang B, Meeploy M, Giwanon R, Benmart Y, Kaewduang M, Supatanakul W. Biological activities of *Asparagus Racemosus*. *Afr J Tradit Complem*. 2008;5(3):230-7.
109. Kim D-O, Lee KW, Lee HJ, Lee CY. Vitamin C equivalent antioxidant capacity (VCEAC) of phenolic phytochemicals. *J Agr Food Chem*. 2002;50:3713-7.
110. Magalhães LM, Segundo MA, Reis S, Lima JLFC. Methodological aspects about in vitro evaluation of antioxidant properties. *Anal Chim Acta*. 2008;613:1-19.

APPENDICES

APPENDIX A

OVEREXPRESSION OF FLIP, Bcl-2, SOD, GPx IN H460 CELLS

FLIP-, Bcl-2-, SOD-, and GPx-overexpressing cells were prepared by stable transfection as described under *Materials and Methods*. The gene transfection resulted in a corresponding increase in the protein expression level over vector-transfected control, as determined by Western blot analysis as shown in Figure 4.28.

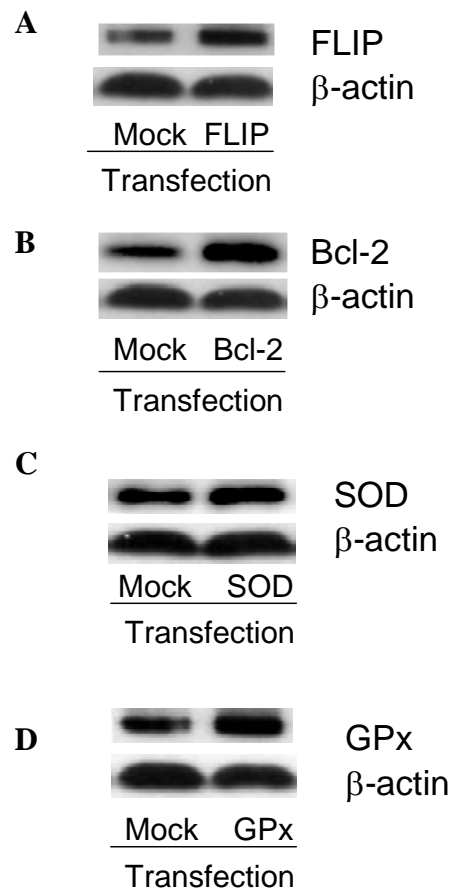


Figure 4.28 H460 cells were stably transfected with FLIP, Bcl-2, SOD, GPx or control pcDNA3 plasmid and determined protein expression level by Western blot analysis.

A, An increase in FLIP expression level over vector-transfected control

B, An increase in Bcl-2 expression level over vector-transfected control

C, An increase in SOD expression level over vector-transfected control

D, An increase in GPx expression level over vector-transfected control

APPENDIX B

ELECTRON SPIN RESONANCE STUDIES

Electron spin resonance (ESR) was used to detect short-lived free radical generation with the aid of the spin trapping agent 5,5-dimethyl-1-pyrroline-*N*-oxide (DMPO). The intensity of the spin adduct signal was used to measure the amount of short-lived radicals trapped, and the hyperfine couplings of the spin adduct were generally characteristics of the original trapped radicals. All ESR measurements were carried out using a Varian E9 ESR spectrometer and a flat cell assembly (Varian Inc., Palo Alto, CA). Reactants were mixed in a test tube in a final volume of 0.5 ml at 37°C. The reaction mixture was then transferred to a flat cell for measurement. Hyperfine couplings were measured (to 0.1 G) directly from magnetic field separation using potassium tetraperoxochromate and 1,1-diphenyl-2-picrylhydrazyl as reference standards. The software EPRDAP, version 2.0, was used for data acquisition and analysis.

The ESR technique allows identification of the specific ROS involved. Cells were treated with LF in the presence or absence of specific ROS scavengers and were analyzed for ROS generation. Non-treated cells with DMPO were used as a negative control. Figure 4.29 shows that in the absence of LF, no ESR signal was observed. However, in the presence of added LF, a clear signal consisting of a 1:2:2:1 quartet was detected. Based on line shape and hyperfine splitting of the spectrum, the signal was assigned to the DMPO-OH[•] adduct, which is indicative of OH[•] generation. The formation of DMPO-OH[•] adduct was detected as early as 5 min and peaked at about 40 min after the treatment, where it gradually declined to the baseline level. Addition of the OH[•] scavenger sodium formate strongly inhibited the ESR signal, indicating the specificity of OH[•] detection. Addition of MnTBAP or CAT also inhibited the signal intensity, indicating that O₂^{•-} and H₂O₂ were generated in LF-treated cells, and that these oxidative species were precursors for OH[•] generation.

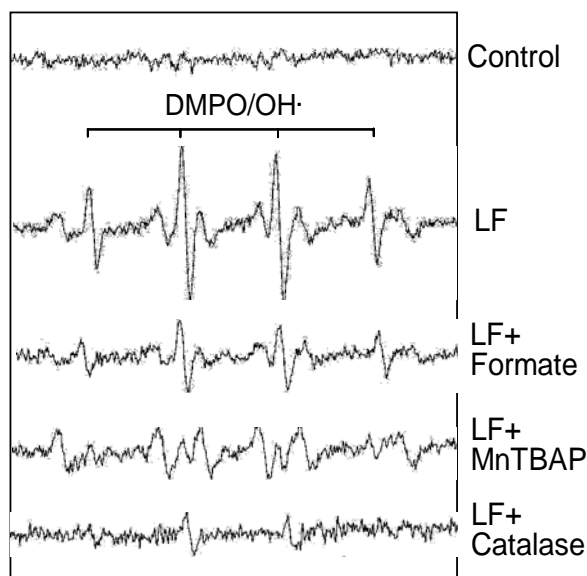


Figure 4.29 H460 cells ($1 \times 10^6/\text{ml}$) were incubated in RPMI medium containing the spin trapper DMPO (10 mM) in the presence or absence of LF (20 $\mu\text{g}/\text{ml}$), sodium formate (10 mM), MnTBAP (100 μM), and catalase (1000 units/ml). ESR spectra were then recorded 30 min after the addition of the test agents. The spectrometer settings were as follows: receiver gain at 1.5×10^5 , time constants at 0.3 second, modulation amplitude at 1.0 G, scan time at 4 min, magnetic field at 3470 ± 100 G.

APPENDIX C

UBIQUITINATION PATHWAY STUDIES

Immunoprecipitation studies were performed to analyze FLIP ubiquitination in cells treated with LF in presence or absence of antioxidants. Cells were washed after treatments with ice-cold phosphate-buffered saline and incubated in lysis buffer (20 mM Tris, pH 7.4, 150 mM NaCl, 10% glycerol, 0.2% NP40, 100 mM phenylmethylsulfonyl fluoride, and a protease inhibitor mixture) for 20 min at 4°C. After centrifugation at 14,000g for 15 min at 4°C, the supernatants were collected and the protein content was determined by bicinchoninic acid protein assay. Cleared lysates were normalized and 60 µg proteins were incubated with 8 µl of anti-Myc agarose bead (Santa Cruz Biotechnology) diluted with 12 µl of protein A-agarose for 4 h at 4°C. The immune complexes were washed 3 times with 500 µl of lysis buffer, resuspended in 2X Laemmli sample buffer, and boiled at 95°C for 5 min. The immune complexes were separated by 10% SDS-PAGE and analyzed by Western blotting as described under *Materials and Methods*.

H460 cells were transiently transfected with ubiquitin and myc-tagged FLIP plasmids, and the resulting immune complexes were analyzed by SDS-PAGE immunoblotting using anti-ubiquitin antibody. Figure 4.30 shows that in the absence of LF, minimum ubiquitinated FLIP was produced. Upon LF treatment, the level of ubiquitinated FLIP was greatly increased. Pretreatment of the cells with MnTBAP strongly inhibited the ubiquitination of FLIP, whereas catalase was less effective. These results indicate the role of O₂^{•-} as the major mediator of FLIP ubiquitination.

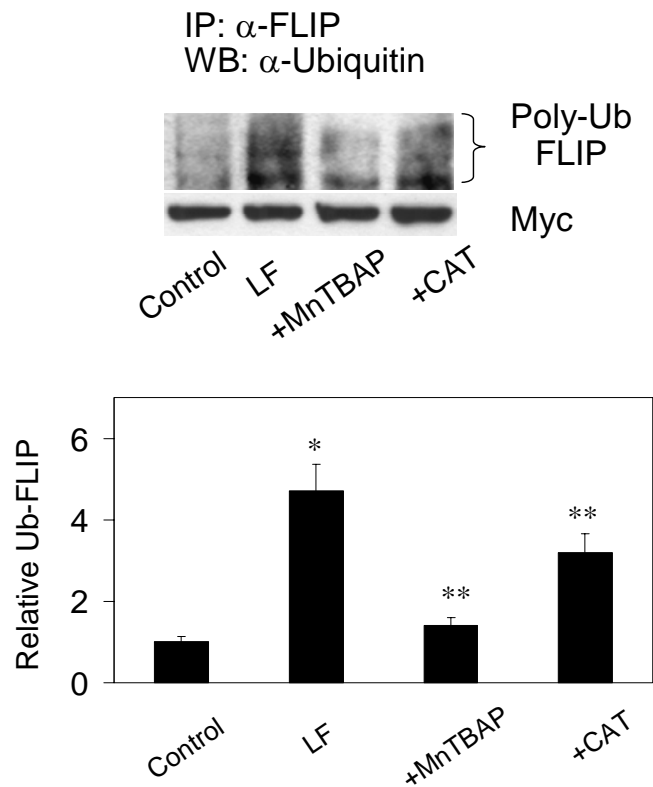


Figure 4.30 H460 cells were transiently transfected with ubiquitin and myc-tagged FLIP plasmids. Thirty six hours later, the cells were treated with LF (20 μ g/ml) in the presence or absence of MnTBAP (100 μ M) or catalase (1000 units/ml). Cell lysates were immunoprecipitated with anti-myc antibody and the immune complexes were analyzed for ubiquitin by Western blotting. Analysis of ubiquitin was performed at 2 h post-treatment where ubiquitination was found to be maximal. Data are mean \pm S.D. (n = 3). *, $p < 0.05$ versus nontreated control; **, $p < 0.05$ versus LF-treated control.

BIOGRAPHY

NAME	Lalana Kongkaneramt
DATE OF BIRTH	5 August 1972
PLACE OF BIRTH	Songkhla, Thailand
INSTITUTIONS ATTENDED	Prince of Songkhla University,(1990-1995) Bachelor of Science in Pharmacy Pharmacist, (1995-1996) Narathiwat Provincial Public Health Office, Narathiwat, Thailand Pharmacist, (1996-1997) Nathawee Hospital, Songkhla, Thailand Chiang Mai University, (1997-2000) Master of Pharmacy (Pharmaceutical Technology) Technical Support (cosmetics), (2000-2001) Research and Development Department, Ceutic Ltd., Bangkok, Thailand Lecturer (2001-present) Department of Pharmaceutical Technology, Faculty of Pharmacy,

Srinakharinwirot University,
Nakhorn Nayok, Thailand.
Mahidol University, (2004-2010)
Doctor of Philosophy
(Pharmaceutics)

RESEARCH GRANT

Commission on Higher Education
(Staff Development Project)

NANOTEC

(Thai Herbal Nano-Cosmeceuticals
Coordinated Research Program)

HOME ADDRESS

120 M. 9, Rong Kwang District,
Rong Kwang, Phare,
54140, Thailand

EMPLOYMENT ADDRESS

Faculty of Pharmacy, Srinakharinwirot
University, 63 M.7, Ongkarak
District, Ongkarak, Nakhon Nayok
Province, 26120, Thailand.
Tel. +66(0)3739 5094-5
Fax. +66(0)37 395096
Position: Lecturer
E-mail : lalana@swu.ac.th